




Fall 11-11-2020

## The Dual Roles of NF- $\kappa$ B Activation in Prx1+ Mesenchymal Cells in Health and Disease

Kang I. Ko

University of Pennsylvania, [gank@upenn.edu](mailto:gank@upenn.edu)

Follow this and additional works at: [https://repository.upenn.edu/dental\\_theses](https://repository.upenn.edu/dental_theses)

 Part of the [Dentistry Commons](#), [Musculoskeletal, Neural, and Ocular Physiology Commons](#), and the [Skin and Connective Tissue Diseases Commons](#)

---

### Recommended Citation

Ko, Kang I., "The Dual Roles of NF- $\kappa$ B Activation in Prx1+ Mesenchymal Cells in Health and Disease" (2020). *Dental Theses*. 54.

[https://repository.upenn.edu/dental\\_theses/54](https://repository.upenn.edu/dental_theses/54)

This paper is posted at ScholarlyCommons. [https://repository.upenn.edu/dental\\_theses/54](https://repository.upenn.edu/dental_theses/54)  
For more information, please contact [repository@pobox.upenn.edu](mailto:repository@pobox.upenn.edu).

---

# The Dual Roles of NF- $\kappa$ B Activation in Prx1+ Mesenchymal Cells in Health and Disease

## Abstract

Nuclear factor kappa-B (NF- $\kappa$ B) was discovered in 1986 and has since been studied extensively for its role as a master inflammatory transcription factor. As inflammation is critical for normal immune response but its chronic presence can be detrimental under pathological conditions, I sought to investigate the role of NF- $\kappa$ B in mesenchymal tissues under diabetic and homeostatic conditions. Aberrant activation of NF- $\kappa$ B and chronic inflammation have been documented in diabetic complications of kidney, eyes and cardiovascular system. Here I found that experimental type 1 diabetes caused hyperactivation of NF- $\kappa$ B in skeletal stem cells (SSCs) in the long bones of mice. Deletion of *Ikkb*, an activator of canonical NF- $\kappa$ B pathway, in Prx1+ (Paired Related Homeobox 1) SSCs prevented NF- $\kappa$ B activity and reversed the effect of diabetes on SSC apoptosis and anti-proliferation. In addition, it rescued the immuno-regulatory property of SSCs by transforming growth factor beta-1 (TGF $\beta$ 1), which in turn promoted macrophage polarization towards pro-resolving phenotype. These findings point to a detrimental role of NF- $\kappa$ B under pathologic condition such as type 1 diabetes. Surprisingly, I observed that NF- $\kappa$ B inactivation in Prx1+ cells caused hyper-inflammation and skin lesion that progressed with aging. The location of lesion was specific to ventral skin, consistent with the pattern of Prx1+ expression in mesenchyme derived from embryonic lateral plate mesoderm. *Ikkb* deletion in Col1a2Cre+ skin fibroblasts, but not Adipoq-Cre+ mature adipocytes, was sufficient to cause local inflammation but not in spleen or bone marrow. Single cell RNA sequencing analysis revealed an immune response that was characterized by an exaggerated inflammatory macrophage and type 2 T cell responses in the experimental animals. Furthermore, Prx1+ fibroblasts that had *Ikkb* deletion overexpressed CCL11 (also known as eotaxin-1), a potent chemoattractant for eosinophils. These results indicate *Ikkb*-NF $\kappa$ B activity in fibroblasts as an important contributor of immune homeostasis against an inflammatory response that mirrors the signs of atopic dermatitis. Thus, *Ikkb*-NF $\kappa$ B exhibits dual and opposing roles in Prx1+ mesenchymal cells where it is critical for homeostasis in dermal immunity, but it is detrimental in diabetic bone healing. These differential responses may be explained by the healthy or diseased status and/or by the niche-specific role of Prx1+ cells.

## Degree Type

Thesis

## Degree Name

DScD (Doctor of Science in Dentistry)

## Primary Advisor

Dana T. Graves

## Keywords

Diabetes, Fracture healing, NF- $\kappa$ B, Inflammation, Skeletal stem cells, Fibroblasts

## Subject Categories

Dentistry | Musculoskeletal, Neural, and Ocular Physiology | Skin and Connective Tissue Diseases



# University of Pennsylvania Dental Medicine

## THE DUAL ROLES OF NF-KB ACTIVATION IN PRX1<sup>+</sup> MESENCHYMAL CELLS IN HEALTH AND DISEASE

---

### THESIS

Presented to the Faculty of Penn Dental Medicine in Fulfillment of  
the Requirements for the Degree of Doctor of Science in Dentistry

Supervisor of Dissertation:

A blue ink signature of Dana T. Graves.

Dana T. Graves, DMD, DMSc

Thesis Committee Chair:

A blue ink signature of Robert P. Ricciardi.

Robert P. Ricciardi, MA, PhD

Dissertation Committee:

A blue ink signature of Sunday Akintoye.

Sunday Akintoye, BDS, DDS, MS

A blue ink signature of Songtao Shi.

Songtao Shi, DDS, MS, PhD

A blue ink signature of Ling Qin.

Ling Qin, PhD

## ACKNOWLEDGEMENT

I would like to thank my primary mentor Dr. Graves for his support, expertise and career guidance. I am particularly thankful for the quick email responses, day and night, in town or traveling. My response on the other hand tends to drag on, but I give myself 24 hours, except of course when I forget. I also thank the thesis committee for their advice, expertise and research enthusiasm.

Thanks to the members of the Graves lab over the past 10 years, many of whom are all over the world now. Special thanks to my two ‘research technicians’ Eileen Hu and Brett DerGarabedian. Both are training to become physicians, and I assume they will be writing prescriptions for my back pain in the future. Thus far they have not agreed to do so. Both are similar in a way that they called me by mean names on multiple occasions. It must be a pre-med thing to do because it can’t possibly be due to my words or behavior as I have been nothing but a pleasant advisor to them. I think.

Thanks to the clinical faculty members of the Department of Periodontics, especially Drs. Fiorellini, Korostoff and Stathopoulou. They have been extremely accommodating with my research schedule. I am sure that the collaboration and intellectual discussion will continue. Thanks to my co-residents for occasionally keeping me sane and insane at the same time. Thanks to the staff members in clinic for voting me as the most grouchy resident in the morning, which led to the discovery of my caffeine addiction.

Lastly, thanks to my family and friends. Mom prefers that I quit research and practice dentistry for more flexible hours and better salary. Unfortunately for her I am the spoiled child that always does opposite of what I am told. I think she has given up on me. She has another son, so I think this is okay.

## ABSTRACT

### **THE DUAL ROLES OF NF-KB ACTIVATION IN PRX1+ MESENCHYMAL CELLS IN HEALTH AND DISEASE**

Kang I. Ko

Dana T. Graves

Nuclear factor kappa-B (NF- $\kappa$ B) was discovered in 1986 and has since been studied extensively for its role as a master inflammatory transcription factor. As inflammation is critical for normal immune response but its chronic presence can be detrimental under pathological conditions, I sought to investigate the role of NF- $\kappa$ B in mesenchymal tissues under diabetic and homeostatic conditions. Aberrant activation of NF- $\kappa$ B and chronic inflammation have been documented in diabetic complications of kidney, eyes and cardiovascular system. Here I found that experimental type 1 diabetes caused hyperactivation of NF- $\kappa$ B in skeletal stem cells (SSCs) in the long bones of mice. Deletion of *Ikkb*, an activator of canonical NF- $\kappa$ B pathway, in Prx1+ (Paired Related Homeobox 1) SSCs prevented NF- $\kappa$ B activity and reversed the effect of diabetes on SSC apoptosis and anti-proliferation. In addition, it rescued the immuno-regulatory property of SSCs by transforming growth factor beta-1 (TGF $\beta$ 1), which in turn promoted macrophage polarization towards pro-resolving phenotype. These findings point to a detrimental role of NF- $\kappa$ B under pathologic condition such as type 1 diabetes. Surprisingly, I observed that NF- $\kappa$ B inactivation in Prx1+ cells caused hyper-inflammation and skin lesion that progressed with aging. The location of lesion was specific to ventral skin, consistent with the pattern of Prx1+ expression in mesenchyme derived from embryonic lateral plate

mesoderm. *Ikkb* deletion in *Col1a2Cre*<sup>+</sup> skin fibroblasts, but not *Adipoq-Cre*<sup>+</sup> mature adipocytes, was sufficient to cause local inflammation but not in spleen or bone marrow. Single cell RNA sequencing analysis revealed an immune response that was characterized by an exaggerated inflammatory macrophage and type 2 T cell responses in the experimental animals. Furthermore, *Prx1*<sup>+</sup> fibroblasts that had *Ikkb* deletion overexpressed CCL11 (also known as eotaxin-1), a potent chemoattractant for eosinophils. These results indicate *Ikkb*-NFκB activity in fibroblasts as an important contributor of immune homeostasis against an inflammatory response that mirrors the signs of atopic dermatitis. Thus, *Ikkb*-NFκB exhibits dual and opposing roles in *Prx1*<sup>+</sup> mesenchymal cells where it is critical for homeostasis in dermal immunity, but it is detrimental in diabetic bone healing. These differential responses may be explained by the healthy or diseased status and/or by the niche-specific role of *Prx1*<sup>+</sup> cells.

The study of *Prx1*<sup>+</sup> SSCs in diabetic bone healing was published in *Diabetes* under the title “Diabetes-Induced NF-κB Dysregulation in Skeletal Stem Cells Prevents Resolution of Inflammation” in 2019 and was modified and reproduced in Chapter 2. The study of *Prx1*<sup>+</sup> dermal fibroblasts in immune homeostasis of skin, in Chapter 3, is under manuscript in preparation.

---

Reference:

Ko KI, Syverson AL, Kralik RM, Choi J, DerGarabedian BP, Chen C, and Graves DT. Diabetes-Induced NF-kappaB Dysregulation in Skeletal Stem Cells Prevents Resolution of Inflammation. *Diabetes*. 2019;68(11):2095-106.

TABLE OF CONTENTS

**ACKNOWLEDGEMENT** ..... ii

**ABSTRACT**..... iii

**TABLE OF CONTENTS** .....v

**LIST OF FIGURES** ..... vii

**CHAPTER 1: INTRODUCTION** .....1

    1.1 IKKB-NFkB canonical signaling pathway .....1

    1.2 Prx1<sup>+</sup> mesenchymal cells in skeleton and skin .....3

    1.3 Diabetic bone healing, stem cells and NF-kB .....4

    1.4 NFkB and dermal homeostasis .....7

    1.5 Overarching goals .....9

**CHAPTER 2: DIABETES-INDUCED NF-κB DYSREGULATION IN SKELETAL STEM CELLS PREVENTS RESOLUTION OF INFLAMMATION**.....10

    2.1 Abstract .....10

    2.2 Introduction .....10

    2.3 SSC ablation causes prolonged inflammation during fracture healing .....13

    2.4 Diabetes enhances NF-kB activation in periosteal cells .....15

    2.5 NF-kB inhibition in SSCs prevents diabetes-mediated inflammation .....17

    2.6 NF-kB inhibition in SSCs, not chondrocytes, restores cartilage formation.....22

    2.7 Diabetes reduces SSC numbers by altering apoptosis and proliferation through NF-kb.....24

    2.8 SSCs modulate M1/M2 polarization through TGF-b1 during fracture healing, which is impaired in diabetes by NF-kB activation.....29

    2.9 TGF-b1 treatment improves inflammation in diabetic fractures.....33

    2.10 Discussion .....35

2.11 Methods.....	38
<b>CHAPTER 3: NF-<math>\kappa</math>B ACTIVITY IN DERMAL PRX1<sup>+</sup> FIBROBLASTS ARE CRITICAL FOR MAINTAINING IMMUNE HOMEOSTASIS IN SKIN.....</b>	<b>43</b>
3.1 Abstract .....	43
3.2 Introduction .....	43
3.3 Ventral skin lesion develops in mice that lack IKK $\beta$ in Prx1 <sup>+</sup> cells .....	45
3.4 Skin lesion progresses with age in postnatal IKK $\beta$ <sup>f/f</sup> mice .....	49
3.5 Dermal inflammation is characterized by excessive myeloid cell infiltration.....	53
3.6 Systemic inflammation in Prx1Cre <sup>+</sup> IKK $\beta$ <sup>f/f</sup> mice .....	55
3.7 NF- $\kappa$ B activity in fibroblasts, not in adipocytes, is critical for immune homeostasis .....	57
3.8 Single cell RNA-sequencing reveals chemokine dysregulation by Ikkb deletion in fibroblasts.....	59
3.9 Discussion .....	73
3.10 Methods.....	76
<b>CHAPTER 4: CONCLUSION AND FUTURE DIRECTIONS.....</b>	<b>80</b>
4.1 Summary .....	80
4.2 Future directions on diabetic healing and NF- $\kappa$ B .....	82
4.3 Future directions on skin lesion by Ikkb deletion .....	83
<b>REFERENCES.....</b>	<b>85</b>



## LIST OF FIGURES

Figure 2.1. SSC ablation by diphtheria toxin enhances inflammation in early fracture healing.....	14
Figure 2.2. SSC ablation prolongs inflammation and reduces cartilage formation .....	15
Figure 2.3. Diabetes enhances NF- $\kappa$ B activation in periosteal cells.....	16
Figure 2.4. Effect of NF- $\kappa$ B inhibition in Prx1+ SSCs on development and STZ-induced hyperglycemia.....	19
Figure 2.5. NF- $\kappa$ B inhibition in SSCs prevents diabetes-mediated inflammation .....	20
Figure 2.6. NF- $\kappa$ B inhibition in BMSSCs prevents high glucose-mediated inflammation .....	21
Figure 2.7. NF- $\kappa$ B inhibition in SSCs, not chondrocytes, restores cartilage formation ....	23
Figure 2.8. Lineage tracing in Prx1Cre+R26TdT and Col2a1Cre+R26TdT mice during fracture healing .....	24
Figure 2.9. Diabetes reduces SSC numbers through NF- $\kappa$ B .....	26
Figure 2.10. CD271 and Sca1 labels Prx1+ cells in healing fractures.....	27
Figure 2.11. Diabetes and high glucose promote apoptosis and inhibits proliferation through NF- $\kappa$ B .....	28
Figure 2.12. Diabetes increases macrophage infiltration to the fracture site that is blocked with NF- $\kappa$ B inhibition in SSCs.....	31
Figure 2.13. Diabetes reduces M2 and enhances M1 in a NF- $\kappa$ B dependent manner.....	31
Figure 2.14. Prx1+ SSCs express TGF $\beta$ 1 which is reduced by diabetes.....	32
Figure 2.15. SSCs modulate M1/M2 polarization through TGF $\beta$ 1, which is impaired by NF- $\kappa$ B activation in high glucose .....	33

Figure 2.16. TGFβ1 treatment improves inflammation in diabetic fractures .....	34
Figure 2.17. Summary cartoon of diabetic fracture healing .....	36.
Figure 3.1. Ventral skin lesion develops in mice that lack IKKβ in Prx1+ cells.....	47
Figure 3.2. Ikkβ deletion in Prx1+ cells block NF-kB activation in dermal fibroblasts and adipocytes .....	48
Figure 3.3. Skin lesion progresses with age in postnatal Ikkβf/f mice .....	50
Figure 3.4. Dermal fibrosis is preceded by myeloid inflammation in young but not neonatal Ikkβf/f mice.....	51
Figure 3.5. Soft cage bedding does not protect Prx1Cre+Ikkbf/f mice from developing inflammation.....	54
Figure 3.6. Systemic inflammation in Prx1Cre+Ikkβf/f mice .....	56
Figure 3.7. NF-kB activity in fibroblasts, not in adipocytes, is critical for immune homeostasis.....	58
Figure 3.8. scRNA-seq analysis of skin cells from control vs. Ikkb deleted mice .....	63
Figure 3.9. Fibroblast heterogeneity and group-specific populations .....	65
Figure 3.10. Differentially expressed genes in Prx1+ fibroblasts between control and Ikkbf/f mice.....	66
Figure 3.11. Immune cell subclusters in the skin of control and Ikkb deleted mice .....	67
Figure 3.12. Ikkb deletion in Prx1+ cells upregulates pro-inflammatory cytokines in macrophages and causes type 2 immune response from lymphoid cells.....	69
Figure 3.13. Fibroblast-specific expression of <i>Ccl11</i> (eotaxin-1) and increased eosinophil-related genes in Ikkb deleted mice.....	71
Figure 3.14. Ikkb deletion in fibroblasts and experimental atopic dermatitis .....	72



## CHAPTER 1: INTRODUCTION

### 1.1 IKK $\beta$ -NF $\kappa$ B canonical signaling pathway

In 1986, David Baltimore's group identified a protein that bound to a specific DNA sequence during B cell maturation and named the protein NF- $\kappa$ B, for nuclear factor binding near the kappa light-chain gene in B cells (Sen and Baltimore, 1986). Since its discovery over 30 years ago, our knowledge of NF- $\kappa$ B has expanded greatly beyond B cell biology. I now know that NF- $\kappa$ B acts as a key transcriptional activator of inflammatory cytokine genes in innate immune cells such as neutrophils and macrophages upon injury and/or bacterial challenge (Hayden and Ghosh, 2011; Sun et al., 2013). NF- $\kappa$ B also regulates critical gene expression responsible for antigen-specific T and B cell proliferation, differentiation and survival (Hayden and Ghosh, 2011). Due to its indispensable regulatory activity in both arms of innate and adaptive immunity, NF- $\kappa$ B is often referred to as the master inflammatory transcription factor.

NF- $\kappa$ B protein family consists of NF- $\kappa$ B1 (p50), NF- $\kappa$ B2 (p52), RelA (p65), RelB and c-Rel, and these five members share a conserved Rel homology domain that mediates DNA binding to the consensus sequence upstream of NF- $\kappa$ B target genes (5'-GGGPuNNPyPyCC-3') (Chen et al., 1998; Ghosh et al., 1998; Oeckinghaus and Ghosh, 2009). These form homo- or heterodimers and remain bound to I $\kappa$ B (inhibitor of  $\kappa$ B) proteins in the cytoplasm during unstimulated phase. Of these, p50/p65 complex is by far the most abundant and found in almost all cell types (Oeckinghaus and Ghosh, 2009). Induction of canonical NF- $\kappa$ B pathway is dependent on the catalytic activity of IKK protein family (inhibitor of nuclear factor kappa-B kinase), which consists of IKK $\alpha$ , IKK $\beta$  and IKK $\gamma$ . Upon stimulation by inflammatory signals (eg. TNF, IL1 $\beta$ , LPS), IKK $\beta$

phosphorylates I $\kappa$ B serine residues and primes I $\kappa$ B for ubiquitination and degradation, which in turn liberates p50/p65 complex to translocate into the nucleus and become transcriptionally active (Ling et al., 1998; Mercurio et al., 1997; Zhang et al., 2017). Non-canonical NF- $\kappa$ B pathway does not involve IKKb, and is distinct from the canonical pathway in its stimulatory signals (CD40, BAFF, lymphotoxin-beta), requirement of NF- $\kappa$ B-inducing kinase/IKKa, and activation of p52/RelB complex (Oeckinghaus and Ghosh, 2009). Inactivation of NF- $\kappa$ B signaling is mediated by the newly synthesized I $\kappa$ B proteins, which is one of the transcriptional targets of NF- $\kappa$ B (Pahl, 1999). NF- $\kappa$ B is then dissociated from DNA by I $\kappa$ B proteins and exported to the cytosol where it remains sequestered until external stimuli are sensed. This negative feedback mechanism prevents chronic activation of NF- $\kappa$ B and achieves resolution of NF- $\kappa$ B transcriptional activity.

The significance of IKKb/NF- $\kappa$ B pathway under physiological condition is well documented in animal models. Global deletion of IKKb or p65 leads to embryonic lethality by severe liver apoptosis (Beg et al., 1995; Li et al., 1999a; Li et al., 1999b), and epidermis-specific deletion of IKKb causes inflammatory skin lesions (Pasparakis et al., 2002). Moreover, IKKb mutation in humans is associated with severe combined immunodeficiency (Pannicke et al., 2013), demonstrating a necessity of IKKb-NF- $\kappa$ B signaling in maintaining immune homeostasis. In chronic disease models, however, NF- $\kappa$ B appears to play a contrasting role by exerting a long-lasting inflammatory effect that is detrimental to organ function. For example, in diabetes, NF- $\kappa$ B activity in myeloid cells is persistent and is linked to high-glucose induced alteration at the epigenetic level to cause constant release of proinflammatory cytokines (El-Osta et al., 2008; Shanmugam et al., 2003). In cancer, NF- $\kappa$ B activity is postulated to play a critical role by linking chronic

inflammation and cancer survival (Taniguchi and Karin, 2018). These findings have led to investigation of specific NF- $\kappa$ B inhibitor as a potential treatment option in chronic diseases such as diabetes and cancer.

## **1.2 Prx1<sup>+</sup> mesenchymal cells in skeleton and skin**

The role of IKKb/NF- $\kappa$ B has been mainly studied in immune cells, despite the broad expression of the protein complex, particularly the p50/p65, in other cell types (Oeckinghaus and Ghosh, 2009). As NF- $\kappa$ B is critical in mounting an inflammatory response, it may function as a sensor of acute inflammatory environment in non-immune cells and elicit appropriate responses. Recent studies have elucidated an important role of NF- $\kappa$ B in mesenchymal cells. Under physiologic condition, TNF stimulates bone marrow derived stromal cells to secrete anti-inflammatory cytokines to modulate inflammation, and this requires transient NF- $\kappa$ B activity (Philipp et al., 2018). Under pathological condition, such as in age-related osteoporosis, NF- $\kappa$ B is aberrantly activated in bone marrow mesenchymal stem cells and shifts their differentiation towards adipogenesis over osteogenesis (Chang et al., 2013; Chang et al., 2009). In skin, old fibroblasts are linked to age-associated inflammation that negatively affects the use of these cells for induced pluripotent stem cells (Mahmoudi et al., 2019). As more genetic tools that target mesenchymal cells become widely available, the field has begun to investigate the role of NF- $\kappa$ B in the mesenchymal cells and its contribution in maintaining physiologic homeostasis and/or disease pathogenesis.

Prx1, or paired related homeobox 1, is a mesenchymal cell marker that is commonly used to study embryologic patterning of cells derived from lateral plate mesoderm. The use of Cre-LoxP system in Prx1Cre<sup>+</sup> reporter mice has shown that Prx1<sup>+</sup> cells trace to limbs,

craniofacial mesenchyme and ventral, but not dorsal, component of dermal mesenchyme (Durland et al., 2008; Logan et al., 2002). A select number of these cells remain as postnatal Prx1+ cells in adult mice and reside in specific skeletal niches such as cranial sutures and periosteum of the long bones (Kawanami et al., 2009; Murao et al., 2013; Ouyang et al., 2014; Wilk et al., 2017). These postnatal Prx1+ cells behave as skeletal stem cells, a subset of mesenchymal stem cells (MSCs), as they differentiate into osteoblasts and chondrocytes in response to injury and are indispensable for skeletal regeneration (Ouyang et al., 2014; Wilk et al., 2017). In the skin, Prx1+ cells trace to the ventral but not dorsal dermis, labeling dermal fibroblasts and adipocytes (Currie et al., 2019; Durland et al., 2008; Sanchez-Gurmaches et al., 2015). Moreover, Prx1+ cells reside as vascular stromal cells in the bone marrow and are critical in maintaining proper hematopoiesis (Greenbaum et al., 2013). One possible explanation to their seemingly distinct function based on the niche may be the microenvironment rigidity. A seminal study demonstrated that mesenchymal stem cells differentiate into neural lineage on soft substrate whereas it is more prone to osteogenic differentiation under stiffer environment (Engler et al., 2006). Given this, even though Prx1-lineage cells are found in multiple mesenchymal niches postnatally, their cell identity and function likely differ in vivo, and thus requires independent investigation.

### **1.3 Diabetic bone healing, stem cells, and NF- $\kappa$ B**

Diabetic complications in multi-organ systems are strongly linked to a chronic inflammatory environment. Organ damage in diabetes is often explained by the impaired mesengenic cellular response such as increased apoptosis and decreased proliferation (Alblowi et al., 2009; Kayal et al., 2010; Siqueira et al., 2010). How diabetic conditions fail to curtail prolonged inflammation in the healing environment remains elusive. Recent

advances made in stem cell therapy demonstrate that mesenchymal stem cells (MSCs), other than their capability to differentiate into many cell types, exhibit potent anti-inflammatory properties (Ma et al., 2014). Given that the diabetic healing environment is often associated with exacerbated inflammation, diabetes may directly affect endogenous MSCs that are needed to control inflammation during healing.

Investigating the physiologic role of endogenous MSCs has been challenging. Wound healing promotes expansion of MSCs through their recruitment and proliferation (Marsell and Einhorn, 2011; Zou et al., 2012). Thus, the wound healing model offers an excellent opportunity to investigate *in vivo* function of MSCs. In mice, fracture healing follows a well-orchestrated pattern of cellular events from acute inflammation, cellular proliferation, cartilage and bone formation and remodeling, and these events are predictably observed based on post-injury days (Claes et al., 2012; Marsell and Einhorn, 2011). This is also well-characterized in oral soft tissue wound healing (Wong et al., 2009). MSCs may play an essential role in the resolution of inflammation and formation of regenerative cells during wound healing (Wang et al., 2013). Furthermore, this may not adequately occur in diabetic healing and lead to prolonged inflammation (Kayal et al., 2010; Pradhan et al., 2011).

MSCs display remarkable anti-inflammatory properties via paracrine and cell-cell contact mechanisms. They have been utilized successfully in the treatment of several autoimmune disorders that have increased inflammation (Wang et al., 2014; Yi and Song, 2012). MSCs are capable of suppressing T cell proliferation via release of soluble mediators such as prostaglandin-E2 (PGE2), transforming growth factor- $\beta$  (TGF $\beta$ ), IL-10, and nitric oxide (English et al., 2007; Sato et al., 2007). Interestingly, MSCs express TGF $\beta$



to induce formation of CD4<sup>+</sup>CD25<sup>+</sup>FoxP3<sup>+</sup> regulatory T cells (English et al., 2007; Patel et al., 2010), essential for reducing inflammation. While there is a significant effort to utilize exogenous MSCs to treat inflammatory diseases due to their potent anti-inflammatory properties, a potential anti-inflammatory role of endogenous MSCs, or lack thereof that may be an underlying pathologic mechanism in diabetic healing, has received surprisingly little attention.

Several animal and human studies suggest that both type 1 and 2 diabetes impair MSC viability and function. In mice, bone marrow MSCs (BMSCs) (Shin and Peterson, 2012) and adipose-derived MSCs (Cramer et al., 2010) isolated from type 2 diabetic animals (db/db) exhibit reduced proliferation and differentiation *in vitro* compared to controls and are less efficacious *in vivo*. MSCs in streptozotocin-induced type 1 diabetic rats have decreased proliferation compared to MSCs from normoglycemic rats (Jin et al., 2010; Stolzing et al., 2010). Moreover, transplantation of autologous MSCs isolated from type 1 diabetic mice to diabetic animals fail to prevent hyperglycemia, whereas MSCs from control mice reverse hyperglycemia (Fiorina et al., 2009).

Diabetes impairs fracture healing in animal models and humans (Alblowi et al., 2009; Claes et al., 2012; Kayal et al., 2010; Loder, 1988) but studies investigating diabetic effect on MSCs are limited to transplantation and *in vitro* experiments. There are few studies examining the role of endogenous MSCs in diabetic fracture or soft tissue healing. In mice, transplantation of MSCs in fractures improve healing (Granero-Molto et al., 2009). In rats, transplantation of MSCs improves cutaneous diabetic wound healing, which is associated with a decrease in inflammatory cell infiltrate (Kuo et al., 2011). These transplantation

findings suggest a potential impairment of endogenous MSCs in diabetic wound healing, but this remains speculative and thus requires further in vivo investigation.

Nuclear factor kappa-B (NF- $\kappa$ B) is a transcription factor that responds to various stressful stimuli and regulates gene transcription that is associated with inflammation (Pahl, 1999). Whereas transient NF- $\kappa$ B activation is essential in innate immune response (Zhang and Ghosh, 2001), dysregulated NF- $\kappa$ B activation is observed in diabetes and contributes to diabetic complications such as renal fibrosis (Wada and Makino, 2013), cardiovascular complications (Fiorentino et al., 2013) and neuropathy (Ganesh Yerra et al., 2013). In mice, increased NF- $\kappa$ B activity is associated with reduced osteogenic differentiation of BMSCs, and a small molecule inhibitor of NF- $\kappa$ B improves osseous calvarial defect healing (Chang et al., 2013). In humans, MSCs isolated from periodontal ligament exhibit reduced proliferation and osteogenic differentiation when cultured in high glucose, and both parameters are reversed with a pharmacologic inhibitor of canonical NF- $\kappa$ B pathway (Kato et al., 2016). These studies highlight the potential adverse role of NF- $\kappa$ B under diabetic condition, which remains to be proven.

#### **1.4 NF- $\kappa$ B and dermal homeostasis**

Initial experiments were designed to translate the findings from diabetic fracture study to oral wound healing model. Unexpectedly, I observed alopecia and, less frequently, ulceration on ventral aspect of the skin in 4 to 5 months old experimental mice that lacked *Ikkb* gene in *Prx1*<sup>+</sup> cells. The experimental female mice, while fertile, were unsuccessful in weaning newborn pups, presumably by failing to nurse them properly due to dermatologic irritation. Moreover, these transgenic mice were easily identified by the skin stiffness while handling and by the limited range of abductive motion of the forearms.

Collectively, the observations indicated that *Ikkb* deletion in *Prx1*<sup>+</sup> cells must have a significant impact on the structural integrity of the skin under normoglycemic condition, unlike that of the long bones.

The skin lesion developed without any experimental injury perturbation, suggesting a dysregulation of homeostatic mechanism that is distinct from fracture healing model. It is thus critical to understand the effects of *Ikkb* deletion in *Prx1* lineage cells on connective tissue homeostasis before its implication in diabetic oral wound healing can be considered. Furthermore, it implicates the homeostatic function of *Prx1*<sup>+</sup> mesenchymal cells as an important factor in regulating or preventing progressive dermatitis, which is a novel idea given that the role of *Ikkb* gene in dermal fibroblasts had not been investigated extensively. It is particularly interesting that the deletion of *Ikkb* and therefore inactivation of NF- $\kappa$ B, an important inflammatory transcription factor, paradoxically leads to a development of dermatitis that is often associated with an overt inflammatory reaction.

While persistent NF- $\kappa$ B activation in diabetic bone healing is strongly associated with healing complications, there exists a contrasting evidence in the skin. In mice lacking SHANK-associated RH domain-interacting protein, NF- $\kappa$ B activity is exacerbated and leads to cutaneous inflammation and lesion development (Liang et al., 2011; Potter et al., 2014; Seymour et al., 2007). Keratinocyte-specific knock-in model of IKKb overexpression (Page et al., 2010) or global deletion of *IkBa* (Klement et al., 1996), both of which caused an aberrant activation of NF- $\kappa$ B, led to severe inflammatory cutaneous lesion. These studies support the negative effects of NF- $\kappa$ B overactivation in skin. In sharp contrast, preventing NF- $\kappa$ B activity by IKKb deletion in keratinocytes also causes inflammation and skin lesion development (Grinberg-Bleyer et al., 2015; Pasparakis et al.,

2002). Altogether, these highlight the opposite roles of NF- $\kappa$ B activity in epidermis, where it supports immune homeostasis under physiological condition but its overactivation is detrimental by causing an overt inflammation in skin. However, the studies are limited to either global gene deletion or keratinocyte-specific knockout models, and both models are typically associated with early neonatal death or blunted postnatal development. Given the abundance of skin inflammatory disorders in humans that has little influence on development (Chiesa Fuxench et al., 2019; Silverberg et al., 2019), these models may not fully represent the practical examples of human dermatitis.

### **1.5 Overarching goals**

The over-arching goal of the thesis is to understand the role of I $\kappa$ kb-NF- $\kappa$ B activation in mesenchymal cells by using two distinct models where the absence of I $\kappa$ kb is either protective or detrimental. To test this, I examined diabetic fracture healing and skin homeostasis using the mice that lacked I $\kappa$ kb gene in Prx1<sup>+</sup> cells. These conditions are unique from each other, where one examines the regeneration of mineralized tissue upon injury, and the other that examines the homeostatic role of mesenchymal cells that prevents spontaneous development of dermatitis. Another important distinction is the non-overlapping identity and function of Prx1<sup>+</sup> cells in bone and skin. Given the existing evidence and our preliminary observations, examining I $\kappa$ kb deletion in Prx1<sup>+</sup> cells in both bone and skin offers a unique advantage to understand a functional duality of NF- $\kappa$ B activation that may be pathologic or protective. In Chapter 2, I will test the hypothesis that NF- $\kappa$ B activation in Prx1<sup>+</sup> cells is responsible for delayed healing in early diabetic fractures. In Chapter 3, I will test the hypothesis that NF- $\kappa$ B activation in Prx1<sup>+</sup> cells is essential for maintaining skin homeostasis by regulating immune response.

## **CHAPTER 2: DIABETES-INDUCED NF- $\kappa$ B DYSREGULATION IN SKELETAL STEM CELLS PREVENTS RESOLUTION OF INFLAMMATION**

### **2.1 Abstract**

Type 1 diabetes (T1D) imposes a significant health burden by its negative impact on tissue regeneration during wound healing. The adverse effect of diabetes is attributed to high levels of inflammation, but the cellular mechanisms responsible remain elusive. Here I show that intrinsic skeletal stem cells (SSCs) are essential for resolution of inflammation to occur during osseous healing by using genetic approaches to selectively ablate SSCs. T1D caused aberrant nuclear factor-kappaB (NF- $\kappa$ B) activation in SSCs and substantially enhanced inflammation *in vivo*. Constitutive or tamoxifen-induced inhibition of NF- $\kappa$ B in SSCs rescued the impact of diabetes on inflammation, SSC expansion, and tissue formation. In contrast, NF- $\kappa$ B inhibition in chondrocytes failed to reverse the effect of T1D. Mechanistically, diabetes caused defective pro-resolving macrophage (M2) polarization by reducing TGF $\beta$ 1 expression by SSCs, which was recovered by NF- $\kappa$ B inhibition or by exogenous TGF $\beta$ 1 treatment. These data identify an underlying mechanism for altered healing in T1D and demonstrate that diabetes induces NF- $\kappa$ B hyperactivation in SSCs to disrupt their ability to modulate M2 polarization and resolve inflammation.

### **2.2 Introduction**

Type 1 diabetes (T1D) exerts a detrimental impact on skeletal health by increasing the risk of fractures and causing poor healing (Sellmeyer et al., 2016; Weber and Schwartz, 2016). A striking feature of T1D complications in skeletal injury is a significantly reduced ability to downregulate inflammatory cytokines such as tumor necrosis factor (TNF) (Xu et al., 2013), which is linked to accelerated cartilage resorption

and reduced bone formation (Alblowi et al., 2009; Pacios et al., 2015). An anti-inflammatory therapy improves regenerative outcomes in diabetic wounds (Alblowi et al., 2009; Mirza et al., 2013), highlighting the importance of limiting inflammation to facilitate healing. While these studies demonstrate the negative impact of chronic inflammation on diabetic healing, little is known about the underlying mechanisms behind the failure to resolve inflammation and maintain homeostasis.

Resolution of inflammation is a critical aspect of tissue regeneration, which is regulated by timely clearance of debris by pro-inflammatory macrophages and transition toward a phenotype that is pro-resolving (Fullerton and Gilroy, 2016). Dysregulated macrophage function leads to excessive tissue destruction and delayed healing (Perdiguero et al., 2011). Studies have demonstrated that macrophages can regulate the behavior of progenitor cells to maintain homeostasis in bone marrow and intestinal microenvironment (Chow et al., 2011; Sehgal et al., 2018) and promote regeneration in muscle injury (Arnold et al., 2007). However, a potential reciprocal regulation by stem cells on inflammatory cells during tissue regeneration is poorly understood and remains a fundamental question in the context of immune and stem cell dialog.

A pool of postnatal stem cells resides in the periosteum, endosteum and stromal compartments in skeletal tissues. In mice, these skeletal stem cells (SSCs) differentiate into chondrocytes and osteoblasts to fully regenerate the lost tissue in response to fracture injury of the long bones (Colnot, 2009). Interestingly, expansion of SSCs occurs early in the healing microenvironment (Einhorn and Gerstenfeld, 2015), suggesting a possible interaction between SSCs and inflammatory cells. SSCs have demonstrated a potent immune-modulatory function *in vitro* and have been utilized to treat symptoms of

inflammatory diseases (Chen et al., 2017; Liang et al., 2010). However, isolation and *in vitro* expansion of SSCs for transplantation use is artificial and does not accurately represent a potential *in vivo* function of SSCs. The role of SSCs in regulation of inflammation *in vivo*, and their potential dysregulation under pathological condition, is surprisingly underexplored.

Nuclear factor kappa-B (NF- $\kappa$ B) is a transcription factor that responds to various stressful stimuli and regulates gene transcription associated with inflammation (Pahl, 1999). Aberrant NF- $\kappa$ B activation is observed in podocytes, peripheral neurons, endothelial and ligament cells in T1D (Ganesh Yerra et al., 2013; Pacios et al., 2015; Suryavanshi and Kulkarni, 2017; Wada and Makino, 2013), which is attributed to increased oxidative stress and inflammation that stems from persistent hyperglycemia (Giacco and Brownlee, 2010). Pharmacologic inhibition of NF- $\kappa$ B improves vascular function in a diabetic animal model (Kassan et al., 2013), implicating a pathologic role of NF- $\kappa$ B in diabetic complications. While these studies implicate a potential involvement of NF- $\kappa$ B in diabetic bone healing, the precise mechanisms and cell types that control homeostasis remain unknown.

Here, I report that SSCs play an essential role in modulating inflammation during fracture injury, and that T1D interferes with this through aberrant activation of NF- $\kappa$ B. Through genetic manipulation and rescue experiments, I demonstrate that diabetes-induced NF- $\kappa$ B suppresses SSC expansion and production of anti-inflammatory TGF $\beta$ 1 to cause the failure of macrophage polarization towards a pro-resolving phenotype. Collectively, our study demonstrates an important reciprocal relationship between immune-stem cell interactions during skeletal regeneration and implicates a potential role of hyperglycemia-

induced NF- $\kappa$ B dysregulation in stem cells in other types of injury where diabetes interferes with the healing process.

### **2.3 SSC ablation causes prolonged inflammation during fracture healing**

To determine if the removal of SSCs has an impact on modulation of inflammation, I selectively ablated SSCs in *Prx1<sup>CreER-GFP+</sup>R26<sup>DTA</sup>* mice with tamoxifen-induced diphtheria toxin expression driven by an SSC-specific promoter element of *Prx1* (Logan et al., 2002). 3- and 6-day post-fracture time points were selected to examine resolution of inflammation and early chondrogenesis phase (Einhorn and Gerstenfeld, 2015), respectively. I followed the loss of SSCs through Prx1-dependent GFP, which is expressed in the fusion protein (Fig. 2.1A). Tamoxifen administration resulted in a significant reduction in GFP<sup>+</sup> SSCs (Fig. 2.1B). SSC ablation led to increased mRNA levels of *Tnf*, *Ilb1* and *Ifn $\gamma$*  compared to the control group (Fig. 2.1C), with a corresponding increase in F4/80<sup>+</sup> macrophages and CD4<sup>+</sup> lymphocytes (Fig. 2.1D, E). SSC ablation also led to a significant reduction in cartilage formation, a measure of tissue regeneration, by day-6 (Fig. 2.2A). The number of proinflammatory TNF<sup>+</sup> cells was maintained at high levels through day-6 fractures when SSCs were removed (Fig. 2.2B). SSC reduction had little effect on basal inflammation in non-injured femurs as measured by the quantity of F4/80<sup>+</sup> and CD4<sup>+</sup> cells (Fig. 2.2C) and MFI per cell (data not shown), indicating that SSCs played a primary role in modulating inflammation when there was an inflammatory perturbation stimulated by injury. These data establish that intrinsic SSCs are necessary in limiting inflammation during an early healing response.



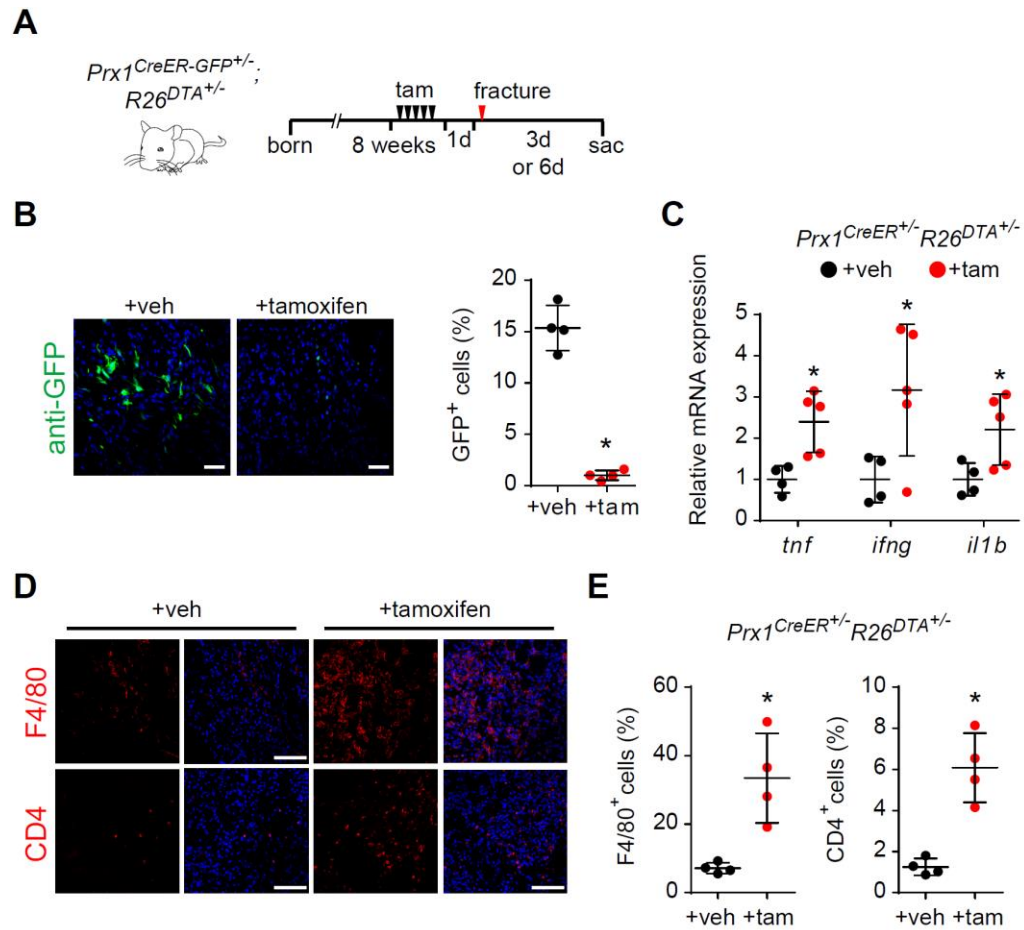


**Figure 2.1. SSC ablation by diphtheria toxin enhances inflammation in early fracture healing.** **A.** Experimental design for diphtheria toxin-induced ablation of SSCs in experimental (*Prx1<sup>CreER-GFP</sup><sup>+/-</sup>R26<sup>DTA</sup><sup>+/-</sup>*) mice. **B.** Immunofluorescence with GFP antibody to detect Prx1<sup>+</sup> cells in day 3 fractures. Quantification of GFP immunopositive cells in experimental mice that received corn oil (+veh) or tamoxifen (+tam). Scale bar, 50um. **C.** mRNA expression of *Tnf*, *il1b*, and *Ifng* from day 3 fractures of experimental mice that received corn oil or tamoxifen, as determined by RT-qPCR. **D.** Representative immunofluorescent images of F4/80 or CD4 immunopositive cells in day 3 fractures in control (+veh) or SSC-ablation group (+tam), scale bar 100um. **E.** Quantification of F4/80 or CD4 immunopositive cells per total nucleated cells in day 3 fractures in experimental mice that received vehicle or tamoxifen.

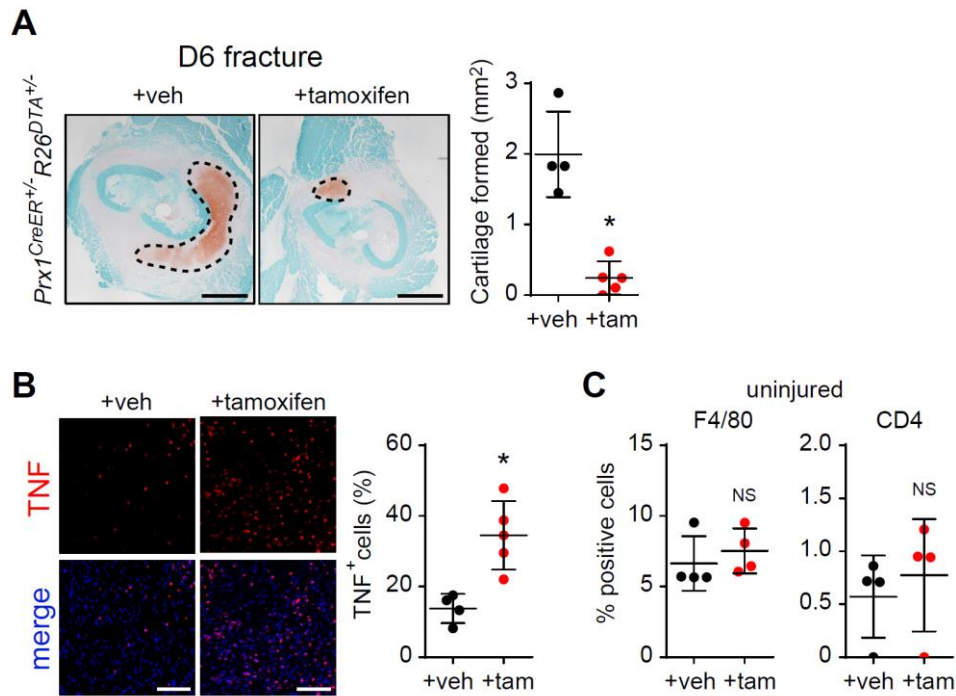


**Figure 2.2. SSC ablation prolongs inflammation and reduces cartilage formation.** **A.** Representative images of day 6 fracture wounds from control or SSC-ablation group, stained with safranin O/fast green. *Right*, quantification of cartilage formed in area (mm<sup>2</sup>). Scale bar, 1mm. **B.** Representative immunofluorescent images of TNF<sup>+</sup> cells in day 6 fracture wounds, analyzed in mesenchymal area between cartilage and muscle compartments. *Right*, quantification of TNF<sup>+</sup> cells in +veh or +tam group. Scale bar, 100um. **C.** Quantification of F4/80 or CD4 positive cells per total nucleated cells (%) in the periosteal layer of uninjured contralateral femurs. NS, not significant. Data are represented as mean  $\pm$  SD. \* $p < 0.05$  comparing corn oil control to tamoxifen groups, two-tailed t-test. N = 4-5 mice each.

## 2.4 Diabetes enhances NF- $\kappa$ B activation in periosteal cells

A hallmark characteristic of diabetic wound healing is a failure to resolve inflammation (Jiao et al., 2015). Because SSC ablation resulted in elevated inflammation that mirrors diabetic fracture healing, I hypothesized that diabetes-enhanced inflammation is due to its impact on SSCs. I first examined activation of NF- $\kappa$ B by its nuclear localization in normoglycemic and streptozotocin-induced diabetic mice. Immunofluorescence with NF- $\kappa$ B antibody demonstrated that diabetes altered nuclear NF- $\kappa$ B localization in skeletal

muscle and periosteum, indicative of its dysregulation, compared to normoglycemic control mice (Fig. 2.3A, C). Induction of fracture injury led to the greatest magnitude of NF- $\kappa$ B activation in periosteal cells (Fig. 2B, D). Given that periosteal cells represent an important SSC population that differentiates into chondrocytes and osteoblasts *in vivo* (Kawanami et al., 2009), I focused our study on the role of NF- $\kappa$ B in SSCs to investigate how its dysregulation affected diabetic healing process.

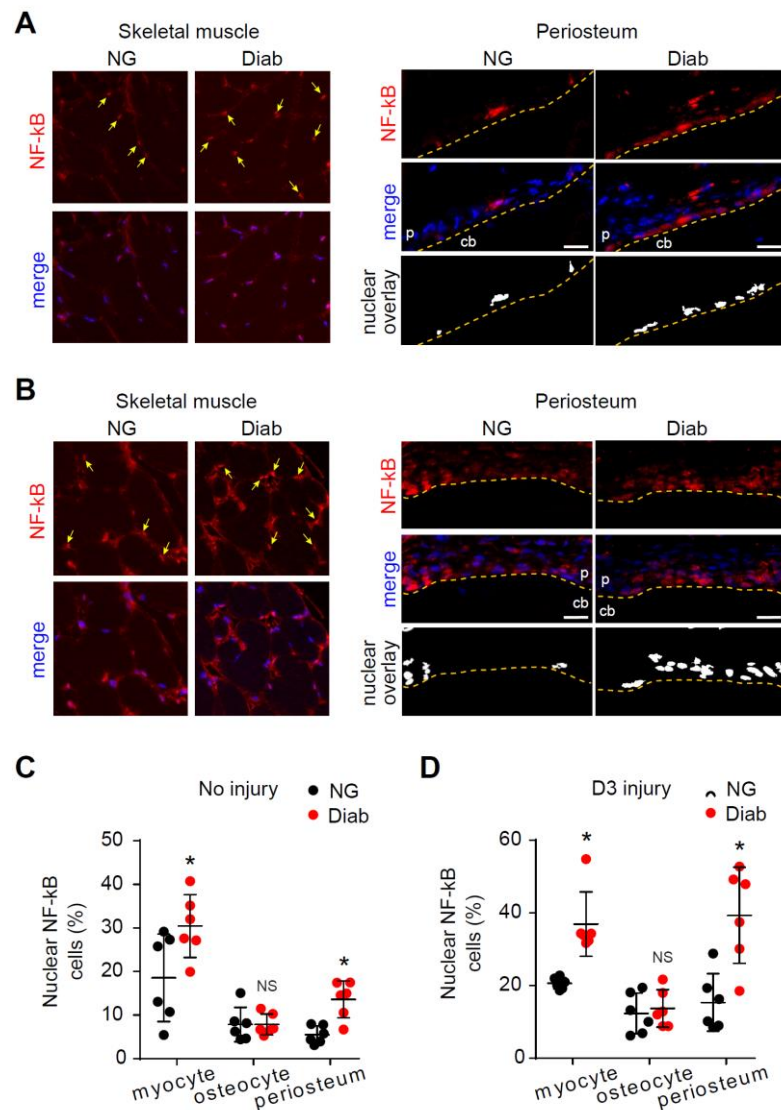


**Figure 2.3. Diabetes enhances NF- $\kappa$ B activation in periosteal cells.** A. Immunofluorescence of NF- $\kappa$ B (p65) in skeletal muscle and periosteum of uninjured femur. Nuclear NF- $\kappa$ B expression is indicated by

arrows (skeletal muscle) or by the nuclear overlay image with DAPI expression (periosteum). Representative images from normoglycemic (NG) and diabetic (Diab) mice are displayed, scale bar: 20um. **B.** Quantification of cells with nuclear NF- $\kappa$ B expression in skeletal muscle (myocyte), cortical bone (osteocyte) and periosteum in uninjured femur of NG or Diab mice. **C.** Immunofluorescence of NF- $\kappa$ B (p65) in NG or Diab mice that received femoral fracture and healed for 3 days. Representative images are shown, scale bar: 20um. **D.** Quantification of cells with nuclear NF- $\kappa$ B expression in NG or Diab mice that healed for 3 days post-fracture (D3 fracture). cb: cortical bone, p: periosteum. Data are represented as mean  $\pm$  SD. \* $p < 0.05$  comparing NG to Diab groups, NS: not significant, two-tailed t-test. N = 6 mice each group.

## 2.5 NF- $\kappa$ B inhibition in SSCs prevents diabetes-mediated inflammation

I next tested the hypothesis that aberrant NF- $\kappa$ B activation in SSCs is responsible for diabetes-dysregulated inflammation during the early response to fracture healing. I used mice with conditional NF- $\kappa$ B inhibition in SSCs using experimental *Prx1<sup>Cre+</sup>Ikk $\beta$ <sup>fl/fl</sup>* mice through deletion of floxed *Ikk $\beta$* , an NF- $\kappa$ B activator (Li et al., 2003). *Ikk $\beta$*  deletion had little to no effect on basal long bone formation, trabeculation, cortical bone area, and weight (Fig. 2.4A-E). *Prx1<sup>+</sup>* SSCs expanded rapidly in the periosteal region 3-days after fracture (Fig. 2.5A). During this period, there was substantial NF- $\kappa$ B activation as shown by its nuclear localization in the periosteal and bone marrow SSCs in diabetic wildtype mice, which was accompanied by significantly elevated levels of inflammatory cytokines *Tnf*, *Il1 $\beta$*  and *Ifn $\gamma$* , and reduced levels of anti-inflammatory cytokine *Tgfb $\beta$ 1* (Fig. 2.5B-D). The increase in *Tnf*, *Il1 $\beta$*  and *Ifn $\gamma$*  caused by diabetes was completely rescued by inhibition of NF- $\kappa$ B in SSCs alone, and the suppression of *Tgfb $\beta$ 1* was reversed (Fig. 2.5B-D). Furthermore, the number of TNF<sup>+</sup> inflammatory cells that was elevated in diabetic wounds returned to normal levels when NF- $\kappa$ B was blocked in SSCs (Fig. 2.5E). A complete reversal of aberrant inflammation by inhibiting NF- $\kappa$ B activation in SSCs suggests a

pathologic role of NF- $\kappa$ B during diabetic healing. Moreover, inhibition of NF- $\kappa$ B in SSCs had little effect in normoglycemic wounds (Fig. 2.5D, E), indicating that there is an aspect to diabetes that induces NF- $\kappa$ B dysregulation that is not present in normoglycemic animals.

I next determined if high glucose could induce NF- $\kappa$ B dysregulation in SSCs by examining bone marrow SSCs (BMSSCs), a heterogeneous population of endosteal and stromal cells that represent a subset of SSCs. High glucose significantly increased NF- $\kappa$ B activation in BMSSCs, elevated mRNA levels of *Tnf* and *Il1 $\beta$* , and greatly reduced *Tgfb1* mRNA levels (Fig. 2.6A, B). High glucose-induced changes were blocked in BMSSCs from experimental mice (Fig. 2.6A, B), consistent with results seen in diabetic animals *in vivo*. In control experiments, BMSSCs isolated from *Prx1<sup>Cre+</sup>Ikk $\beta$ <sup>fl/fl</sup>* mice had reduced IKK $\beta$  protein and mRNA expression when compared to BMSSCs from control mice (Fig. 2.6C, D).

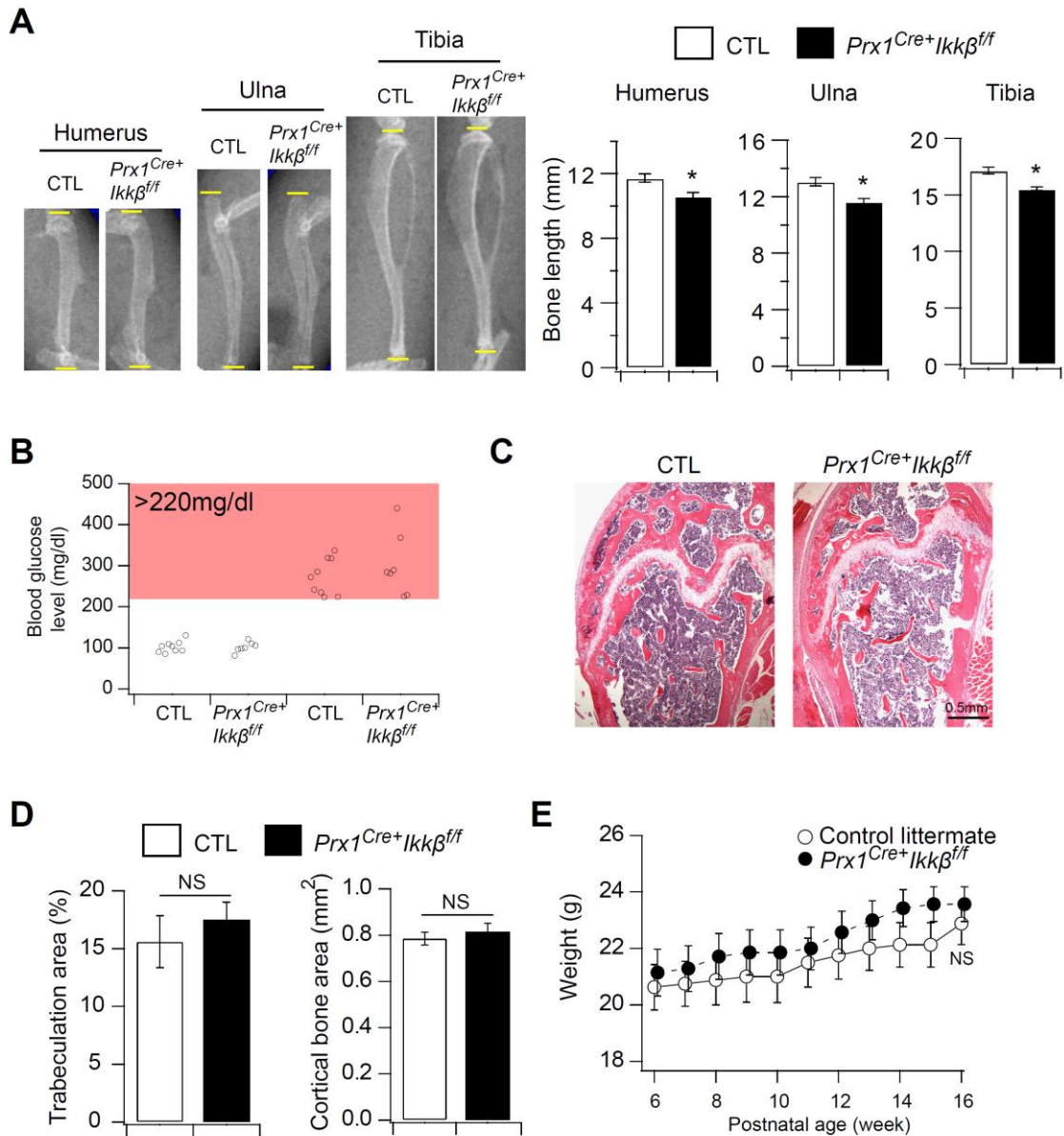


**Figure 2.4. Effect of NF- $\kappa$ B inhibition in *Prx1*<sup>+</sup> SSCs on development and STZ-induced hyperglycemia.** **A.** Radiographic assessment of the long bone lengths in 16 weeks old mice. Humerus, ulna, and tibia were placed perpendicular to the path of radiographic beam to generate images showing sagittal view of the long bones. There was a minimal decrease in the lengths of the humerus (10%), ulna (9%), and tibia (10%) of the experimental groups compared to control littermates. *n* = 4-5 animals each. **B.** Blood glucose level in control and experimental groups after buffer or STZ injection. Both control and experimental mice achieved diabetic status after STZ injection. *n* = 7-9 animals each. **C.** H&E staining of the femoral metaphysis in control and experimental mice. **D.** Quantification of

metaphyseal trabeculation and cortical bone area from control and experimental mice. There was no statistical difference in these parameters between the groups, n = 5 animals each. **E.** Weight changes in control and experimental mice. There was no statistically different weight changes. n = 10 animals each. \*p < 0.05, two-tailed t-test. NS: not significant. All data show mean +/- SD.

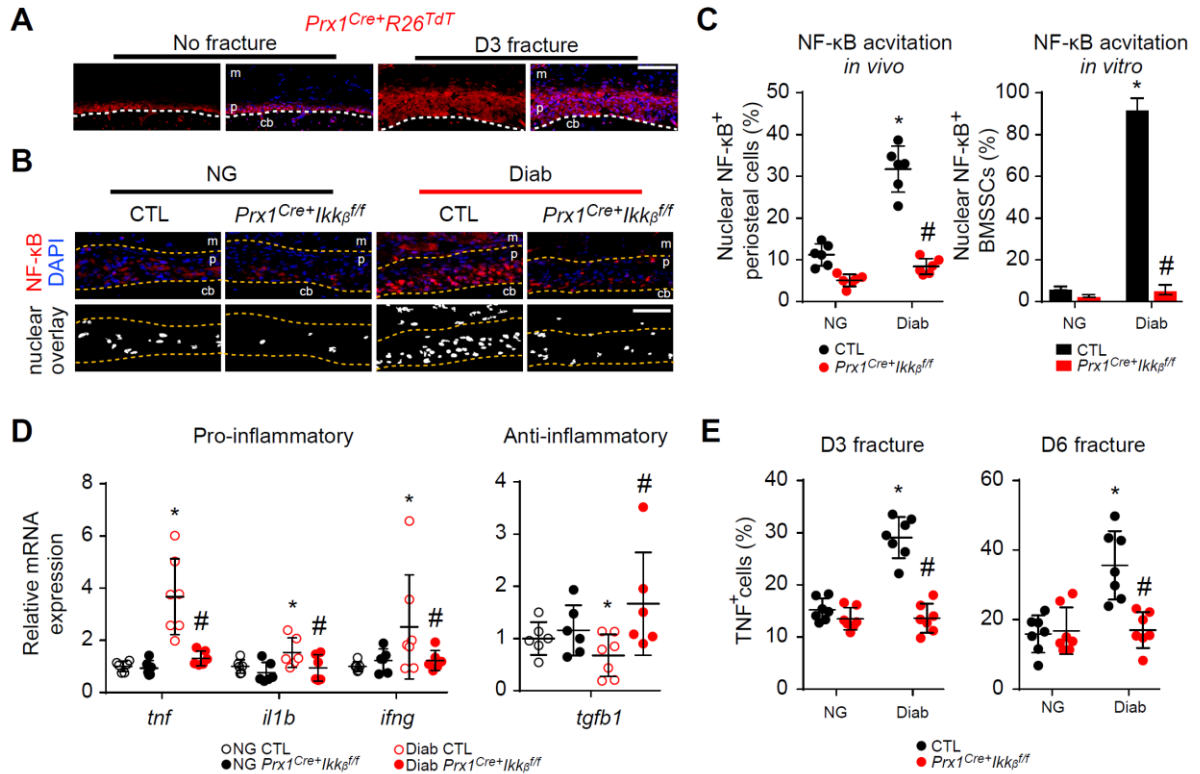


**Figure 2.5. NF-κB inhibition in SSCs prevents diabetes-mediated inflammation.** **A.** Lineage tracing in *Prx1<sup>Cre+</sup>R26<sup>TdtTomato</sup>* mice. Representative images of periosteum in unfractured femur and 3-day fracture. m = muscle, p = periosteum, cb = cortical bone. Scale bar, 100um. **B.** Nuclear NF-κB expression by immunofluorescence in periosteum of 3-day fracture from normoglycemic (NG) or diabetic (Diab) control (CTL, *Prx1<sup>Cre+</sup>Ikkβ<sup>fl/fl</sup>*) and experimental (*Prx1<sup>Cre+</sup>Ikkβ<sup>fl/fl</sup>*) mice. Nuclear NF-κB expression is identified through its overlap with DAPI expression (nuclear overlay). Scale bar, 50um. **C.** Quantification of periosteal (left) and bone marrow derived (right) SSCs with nuclear NF-κB expression, per total nucleated cells. **D.** mRNA expression of *Tnf*, *Il1b*, *Ifng*, and *Tgfb1* from day 3 fractures, as determined by RT-qPCR. **E.** TNF<sup>+</sup> immunopositive cells were counted and quantified by percent of total nucleated cells in day 3 and 6 fractures. Data are represented as mean ± SD, \*p<0.05 comparing NG CTL to Diab CTL



groups, #p<0.05 comparing Diab CTL to Diab experimental groups; two-way ANOVA with Tukey's post-hoc test for multi-group comparisons. N = 6-7 each group.

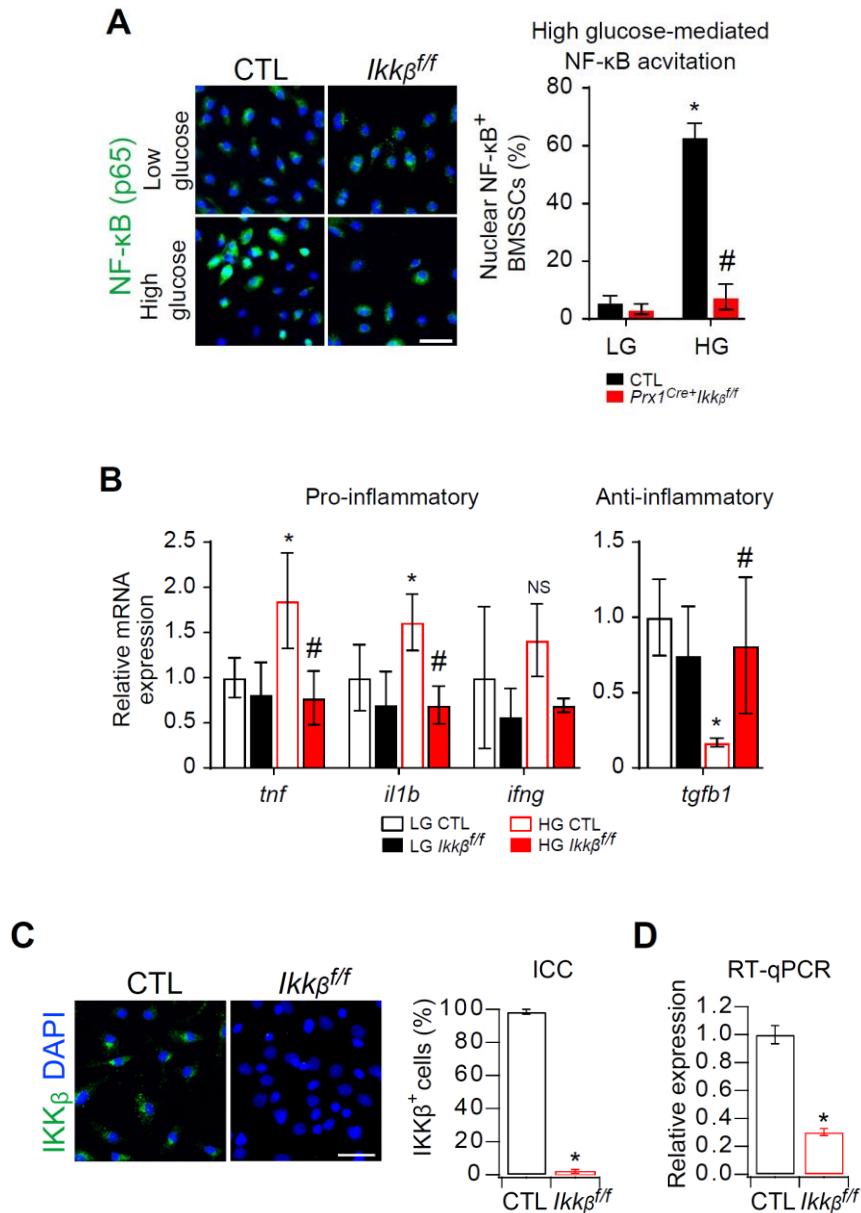


**Figure 2.6. NF-κB inhibition in BMSSCs prevents high glucose-mediated inflammation. A.** ICC with NF-κB antibody in BMSSC cultures incubated under low (4.5mM, LG) or high glucose (25mM, HG) condition. Cells immunopositive for nuclear NF-κB were quantified as percent of total cells. Scale bar, 20um. **B.** mRNA expression of *Tnf*, *Il1b*, *Ifng*, and *Tgfb1* cytokines in BMSSCs isolated from CTL or experimental mice, as determined by RT-qPCR. **C.** Representative images of ICC with IKKβ antibody in



BMSSCs isolated from control (CTL) or experimental (*Ikkβ<sup>ff</sup>*) mice. Quantification of IKKβ immunopositive cells per total nucleated cells. Scale bar, 20um. **D.** mRNA expression of *Ikkβ* from control or experimental BMSSCs as determined by RT-qPCR. Data are represented as mean ± SD. \*p<0.05 comparing NG CTL to HG CTL groups, #p<0.05 comparing HG CTL to HG experimental groups; two-way ANOVA with Tukey's post-hoc test for multi-group comparisons (B) or t-test (A, C, D). N = three independent experiments from 3 mice.

## 2.6 NF-κB inhibition in SSCs, not chondrocytes, restores cartilage formation

To determine whether NF-κB activation in SSCs had an impact on subsequent healing events, I examined callus size and production of cartilage matrix. Diabetic mice had significantly reduced callus size and cartilage production by 39% and 58%, respectively (Fig. 2.7A, B). NF-κB inhibition in SSCs completely rescued the production of callus and cartilage in diabetic fractures (Fig. 2.7B). Of note, lineage tracing of *Prx1<sup>+</sup>* SSCs showed labelled SSCs near injury site in day-3 fractures but also labelled chondrocytes that derived from SSCs by day-6 (Fig 2.8A, B), raising a possibility that genetic perturbation in chondrocytes may contribute to the rescued phenotype. To test if chondrocyte-specific NF-κB inhibition reversed the effects of diabetes, I generated *Col2α1<sup>Cre+</sup>Ikkβ<sup>ff</sup>* mice (Ovchinnikov et al., 2000). NF-κB inhibition in chondrocytes failed to rescue the negative effect of diabetes on callus and cartilage formation (Fig. 2.7C, D), ruling out chondrocytes as a potential rescue source. Lastly, I asked whether post-natal SSCs are responsible for preventing the impact of diabetes by generating mice with tamoxifen-inducible NF-κB inhibition (*Prx1<sup>CreER+</sup>Ikkβ<sup>ff</sup>*). I first confirmed through lineage tracing in *Prx1<sup>CreER+</sup>R26<sup>TdTomato</sup>* mice that post-natal SSCs are labelled by day-3 and expand rapidly throughout day-6 post-fracture (Fig. 2.7E). Similar to results with constitutive NF-κB inhibition, conditional tamoxifen-induced NF-κB inhibition in SSCs reversed the

reduction in cartilage formation caused by diabetes (Fig. 2.7F, G). Thus, by both constitutive and induced blockage of NF- $\kappa$ B activation, I demonstrated that SSCs but not chondrocytes are critical in rescuing the impact of diabetes on the early events of fracture repair.

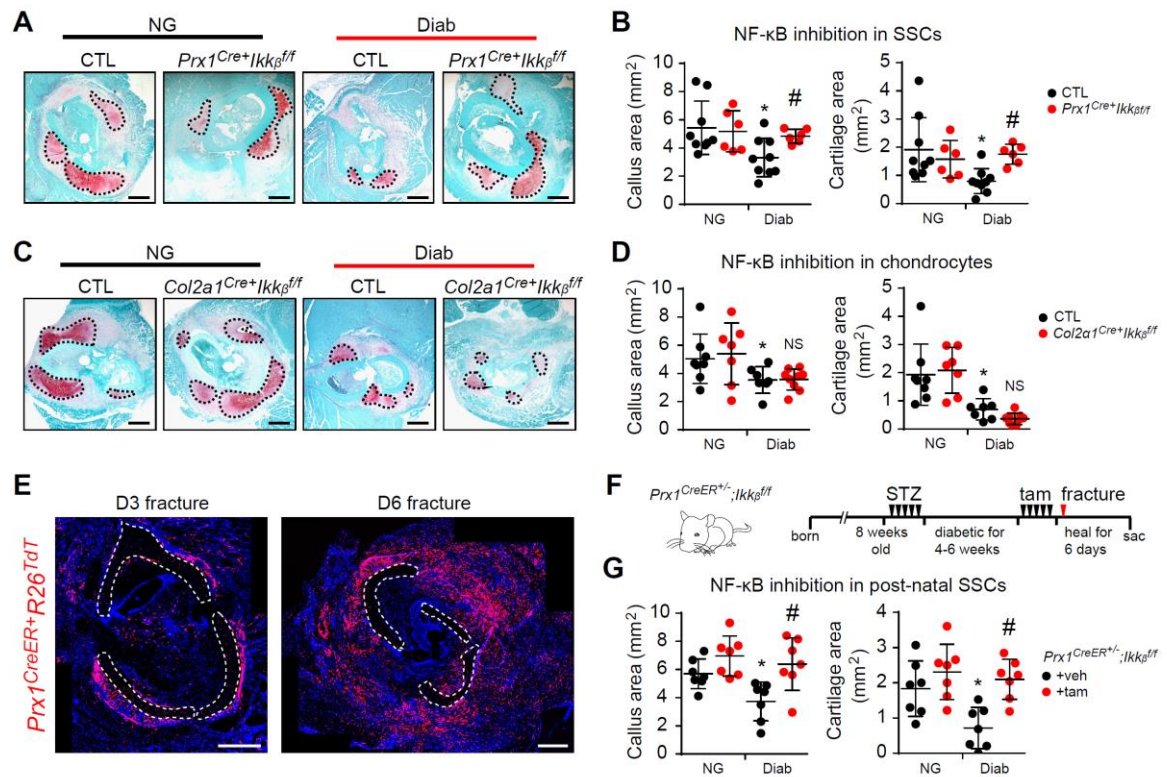


**Figure 2.7. NF- $\kappa$ B inhibition in SSCs but not chondrocytes restores cartilage formation.** **A.** Safranin-O and fast green staining in day 6 fractures of normoglycemic (NG) or diabetic (Diab) control (CTL, *Prx1Cre<sup>+</sup>Ikkβ<sup>ff</sup>*) and experimental (*Prx1Cre<sup>+</sup>Ikkβ<sup>ff</sup>*) mice. Representative images are shown; scale bar: 0.5mm. **B.** Histomorphometric analysis of callus area (left) and cartilage formation (right) in NG or Diab CTL and experimental mice with NF- $\kappa$ B inhibition in SSCs. **C.** Safranin-O and fast green staining in day 6 fractures of NG or Diab CTL (*Col2a1Cre<sup>+</sup>Ikkβ<sup>ff</sup>*) and experimental (*Col2a1Cre<sup>+</sup>Ikkβ<sup>ff</sup>*) mice. Representative images are shown; scale bar: 0.5mm. **D.** Quantification of callus area (left) and cartilage formation (right) in NG or Diab CTL and experimental mice with NF- $\kappa$ B inhibition in chondrocytes. **E.** Lineage tracing in *Prx1CreER<sup>+</sup>R26<sup>TdTomato</sup>* mice that healed for 3 (left) or 6 days (right) post fracture. Representative stitched images are shown, scale bar: 0.5mm. **F.** Schematic diagram of experimental

approach for NF- $\kappa$ B inhibition in postnatal SSCs. **G.** Callus and cartilage area quantification in day 6 fractures of *Prx1CreER<sup>+/-</sup>Ikk $\beta$ <sup>fl/fl</sup>* NG or Diab mice with corn oil (+veh) or tamoxifen (+tam) administration. Data are represented as mean  $\pm$  SD. \* $p$ <0.05 comparing NG CTL to Diab CTL groups, # $p$ <0.05 comparing Diab CTL to Diab experimental groups, NS: not significant; Two-way ANOVA with Tukey's post-hoc test. N = 6-9 each group.

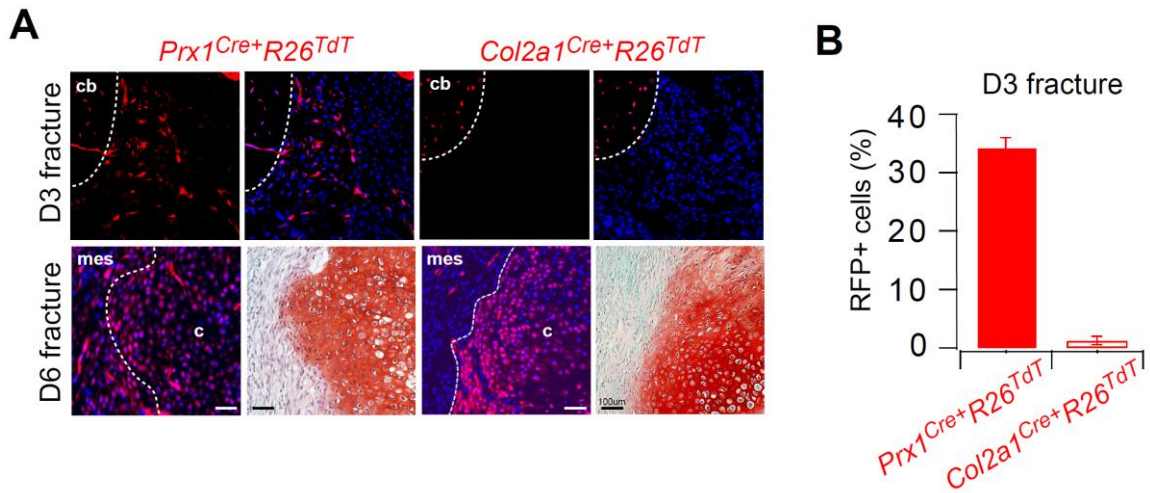


**Figure 2.8. Lineage tracing in *Prx1Cre<sup>+</sup>R26<sup>TdT</sup>* and *Col2a1Cre<sup>+</sup>R26<sup>TdT</sup>* mice during fracture healing.**

**A.** Representative images of 3- and 6-day fracture specimens from *Prx1Cre<sup>+</sup>R26<sup>TdT</sup>* and *Col2a1Cre<sup>+</sup>R26<sup>TdT</sup>* mice. cb: cortical bone, c: cartilage, mes: mesenchymal tissue. Serial section stained with safranin O and fast green was used to identify the cartilage-mesenchymal tissue border. Scale bar: 100 $\mu$ m. **B.** Quantification of red fluorescent protein (RFP) positive cells per total nucleated cells in day 3 fractures near the injury site. *Prx1Cre<sup>+</sup>R26<sup>TdT</sup>* mice had approximately ~30% labeled cells whereas *Col2a1Cre<sup>+</sup>R26<sup>TdT</sup>* mice did not show positive cells.

## 2.7 Diabetes reduces SSCs by altering apoptosis and proliferation through NF- $\kappa$ B

To examine a downstream effect of dysregulated NF- $\kappa$ B activation in SSCs, I assessed its impact on SSC numbers quantified by immunofluorescence with antibodies specific to SSC markers, CD271 and Sca1 (Alvarez et al., 2015; Xiao et al., 2013). Diabetes caused a large decrease in CD271<sup>+</sup> SSCs on day-3 and -6 fractures compared to normoglycemic mice, and this loss was prevented by NF- $\kappa$ B inhibition (Fig. 2.9A, B).

Similar results were obtained for Sca1<sup>+</sup> SSCs (Fig. 2.9A, C). Further experiments demonstrated that diabetes-induced loss of SSCs was also blocked by conditional NF- $\kappa$ B inhibition in post-natal SSCs (Fig. 2.9D). In control experiments, I determined that CD271 and Sca1 co-localized with red fluorescent protein produced by *Prx1*<sup>Cre+</sup>*R26*<sup>TdTomato</sup> reporter mice, consistent Prx1 lineage-specific expression in SSCs (Duchamp de Lageneste et al., 2018), whereas SSCs did not express CD45, a hematopoietic cell marker (Fig 2.10A-C).

The above results demonstrate that diabetes caused the loss of SSCs and linked this decrease to aberrant NF- $\kappa$ B activation in SSCs. I next examined potential mechanisms by examining the impact of NF- $\kappa$ B dysregulation on SSC apoptosis and proliferation. SSC apoptosis was assessed by counting double positive CD271<sup>+</sup>TUNEL<sup>+</sup> cells in the healing fractures. Diabetes led to a substantial 86% increase in SSC apoptosis, which was completely blocked by NF- $\kappa$ B inhibition in SSCs (Fig. 2.11A). Mechanistically, this was linked to the effect of high glucose, which mimicked diabetes-induced increase in BMSSC apoptosis *in vitro* that was reversed by NF- $\kappa$ B inhibition (Fig. 2.11B). Diabetes *in vivo* and high glucose *in vitro* also reduced SSC proliferation that was rescued by inhibition of NF- $\kappa$ B, although the magnitude of the effect was less than that of apoptosis (Fig. 2.11C-D). To further establish how high glucose modulated SSC apoptosis and proliferation, I examined downstream gene expression. High glucose led to increased expression of apoptotic genes (*casp3* and *casp8*) and cell cycle arrest genes (*p21* and *p27*), which was blocked in BMSSCs that were derived from experimental mice that had lineage-specific NF- $\kappa$ B inhibition (Fig. 2.11E). Thus, diabetes caused a loss of SSCs due to increased apoptosis

and to a lesser effect, reduced proliferation, both of which are mediated by aberrant NF- $\kappa$ B activation that can be induced by high glucose levels.

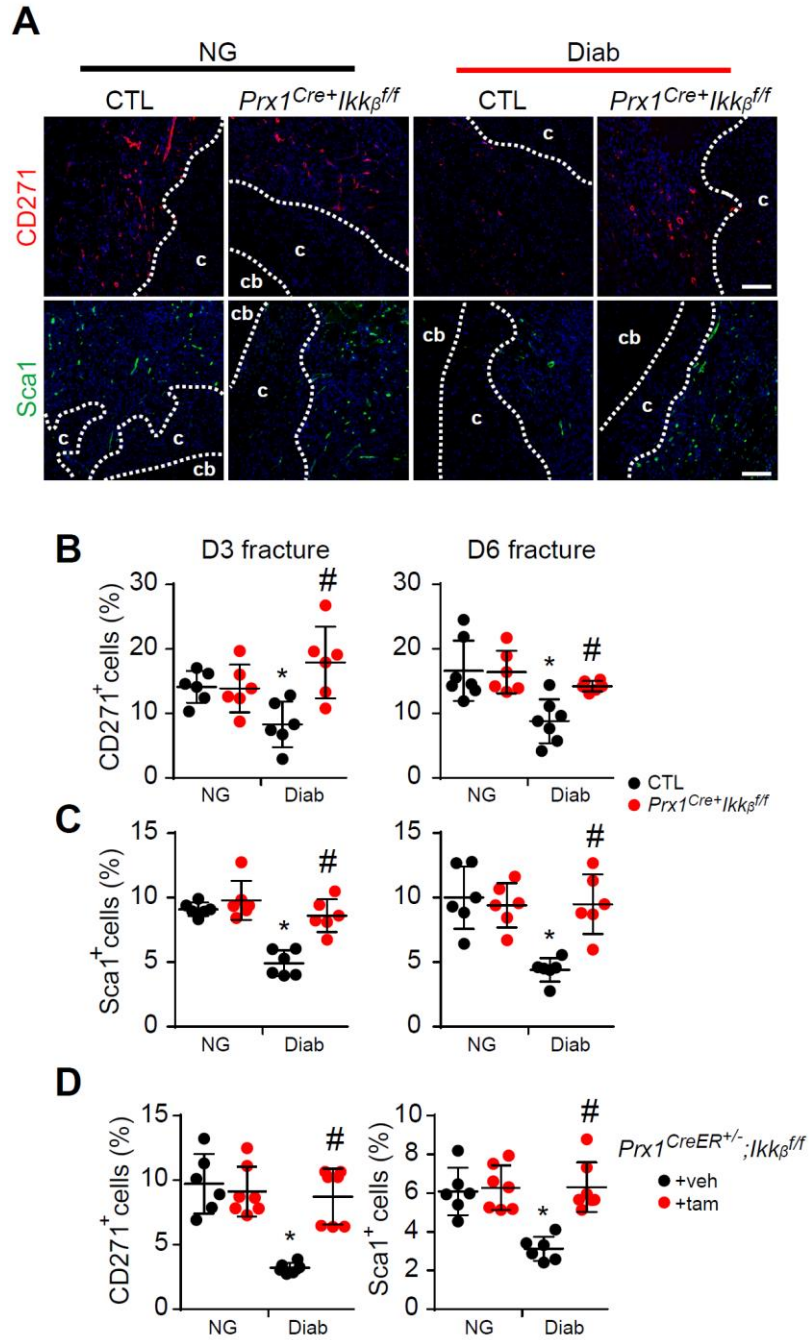


**Figure 2.9. Diabetes reduces SSC numbers through NF- $\kappa$ B.** **A.** Immunofluorescence of CD271 (top panels) and Sca1 (bottom panels) in normoglycemic (NG) or diabetic (Diab) control (CTL) and experimental (*Prx1<sup>Cre+</sup>Ikk $\beta$ <sup>ff</sup>*) mice. Representative images are shown; scale bar: 100 $\mu$ m. cb: cortical

bone, c: cartilage. **B, C.** Quantification of CD271 (**b**) and Sca1 (**c**) immunopositive cells per total nucleated cells in NG or Diab CTL and *Prx1Cre<sup>+</sup>Ikkβ<sup>fl/fl</sup>* mice. Data from day 3 (left) and day 6 (right) fractures are shown. **D.** Quantification of CD271 and Sca1 immunopositive cells in *Prx1CreER<sup>+/+</sup>Ikkβ<sup>fl/fl</sup>* NG or Diab mice with corn oil (+veh) or tamoxifen (+tam) administration. Data are represented as mean  $\pm$  SD. \* $p < 0.05$  comparing NG CTL to Diab CTL groups, # $p < 0.05$  comparing Diab CTL to Diab experimental groups; two-way ANOVA with Tukey's post-hoc test for multi-group comparisons. N = 6-7 mice each group.

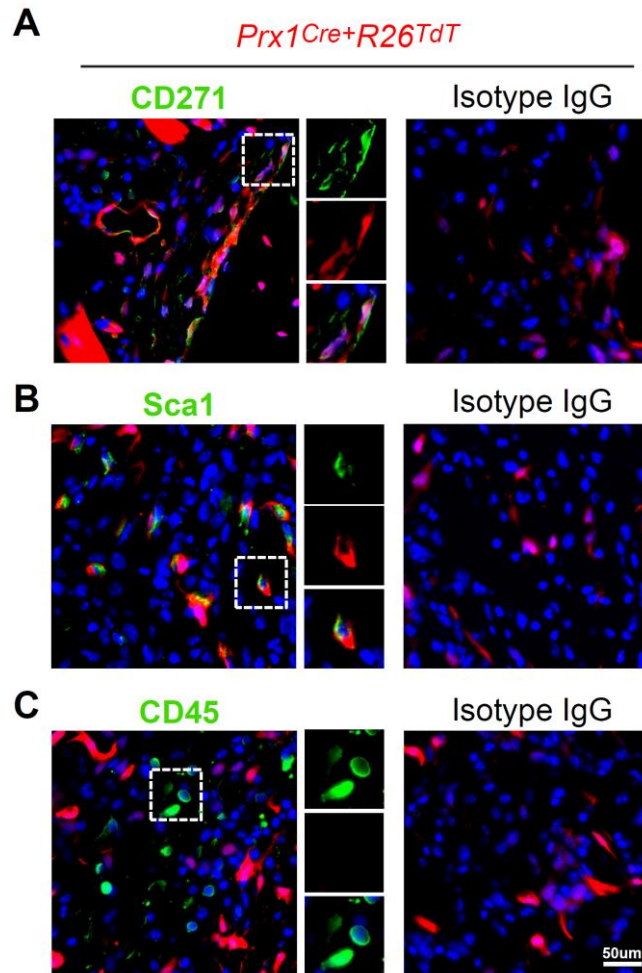


**Figure 2.10. CD271 and Sca1 labels Prx1+ cells in healing fractures.** A-C. Representative images from immunofluorescence experiments with CD271 (A), Sca1 (B) or CD45 (C) antibody in *Prx1Cre<sup>+</sup>R26<sup>TdT</sup>* reporter mice. Co-localization was observed for CD271 and Sca1 with Prx1 cells, whereas CD45, a marker for hematopoietic cells, did not co-localize with Prx1+ cells. Isotype IgG controls



were used for all experiments, which showed negative staining. Experiments were performed on 3 mice with similar results. Scale bar, 50um.

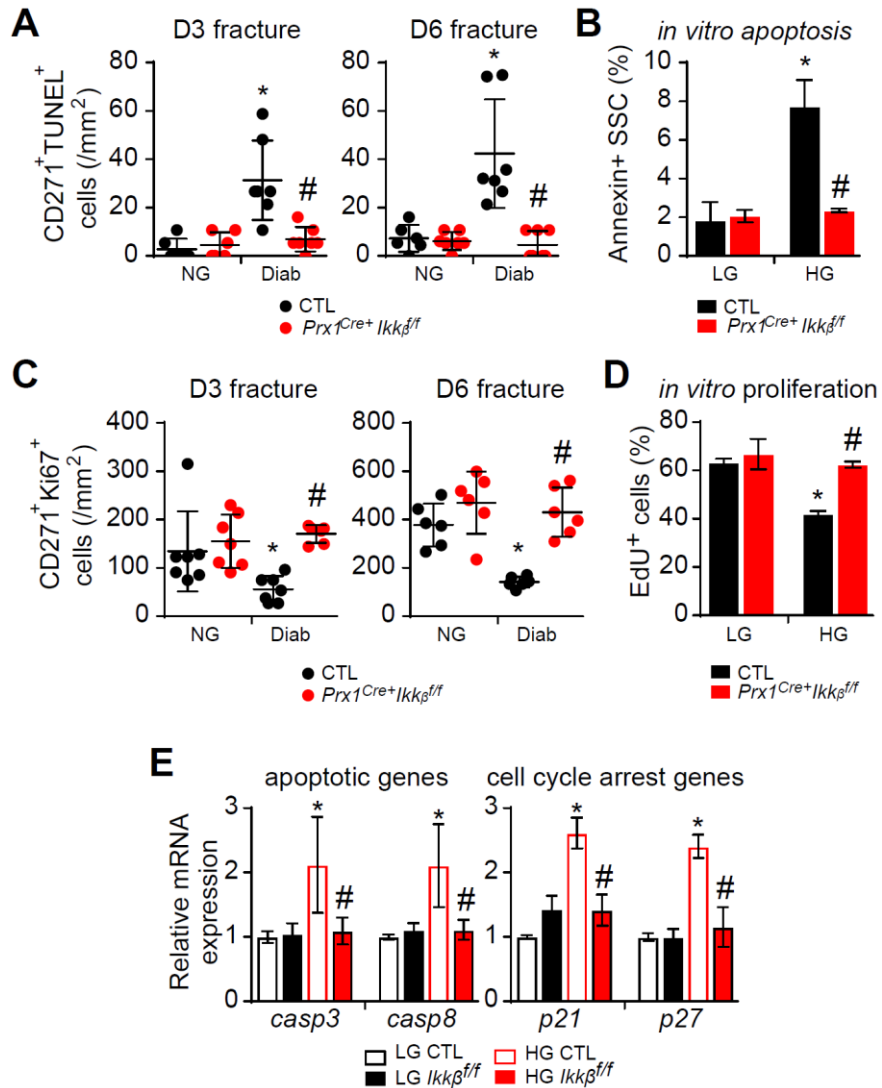


**Figure 2.11. Diabetes and high glucose promote apoptosis and inhibits proliferation through NF-**

**kB. A.** Immunofluorescence of CD271 and TUNEL to count double-positive cells (apoptotic SSCs) in day 3 and 6 fractures of NG or Diab CTL and *Prx1*<sup>Cre+</sup>*Ikkβ*<sup>ff</sup> mice. **B.** Control or experimental BMSSCs were isolated and incubated in low (4.5mM, LG) or high glucose (25mM, HG) for 5 days under low-serum condition, followed by ICC with annexin to detect apoptotic BMSSCs *in vitro*. Quantification of annexin<sup>+</sup> cells per total nucleated cells. **C.** Immunofluorescence of CD271 and Ki67 to count proliferative SSCs as CD271<sup>+</sup>Ki67<sup>+</sup> cells. Quantification of double positive cells in day 3 and 6 fractures of NG or Diab CTL and *Prx1*<sup>Cre+</sup>*Ikkβ*<sup>ff</sup> mice. **D.** Serum-induced proliferation of control or experimental BMSSCs

after LG or HG incubation for 5 days, quantified by EdU incorporation. EdU+ cells per total nucleated cells were quantified by ICC *in vitro*. **E.** mRNA expression of apoptotic genes (*casp3* and *casp8*) and cell cycle arrest genes (*p21* and *p27*) in control and experimental BMSSCs incubated under LG or HG condition, as determined by RT-qPCR. Data are represented as mean  $\pm$  SD. \* $p < 0.05$  comparing NG CTL to Diab CTL groups, # $p < 0.05$  comparing Diab CTL to Diab experimental groups; two-way ANOVA with Tukey's post-hoc test for multi-group comparisons. N = 6-7 mice each group (A, C); three independent experiments from 3 mice (B, D, E).

## **2.8 SSCs modulate M1/M2 polarization through TGF- $\beta$ 1 during fracture healing, which is impaired in diabetes by NF- $\kappa$ B activation**

I next examined how SSCs limit inflammation during healing by examining a downstream cellular event. Given the relatively high number of macrophages (Fig. 2.12A, B), I postulated that SSCs promote resolution of inflammation by inducing M2 polarization and that diabetes interferes with the capacity of SSCs to regulate polarization due to altered NF- $\kappa$ B regulation. Immunofluorescence was carried out to quantify pro-inflammatory M1 as F4/80<sup>+</sup>iNOS<sup>+</sup> cells and pro-resolving M2 as F4/80<sup>+</sup>CD163<sup>+</sup> cells (Edin et al., 2012). Diabetic fractures had a significantly higher M1 count compared to normoglycemic fractures, whereas M2 numbers were drastically reduced (Fig. 2.13A, B). Surprisingly, the low level of M2 macrophages and high level of M1 macrophages caused by diabetes was completely rescued by lineage-specific NF- $\kappa$ B inhibition in SSCs. Thus, through NF- $\kappa$ B activation in SSCs, diabetes causes an imbalance in the M1/M2 macrophage ratio that is pro-inflammatory.

To identify a mechanism through which NF- $\kappa$ B in SSCs affects macrophage polarization, I examined expression of TGF $\beta$ 1, a cytokine known to modulate M1/M2 balance (Gong et al., 2012; Zhang et al., 2016). Prx1<sup>+</sup> SSCs expressed TGF $\beta$ 1 during early



fracture healing in normoglycemic mice (Fig. 2.14A). Diabetes largely decreased TGF $\beta$ 1 expression, which was reversed *in vivo* by lineage-specific NF- $\kappa$ B inhibition (Fig. 2.14B). Incubating BMSSCs in high glucose closely reproduced the effect of diabetes on reducing TGF $\beta$ 1 protein levels *in vitro* (Fig. 2.14C). The loss of TGF $\beta$ 1 was directly linked to NF- $\kappa$ B, as high glucose-inhibited TGF $\beta$ 1 expression was blocked in BMSSCs obtained from experimental mice with *Ikk $\beta$*  deletion. To test this further, I incubated BMMs with conditioned medium from BMSSC cultures (BMSSC-CM) and low-dose LPS or IL4 to avoid saturation of M1 and M2 responses, respectively. Under standard conditions, BMSSC-CM had little effect on M1 but stimulated high levels of M2 polarization (Fig. 2.15A, B). M1 polarization was significantly increased by conditioned medium from BMSSCs incubated with high glucose, whereas M2 polarization was inhibited (Fig. 2.15A, B). Blocking NF- $\kappa$ B activation in BMSSCs rescued the effect of high glucose on BMSSC-induced macrophage polarization. TGF $\beta$ 1 neutralizing antibody prevented BMSSC-CM from upregulating M2 polarization under standard conditions (Fig. 2.15C) and prevented M2 polarization induced by BMSSC-CM from experimental BMSSCs in high glucose. These experiments demonstrate that TGF $\beta$ 1 is a key mediator expressed by SSCs to modulate M2 polarization and that the inability of SSCs to induce M2 polarization through TGF $\beta$ 1 in high glucose is due to NF- $\kappa$ B activation.

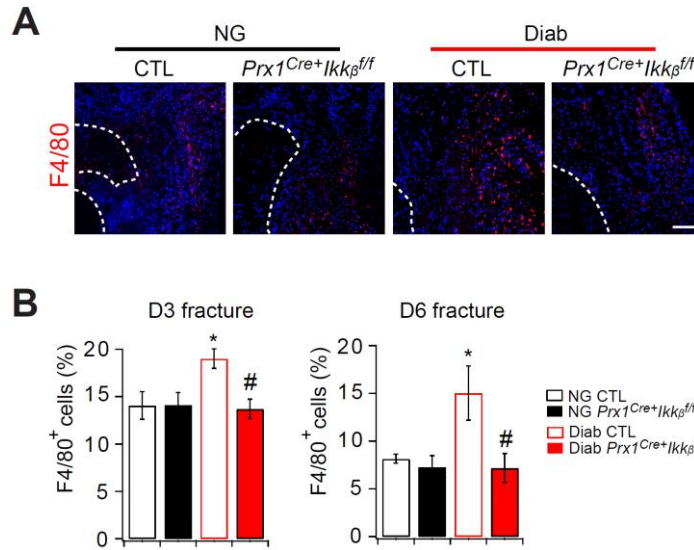


**Figure 2.12. Diabetes increases macrophage infiltration to the fracture site that is blocked with NF-κB inhibition in SSCs. A.** Representative immunofluorescent images of F4/80<sup>+</sup> macrophages in day 3 fractures of normoglycemic (NG) or diabetic (Diab) control or *Prx1Cre<sup>+</sup>Ikkβ<sup>ff</sup>* mice. Scale bar, 200um. Dashed line demarcates cortical bone. **B.** Quantification of F4/80<sup>+</sup> macrophage percent in day 3 and day 6 fractures of NG or Diab CTL and experimental mice, n = 6 each. \*,#p<0.05 by two-way ANOVA followed by Tukey's post-hoc test.

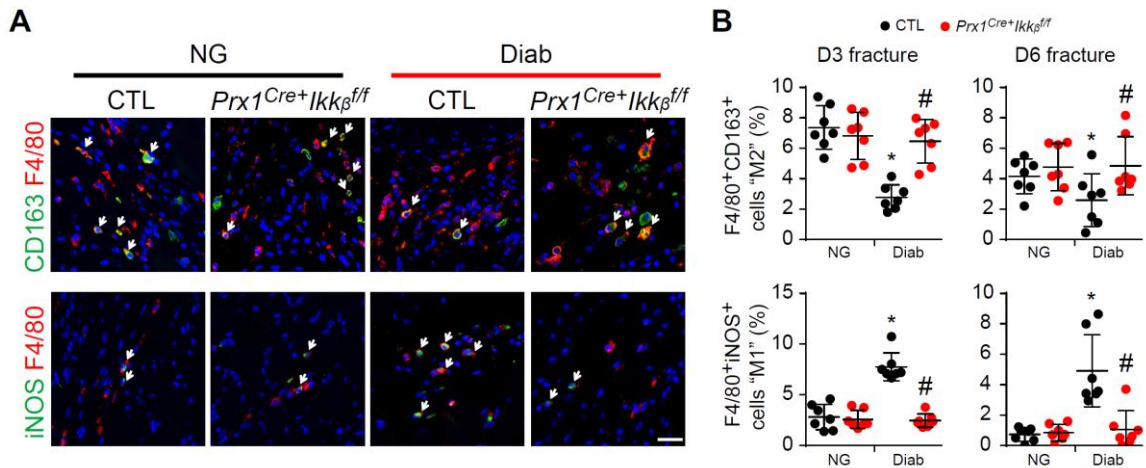


**Figure 2.13. Diabetes reduces M2 and enhances M1 in a NF-κB dependent manner. A.** Double immunofluorescence to detect M2 (F4/80<sup>+</sup>CD163<sup>+</sup>) and M1 (F4/80<sup>+</sup>iNOS<sup>+</sup>) macrophages in NG and Diab control (*Prx1Cre-Ikkβ<sup>ff</sup>*) or experimental (*Prx1Cre<sup>+</sup>Ikkβ<sup>ff</sup>*) mice. Representative images show arrows pointing to M2 in day 3 fractures and M1 in day 6 fractures. Scale bar, 50um. **B.** Quantification of M2

and M1 immunopositive cells per total nucleated cells in day 3 and day 6 fractures, as determined by immunofluorescence. Data are represented as mean  $\pm$  SD. \* $p$ <0.05 comparing NG CTL to Diab CTL, # $p$ <0.05 comparing Diab CTL to Diab experimental mice; two-way ANOVA with Tukey's post-hoc test. N = 6-7 each group.

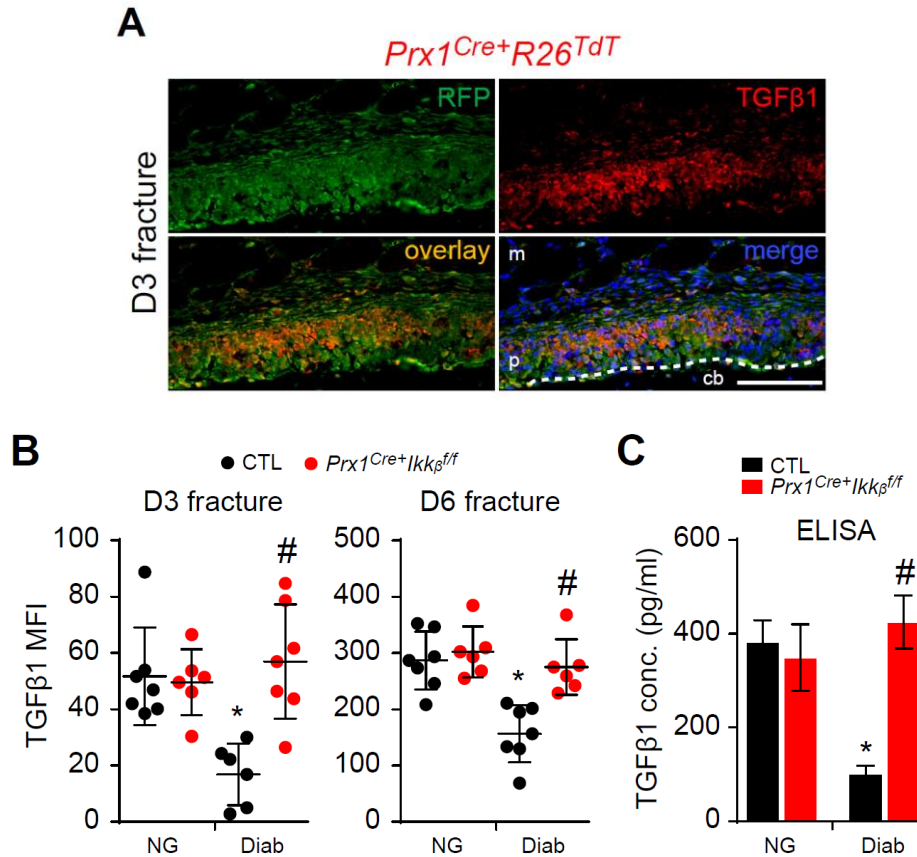


**Figure 2.14. *Prx1*<sup>+</sup> SSCs express TGFβ1 which is reduced by diabetes-mediated NF-κB. A.** Immunofluorescence with RFP (detection with Alexa-488) and TGFβ1 (detection with Cy5) antibody in day 3 fracture periosteum from *Prx1<sup>Cre</sup>;R26<sup>TdTomato</sup>* mice. Scale bar, 100um. **B.** TGFβ1 expression as determined by immunofluorescence with TGFβ1 antibody in day 3 and day 6 fracture of NG or Diab control or experimental mice. Data are expressed as mean fluorescent intensity (MFI). **C.** TGFβ1 concentration in conditioned medium of BMSSCs from control or experimental mice, incubated in low (LG) or high glucose (HG) condition, as determined by ELISA. Data are represented as mean  $\pm$  SD. \* $p$ <0.05 comparing NG CTL to Diab CTL, # $p$ <0.05 comparing Diab CTL to Diab experimental mice; two-way ANOVA with Tukey's post-hoc test. N = 6-7 each group (B) and 3 biological replicates (C).

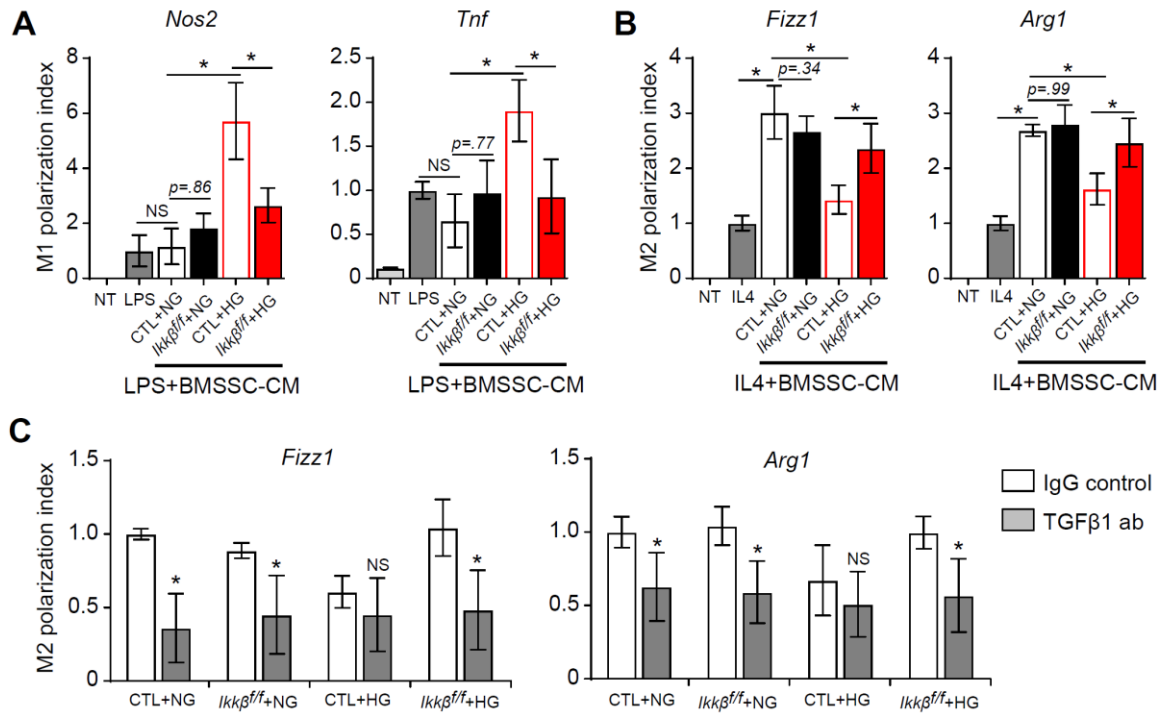


**Figure 2.15. SSCs modulate M1/M2 polarization through TGFβ1, which is impaired by NF-κB activation in high glucose.** **A.** M1 polarization index from bone marrow macrophages (BMMs) stimulated with LPS and BMSSC-CM from control or experimental BMSSCs with low (LG) or high glucose (HG) incubation, as determined by RT-qPCR for *Nos2* and *Tnf*. Data are normalized to LPS alone (10ng/ml). **B.** M2 polarization index from BMMs stimulated with IL-4 with or without BMSSC-CM, as determined by RT-qPCR for *Fizz1* and *Arg1*. Data are normalized to IL-4 alone (1.25ng/ml). **C.** M2 polarization index from BMMs incubated in BMSSC-CM with IL-4 plus TGFβ1 neutralizing antibody or control IgG, as determined by RT-qPCR for *Fizz1* and *Arg1*. Data are normalized to BMSSC-CM IgG control group. Data are represented as mean ± SD. \*p<0.05, one-way ANOVA with Tukey's post-hoc test. Student's t-test for (C). N = three independent experiments from 3 mice.

## 2.9 TGF-β1 treatment improves inflammation in diabetic fractures

Based on our results above, I speculated that exogenous delivery of TGFβ1 would compensate for the lack of its expression by SSCs and reverse overt inflammation in diabetic fractures. To test this, I administered recombinant TGFβ1 or vehicle in the fracture site of normoglycemic or diabetic mice, 24h post-injury to focus on resolution of

inflammation rather than the first inflammatory events (Fig. 2.16A). I found that TGF $\beta$ 1 administration led to a large reduction of TNF<sup>+</sup> cells in diabetic fractures (Fig 2.16B, C). Consistently, the number of M2 was rescued in diabetic mice that received TGF $\beta$ 1, returning to normal levels (Fig. 2.16D). Therefore, TGF $\beta$ 1 treatment substantially reversed diabetes-mediated dysregulation of M2 polarization and inflammation.

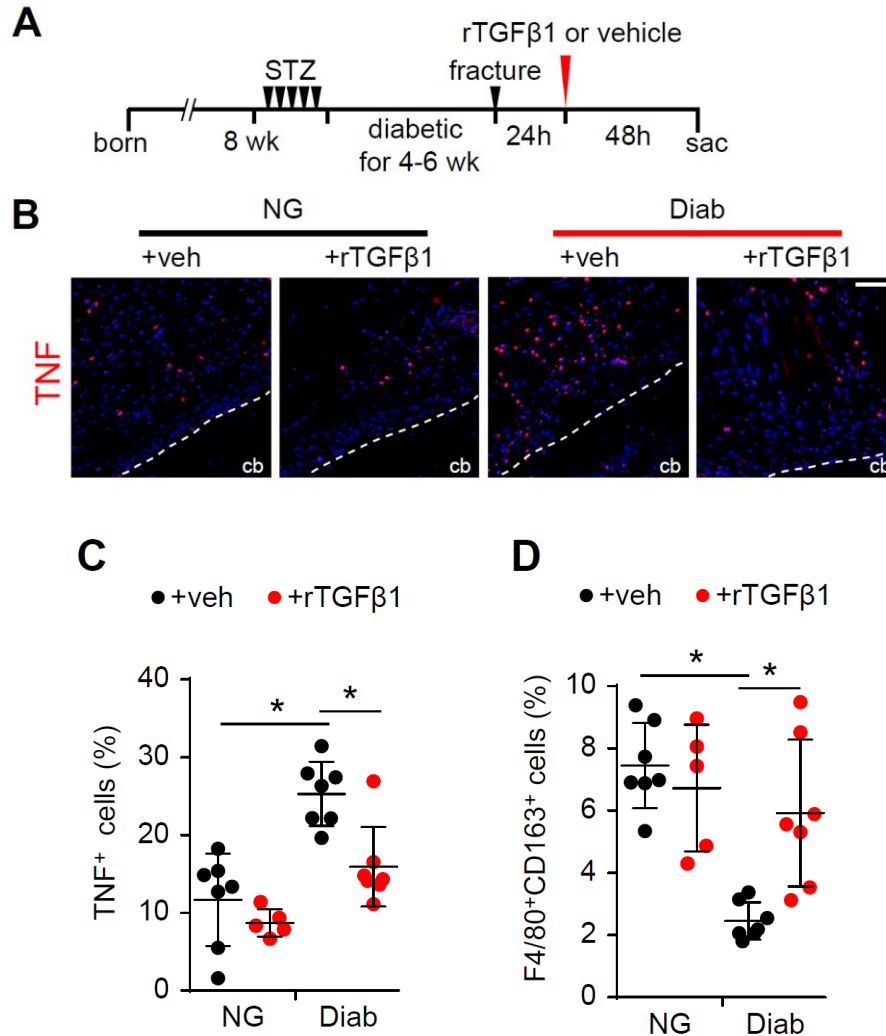


**Figure 2.16. TGF $\beta$ 1 treatment improves inflammation in diabetic fractures.** **A.** Experimental approach for TGF $\beta$ 1 treatment. **B.** Immunofluorescence with TNF antibody in normoglycemic (NG) or diabetic (Diab) mice that received PBS only (+veh) or recombinant TGF $\beta$ 1 (+rTGF $\beta$ 1). Dashed line demarcates cortical bone (cb). Scale bar, 100 $\mu$ m. **C.** Quantification of TNF<sup>+</sup> cells per total nucleated cells

in day 3 fractures of NG or Diab mice that received PBS or recombinant TGF $\beta$ 1. **D.** Quantification of M2 (F4/80<sup>+</sup>CD163<sup>+</sup> immunopositive cells) per total nucleated cells in day 3 fractures. Data are represented as mean  $\pm$  SD. \*p<0.05; two-way ANOVA with Tukey's post-hoc test. N = 5-7 each group.

## 2.10 Discussion

The underlying cause for a failure to resolve elevated inflammation in diabetic wounds is poorly understood. Here I report that endogenous SSCs play a pivotal role in downregulating inflammation during the early healing process of osseous wounds and that diabetes interferes with this resolution specifically through aberrant NF- $\kappa$ B activation in SSCs. Specific ablation of SSCs in healing fractures led to persistent inflammation, suggesting a critical link between proper SSC expansion and resolution of inflammation. Surprisingly, diabetes affected fracture healing through a reduction of SSCs and enhanced inflammation, both of which were caused by hyperactivation of NF- $\kappa$ B. Lineage-specific inhibition of NF- $\kappa$ B in SSCs through *Ikk $\beta$*  deletion reversed diabetes-enhanced apoptosis and reduced proliferation of SSCs, thus preventing the loss of SSCs and restoring tissue regeneration. Aberrant NF- $\kappa$ B activation also impaired the ability of SSCs to express TGF $\beta$ 1 and induce the formation of M2 macrophages, which was rescued in experimental animals. In diabetic animals, macrophage polarization favored pro-inflammatory M1 over pro-resolving M2 polarization *in vivo*. The negative impact of diabetes was reversed by increasing TGF $\beta$ 1 either by restoring SSC-produced TGF $\beta$ 1 through inhibition of NF- $\kappa$ B or by administration of recombinant TGF $\beta$ 1. Taken together, our findings provide definitive evidence that diabetes leads to NF- $\kappa$ B dysregulation in endogenous SSCs, which is a central pathologic factor in disrupting the early repair process (Fig 2.17).

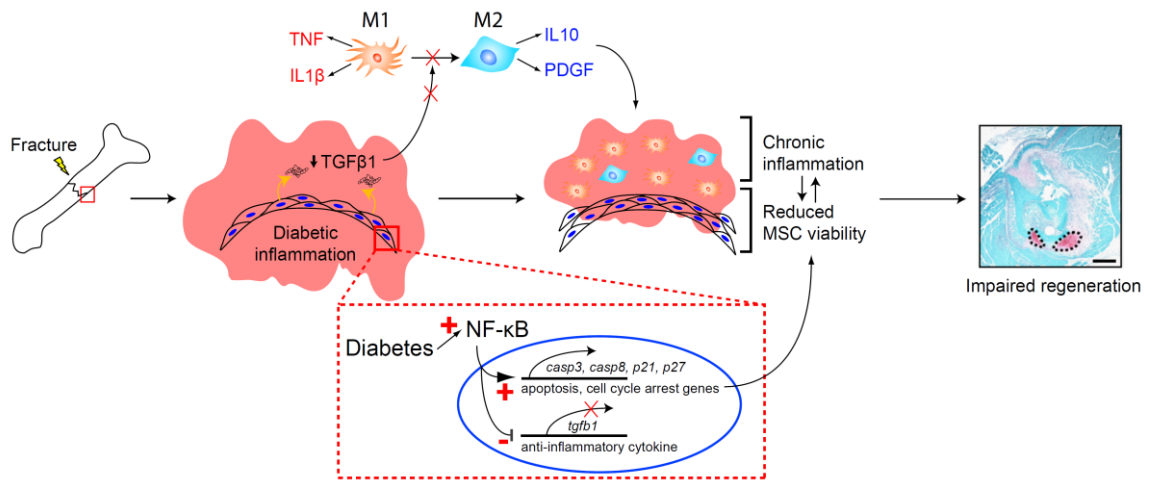


**Figure 2.17. Diabetes-induced NF-κB dysregulation in skeletal stem cells prevents resolution of inflammation.** Summary cartoon depicting the negative impact of NF-κB on pro-resolving and viability gene expression by the SSCs to negatively influence macrophage polarization and skeletal expansion to delay bone regeneration.

*In vivo* evidence demonstrating a role of SSCs on modulating inflammation has been limited because of relatively low abundance of SSCs under homeostatic conditions. Using fracture healing model where SSCs expand, and with genetic tools to selectively ablate them, I demonstrated that the loss of SSCs was a key factor that causes the failure to resolve inflammation indicated by the high TNF levels. Persistent TNF signalling is detrimental for proper tissue regeneration and homeostasis in most organs through its impact on stem cell proliferation (Baker et al., 2011; Palacios et al., 2010; Zhou et al., 2012). In particular, high levels of TNF is characteristic of diabetic fracture healing (Alblowi et al., 2009; Kayal et al., 2010; Tevlin et al., 2017), and specific inhibition of TNF can partly restore bone formation (Ko et al., 2015). Given the negative impact of unresolved TNF levels on stem cells, its dysregulation by impaired SSC function may

trigger a pathologic positive feedback loop to further compromise the expansion of SSCs, consequently attributing to delayed tissue regeneration.

I investigated a potential role of NF- $\kappa$ B during diabetic osseous healing and discovered that it had a detrimental effect on SSC expansion by promoting apoptosis and inhibiting proliferation. Although NF- $\kappa$ B typically has a direct anti-apoptotic effect (Hoesel and Schmid, 2013), it has been reported to promote apoptosis and inhibit proliferation under diabetic conditions (Kato et al., 2016; Tsai et al., 2012). This polarizing role of NF- $\kappa$ B may be explained by its diverse crosstalk with other signalling pathways (Oeckinghaus et al., 2011) and/or an epigenetic signature that is modified by persistent hyperglycemia (El-Osta et al., 2008). I also found that NF- $\kappa$ B dysregulation in SSCs interfered with resolution of inflammation in diabetic fractures, similar to that seen with selective SSC ablation. Thus, maintaining SSC numbers during fracture healing is critical for limiting inflammation, and in diabetic fractures, this process is interrupted through aberrant NF- $\kappa$ B activation in SSCs. Our results also provide an explanation for why diabetes decreases the efficacy of transplanted SSCs to enhance hard and soft tissue repair (Sui et al., 2017; van de Vyver, 2017) by suggesting that diabetic environment is unfavorable for normal SSC function. Interestingly, NF- $\kappa$ B inhibition in SSCs had minimal effects in normoglycemic wounds, likely due to relatively little NF- $\kappa$ B activation in SSCs in normal compared to those in diabetic wounds (Fig. 2.7A, C).

The second major effect of diabetes on fracture wounds was the impairment of macrophage transition from M1 to M2, which was rescued when NF- $\kappa$ B was blocked in SSCs. This finding indicates that SSCs are responsible for the proper M1/M2 balance during osseous healing and are disrupted under diabetic conditions. SSC dysregulation



through NF- $\kappa$ B is likely to contribute to other types of diabetic wounds where persistent inflammation and predominance of M1 over M2 is observed (Bannon et al., 2013; Finley et al., 2016). Mechanistically, this was due to NF- $\kappa$ B-mediated reduction of TGF $\beta$ 1 expression by SSCs caused by diabetes *in vivo* and by high glucose *in vitro*. Conditioned media from BMSSC culture stimulated M2 polarization, which was blocked by glucose-induced NF- $\kappa$ B activation that was directly related to a failure to express TGF $\beta$ 1. In humans, early fracture healing coincides with an increase in TGF $\beta$ 1 serum concentration levels, whereas subjects that experience difficulty in healing such as formation of non-unions exhibit significantly lower TGF $\beta$ 1 levels (Jiao et al., 2015; Zimmermann et al., 2005). While our findings clearly demonstrate M1/M2 imbalance in diabetic fracture wounds and suggest modulation of phenotype-switching by TGF $\beta$ 1 as a mechanism, I cannot rule out other potential cellular events such as differential recruitment of M1 or M2 egression. Moreover, our results suggest that the formation of M2, which occurs in normoglycemic but not diabetic wounds, is important in resolving inflammation in early fracture repair. The important role of TGF $\beta$ 1 in modulating inflammation and promoting skeletal regeneration is further supported by the findings that diabetic inflammation was largely reduced along with the recovery of M2 when recombinant TGF $\beta$ 1 was administered during early fracture healing. Thus, suppression of TGF $\beta$ 1 signaling is a key mechanism by which diabetes-enhanced NF- $\kappa$ B activation limits the capacity of SSCs to resolve inflammation in diabetic fracture wounds.

In summary, our study unveils a mechanism where T1D impairs endogenous SSCs to enhance inflammation and impair healing response, for which aberrant activation of NF- $\kappa$ B plays a key role. The deficit in SSC function due to NF- $\kappa$ B dysregulation can be linked

to the loss of SSC numbers as well as reduced capacity of SSCs to produce TGF $\beta$ 1 that modulates macrophage polarization. Although our study used T1D model, the findings may be applicable to impaired skeletal healing in type 2 diabetes, as downstream activation of NF- $\kappa$ B has been implicated in T2D complications in other cell types (Suryavanshi and Kulkarni, 2017). Furthermore, these results also point to disruption of a critical pathway in SSCs caused by diabetes and may represent a general mechanism for diabetic complications where stem cells and inflammation play a role in the response to perturbation.

## 2.11 Methods

**Animal Studies** All animal experiments were initiated on 8-10 weeks old male and female mice conforming to a protocol approved by the University of Pennsylvania Institutional Animal Care and Use Committee. The following mice were purchased from Jackson Laboratory: C57BL/6J, *B6.Cg-Tg(Prrx1-cre)1Cjt/J (Prrx1<sup>Cre</sup>)*, *B6.Cg-Tg(Prrx1-cre/ERT2,-EGFP)1Smkm/J (Prrx1<sup>CreER</sup>)*, *B6.Cg-Gt(ROSA)26Sor<sup>tm9(CAG-tdTomato)Hze/J (R26<sup>TdTomato</sup>)</sup>*, *B6.129P2-Gt(ROSA)26Sor<sup>tm1(DTA)Lky/J (R26<sup>DTA</sup>)</sup>*. *B6;SJL-Tg(Col2a1-cre)1Bhr/J* mice (*Col2a1<sup>Cre</sup>*) were obtained from Dr. Patrick O'Connor (Rutgers University, Newark), and floxed *Ikk $\beta$*  mice (*Ikk $\beta$ <sup>ff</sup>*) from Dr. Michael Karin (UCSD, La Jolla). Low-dose streptozotocin injection was performed intraperitoneally for T1D induction (5 consecutive days, 50mg/kg, Cayman Chemical) as previously described (Alblowi et al., 2013). Animals were considered diabetic when blood glucose was >220mg/dl one week after last injection, and remained diabetic for 4-6 weeks prior to fracture surgery.

**Fracture Induction** A closed-transverse femoral fracture was induced as previously described (Alblowi et al., 2009). Briefly, 27G-needle was used to access femoral marrow space via articular cartilage. 30G-pin was inserted into the marrow for wound stabilization.

Fracture injury was induced at mid-diaphysis with controlled weight on a guillotine-like apparatus.

**Tamoxifen Injection** Tamoxifen (5mg/25g, Sigma) or corn oil was administered via oral gavage for 5 consecutive days. Fracture injury was induced 24h after last injection.

**Immunofluorescence** Harvested fracture samples were fixed in 10% formalin at 4°C for 24h, decalcified in 14% EDTA (pH 7.4) for 2 weeks at 4°C with constant agitation, and processed in paraffin or frozen blocks. Immunofluorescence was performed using following primary antibodies: anti-GFP (NB100-1770, Novus Biological), anti-Ki67 (14-5698-82, eBioscience), anti-RFP (600-901-379, Rockland), anti-NF-κB (ab16502, Abcam), anti-TNF (ab34674), anti-F4/80 (ab6640), anti-CD4 (ab183685), anti-IKKb (ab124957), anti-CD271 (ab52987), anti-Sca1 (ab51317), anti-iNOS (ab15323), anti-CD163 (ab182422), anti-TGFb1 (ab92486). DeadEnd<sup>TM</sup>-TUNEL System (G3250, Promega) or Annexin-V (A13204, Invitrogen) was used to detect apoptotic cells. Percent-positive cells and mean fluorescent intensity (MFI) were quantified using NIS-Element software (Nikon).

**RT-qPCR** Fractures samples were dissected, snap-frozen in liquid nitrogen, and stored in -80°C freezer. Samples were pulverized in liquid nitrogen by using pre-chilled mortar and pestle. RNA isolation (AM1912, ThermoFisher) and cDNA preparation (4368813, ThermoFisher) were performed following manufacture's protocols. RT-qPCR was performed with Fast SYBR Green (4385614, ThermoFisher) on StepOnePlus System (Applied Biosystems). Primer sequences were, in 5' → 3' direction, as follows: *L32*, F: TTAAGCGAAACTGGCGGAAAC, R: TTGTTGCTCCCATAACCGATG; *Fizz1*, F: CCAATCCAGCTAACTATCCCTCC, R: CCAGTCAACGAGTAAGCACAG; *Nos2*, F:

GTTCTCAGCCCAACAATACAAGA, R: GTGGACGGGTCGATGTCAC; *Il1b*, F: TGCCACCTTTTGACAGTGATG, R: ATGTGCTGCTGCGAGATTTG; *Il10*, F: GCTCTTACTGACTGGCATGAG, R: CGCAGCTCTAGGAGCATGTG; *Il6*, F: TAGTCCTTCCTACCCCAATTTCC, R: TTGGTCCTTAGCCACTCCTTC; *Tnf*, F: CCCTCACACTCAGATCATCTTCT; R: GCTACGACGTGGGCTACAG; *Ifng*, F: ACAGCAAGGCGAAAAAGGATG, R: TGGTGGACCACTCGGATGA; *Ikkb*, F: ACAGCCAGGAGATGGTACG, R: CAGGGTGACTGAGTCGAGAC; and *Tgfb1*, F: CAACAATTCCTGGCGTTACCTTGG, R: GAAAGCCCTGTATTCCGTCTCCTT.

Data were normalized to housekeeping gene expression (*L32*). In a pilot study, *Tgfb1* had more pronounced effect than *Il10*, therefore *Tgfb1* was investigated further.

***In Vitro Experiments*** Primary bone marrow SSCs from female mice were prepared by flushing femur/tibiae marrow cavity as previously described (Chen et al., 2017). Briefly,  $15 \times 10^6$  cells were seeded in 100mm dishes (Genesee Scientific). Non-adherent cells were removed after initial 24h-incubation in 5% CO<sub>2</sub> at 37°C, and adherent cells were cultured for 14 days in  $\alpha$ -MEM supplemented with 20% FBS, 2mM L-glutamine (Invitrogen), 55uM 2-mercaptoethanol (Invitrogen) and 100U/ml penicillin and 100ug/ml streptomycin (Invitrogen). For high glucose experiments, wildtype BMSSCs and BMSSCs with *Ikk $\beta$*  deletion were incubated under low (4.5mM) or high glucose (25mM) condition in low-serum media containing 2% FBS for 5 consecutive days. TGF $\beta$ 1 ELISA was performed according to the manufacturer's protocols (DY1679-05, R&D Systems), including activation of latent TGF $\beta$ 1.

Bone marrow-derived macrophages (BMMs) were prepared following published protocol (Zhang et al., 2016) using M-CSF (315-02, 20ng/ml, PeproTech). BMMs were stimulated

for 24h with low-dose LPS (10ng/ml) for M1 and IL-4 (1.25ng/ml) for M2 polarization, in combination with BMSSC-conditioned medium. All conditioned media contained 20% FBS and low glucose (4.5mM), which were prepared by incubating BMSSCs for 48h after low or high glucose treatment as described above. For TGF $\beta$ 1 neutralizing experiments, BMMs were stimulated as above with isotype IgG or TGF $\beta$ 1 antibody (5ug/ml, MAD240, R&D Systems) for 24h.

**Recombinant TGF $\beta$ 1 Treatment** After 24h post-fracture, mice received 100ng of recombinant TGF $\beta$ 1 (Cat: 240-B-002, R&D Systems) dissolved in 200ul of PBS, administered circumferentially around fracture periosteal layer. Control mice received PBS only.

**Statistical Analysis** Statistical analysis was performed using Prism software (GraphPad-ver.7.03). All data are expressed as the mean  $\pm$  SD. *In vivo* experiments comparing multiple groups used two-way ANOVA followed by Tukey's post-hoc test to determine significance. When comparing two groups, Student's T-test was performed. *In vitro* experiments with multiple groups were analyzed with one-way ANOVA. P<0.05 was considered statistically significant. Individual animal was used as a unit of measurement, and sex was not considered as a factor in the analyses.

## CHAPTER 3: NF- $\kappa$ B ACTIVITY IN DERMAL PRX1<sup>+</sup> FIBROBLASTS ARE CRITICAL FOR MAINTAINING IMMUNE HOMEOSTASIS IN SKIN

### 3.1 Abstract

The transcription factor NF- $\kappa$ B plays a central role in mediating inflammatory responses. While its protective and destructive function in epidermis is well documented, the role of NF- $\kappa$ B activation in dermal fibroblasts is not fully understood. Here, I found that deletion of *Ikkb* in Prx1<sup>+</sup> fibroblasts led to NF- $\kappa$ B inactivation and unexpected development of dermal inflammatory lesion. The lesion was characterized by overt inflammation that preceded alopecia and ulceration. The inflammatory infiltrate was predominantly CD11b<sup>+</sup>F4/80<sup>+</sup> myeloid cells, and this was not due to the micro-irritation by the hard or soft bedding material. Inducible perinatal deletion of *Ikkb* in Col1a2<sup>+</sup> fibroblasts or Prx1<sup>+</sup> mesenchymal cells caused dermal inflammation, whereas the effect was absent in mice with adipocyte-specific deletion of *Ikkb*. Single cell RNA-sequencing demonstrated that Prx1<sup>+</sup> fibroblasts with *Ikkb* deletion had elevated *Ccl11* (encoding eotaxin-1) levels, and the immune cells were characterized by inflammatory macrophage and type 2 lymphocyte phenotype. Collectively the data demonstrate importance of basal activity of NF- $\kappa$ B in dermal fibroblasts for maintaining immune homeostasis, and that the lesion may represent clinical atopic dermatitis model in which *Ccl11* expression by the fibroblasts may provide the mechanism for disease pathogenesis.

### 3.2 Introduction

Skin is the largest organ in human body and provides a niche for diverse immune cell types that have anti-microbial and repair functions (Eyerich et al., 2018). Skin disorders are responsible for 41.6 million years lost to disease plus lived with disability

globally, as well as affecting nearly 85 million people in the U.S., thus posing a significant public health issue (Karimkhani et al., 2017; Lim et al., 2017). Though significant advances have been made identifying immune and keratinocyte dysfunction as a contributing factor for dermatologic disorders (Schwingen et al., 2020), it is unclear if fibroblasts, the most abundant cell type in dermis, play a causative role in development of skin diseases. Given the re-emerging concept of fibroblasts as immune modulators in multiple organs (Van Linthout et al., 2014; Yoshitomi, 2019), it is critical to understand the crosstalk between fibroblasts and immune cells to fully understand the pathogenetic mechanism behind skin disorders.

Dermatitis (atopic, contact and seborrheic) is responsible for the highest global burden among skin disorders (Karimkhani et al., 2017). Atopic dermatitis (AD), the most common chronic inflammatory skin disorder, alone affects 7.3% of US adult population (Chiesa Fuxench et al., 2019; Silverberg et al., 2019). While the cause is undoubtedly multifactorial, the disease is well characterized by the abundance of type 2 immune cytokines, eosinophilia and IgE (Kim et al., 2019). Dupilumab, a monoclonal antibody that targets IL-4 alpha receptor to block type 2 immune response, was recently found to have a positive outcome in patients with moderate to severe atopic dermatitis as compared to placebo group (Gooderham et al., 2018; Simpson et al., 2016). However, the symptoms were alleviated in just 37-38% of the subjects, suggesting that the AD pathogenesis may be more complex, and that further understanding is necessary to develop viable therapeutic approaches for patients who are refractory to currently available options.

Ikkb-NFkB is a key master inflammatory pathway that is often implicated in animal models of dermatitis. Hyperactivation of NF-kB in SHARPIN-deficient mice

(Liang et al., 2011; Potter et al., 2014; Seymour et al., 2007), by *Ikkb* overexpression in keratinocytes (Page et al., 2010), or by deleting NF- $\kappa$ B inhibitor I $\kappa$ B $\alpha$  (Klement et al., 1996) all lead to the development of dermatitis with severe inflammatory infiltration in the skin. In contrast, inactivation of NF- $\kappa$ B in keratinocytes by deleting p65 (Grinberg-Bleyer et al., 2015) or *Ikkb* (Pasparakis et al., 2002) also lead to development of dermatitis in neonatal mice. These studies demonstrate that either deficiency or overactivation of NF- $\kappa$ B is harmful and suggest its basal activation to be a critical component of skin immune homeostasis. However, the animal models are either global or keratinocyte-specific gene deletion, and the animals do not survive long-term, suggesting that it may not fully reflect the human model of dermatitis.

Given the important role of NF- $\kappa$ B in skin immunity, I initially sought to investigate the role of NF- $\kappa$ B in skin fibroblasts under chronic inflammatory condition. Surprisingly, I observed that the animals lacking *Ikkb* in Prx1<sup>+</sup> mesenchymal cells spontaneously developed skin lesion in the venter. Thus, I tested the hypothesis that the basal level of inflammation by *Ikkb*-NF $\kappa$ B pathway is necessary in skin fibroblasts in order to maintain immune homeostasis of the dermis.

### **3.3 Ventral skin lesion develops in mice that lack IKK $\beta$ in Prx1<sup>+</sup> cells**

To determine if NF- $\kappa$ B activity in mesenchymal cells is important in skin homeostasis, I generated Prx1<sup>+</sup>*Ikkbf/f* mice that lack *Ikkb* gene, an activator of canonical NF- $\kappa$ B pathway, specifically in Prx1-lineage stromal cells. At 4 months of age, I found that the experimental mice that lacked *Ikkb* in Prx1<sup>+</sup> cells spontaneously developed a severe skin lesion, whereas the littermates that lacked Cre recombinase did not (Figure 3.1A). Histological analysis revealed thickening of the dermal layer in the ventral skin of



Prx1Cre+Ikbbf/f mice, indicative of fibrosis, whereas that of dorsal skin was not affected (Figure 3.1B-D). In Prx1Cre<sup>+</sup>R26R<sup>TdTomato</sup> mice, Prx1-lineage positive cells were found in ventral but not dorsal skin (Figure 3.1E), consistent with the reported ventral patterning of lateral somatic lineage of Prx1<sup>+</sup> cells during embryonic development (Durland et al., 2008; Logan et al., 2002). Mechanical testing demonstrated that the ventral skin of experimental mice was less resistant to stretch-till-failure, as revealed by reduced stiffness and maximum load until failure (Figure 3.1F), suggesting that there must be another component to the lesion other than fibrosis to weaken the structural integrity of skin.

Because Prx1-lineage cell population in skin includes fibroblasts and adipocytes (Currie et al., 2019; Durland et al., 2008; Sanchez-Gurmaches et al., 2015), I examined if Ikbb deletion in Prx1<sup>+</sup> cells affected the basal activity of NF-κB in these cells by immunofluorescence with p65 antibody. In both vimentin<sup>+</sup> fibroblasts and perilipin<sup>+</sup> adipocytes, Ikbb deletion reduced the number of cells with nuclear NF-κB expression, indicative of its activation (Figure 3.2A-B). These results demonstrate that physiological NF-κB activation in Prx1<sup>+</sup> mesenchymal cells is essential for maintaining structural integrity of skin.

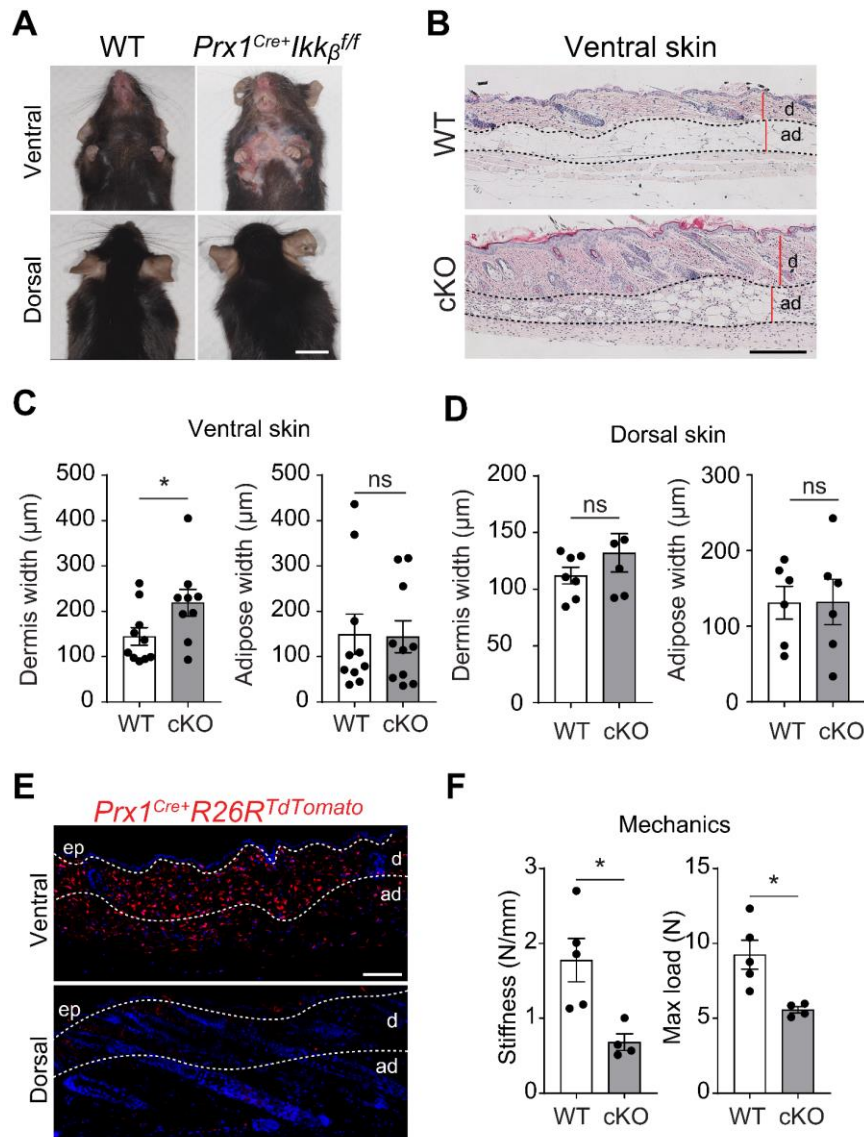


**Figure 3.1. Ventral skin lesion develops in mice that lack IKK $\beta$  in *Prx1*<sup>+</sup> cells.** **A.** Representative photograph images of ventral and dorsal skin in 16 weeks old control (WT) and experimental (*Prx1Cre<sup>+</sup>Ikk $\beta$ <sup>ff</sup>*) mice. **B.** H&E images of ventral skin from WT or conditional knockout mice (cKO, *Prx1Cre<sup>+</sup>Ikk $\beta$ <sup>ff</sup>*); d, dermis, ad, adipose layers. Scale bar, 0.5mm. **C.** Dermis and adipose width in ventral skin of WT and cKO mice. **D.** Dermis and adipose width in dorsal skin of WT and cKO mice. **E.** TdTomato expression in ventral and dorsal skins of *Prx1Cre<sup>+</sup>R26R<sup>TdTomato</sup>* mice demonstrating ventral-specific expression pattern; ep, epithelium, scale bar: 0.1mm. **F.** Mechanical testing of ventral skins of WT and cKO mice; stiffness and max load until failure (tear) were quantified. Data are represented as mean  $\pm$  SEM. \* $p < 0.05$ ; students t-test comparing WT to cKO groups. N = 9-10 (C), 6-7 (D), 4-5 (F).

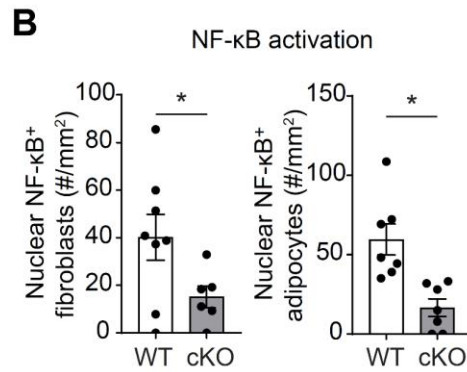
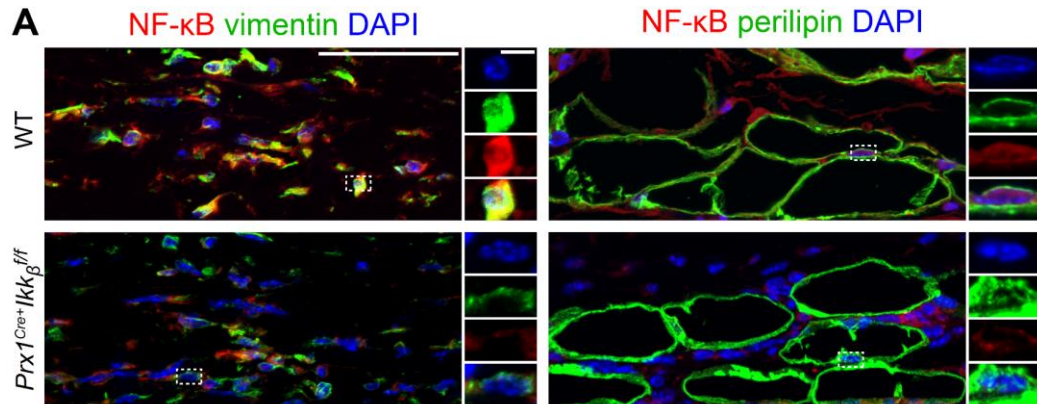


**Figure 3.2.** *Ikk $\beta$*  deletion in *Prx1*<sup>+</sup> cells block NF- $\kappa$ B activation in dermal fibroblasts and adipocytes.

**A.** Representative immunofluorescent images of ventral skin stained with NF- $\kappa$ B (p65) antibody and vimentin (fibroblast marker) or perilipin (adipocyte marker) in 16 weeks old control (WT) or *Prx1Cre*<sup>+</sup>*Ikkb*<sup>flf</sup> mice. **B.** Quantification of vimentin<sup>+</sup> fibroblasts with nuclear NF- $\kappa$ B expression (left), and perilipin<sup>+</sup> adipocytes with nuclear NF- $\kappa$ B expression (right). Data are represented as mean  $\pm$  SEM.

\* $p < 0.05$ ; students t-test comparing WT to cKO groups. N = 7-8 each group.

### 3.4 Skin lesion progresses with age in postnatal IKK $\beta$ <sup>f/f</sup> mice

I next examined the skin of postnatal mice in different ages to determine the timing of disease emergence. I observed that alopecia first developed at 10<sup>th</sup> week of experimental Prx1CreIkkb<sup>f/f</sup> mice, which always preceded ulceration (Figure 3.3A, B). Furthermore, the affected area progressively increased with aging (Figure 3.3C). Alopecia indicated a possible dysregulation of hair follicle niche that may be responsible for the eventual ulcer. Thus, I examined the number of hair follicles histologically and by CD34<sup>+</sup> immunofluorescence and found that there was no significant changes in hair follicle numbers between control and experimental mice (Figure 3.3D).

I next tested if the experimental mice exhibited histologic signs of lesion development at time points where clinical lesions were never found, such as in 1-day old (P1) or in 4-weeks old mice. I found that P1 neonatal mice had ventral skin that was histologically indistinguishable between wildtype control versus experimental mice that lacked Ikkb in Prx1<sup>+</sup> cells (Figure 3.4A, C). However, at 4 weeks old, Prx1Cre<sup>+</sup>Ikkb<sup>f/f</sup> mice had a significant infiltration of inflammatory cells while its dermal thickness was unchanged (Figure 3.4B, D). These results demonstrate that the skin lesion occurs perinatally and is not due to a perturbation during embryonic development. Moreover, the data point to inflammation as a precipitating cellular event that may explain dermal fibrosis observed in adult mice at 16-20 weeks old.

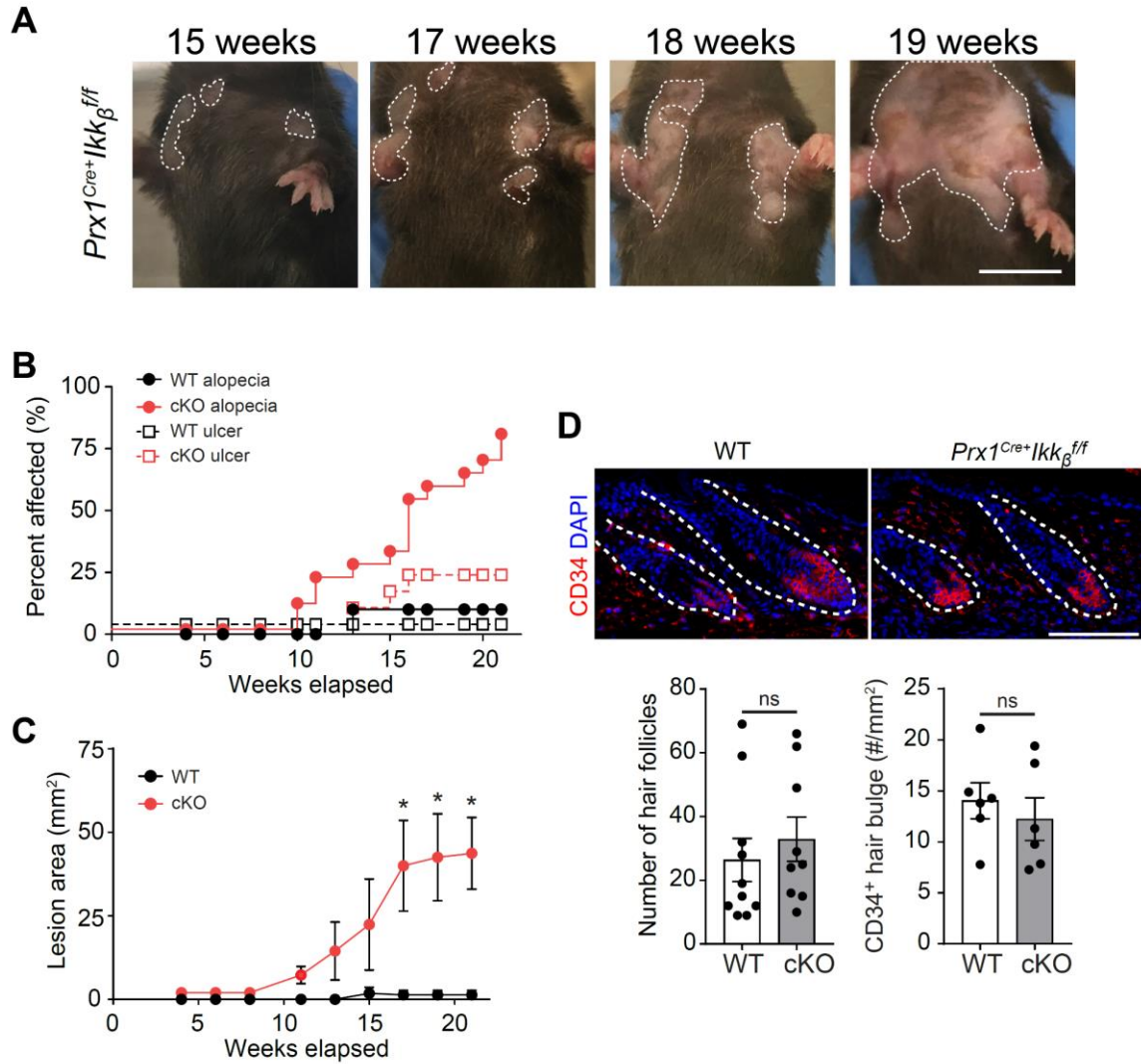


**Figure 3.3. Skin lesion progresses with age in postnatal *Ikk $\beta$ <sup>ff</sup>* mice.** **A.** Representative images of clinical lesion developing in *Prx1<sup>Cre+</sup>Ikk $\beta$ <sup>ff</sup>* (cKO) mice from 15<sup>th</sup> to 19<sup>th</sup> weeks old in age. Scale bar, 1cm. **B.** Quantification of percent affected by alopecia or ulceration in function of age from 4 to 21 weeks. **C.** Lesion area quantified in mm<sup>2</sup> over the observational period. **D.** Quantification of hair follicles from histologic analysis or by CD34 staining. Top, representative immunofluorescent images of CD34<sup>+</sup> hair follicle niche. Bottom: left, histological analysis of hair follicle numbers per mm<sup>2</sup> from H&E staining of ventral skin in WT and cKO mice; right, the number of CD34<sup>+</sup> hair follicles per mm<sup>2</sup>. Data are represented as mean  $\pm$  SEM. \* $p < 0.05$ , ns = not significant; students t-test comparing WT to cKO groups. N = 6-10 each group.

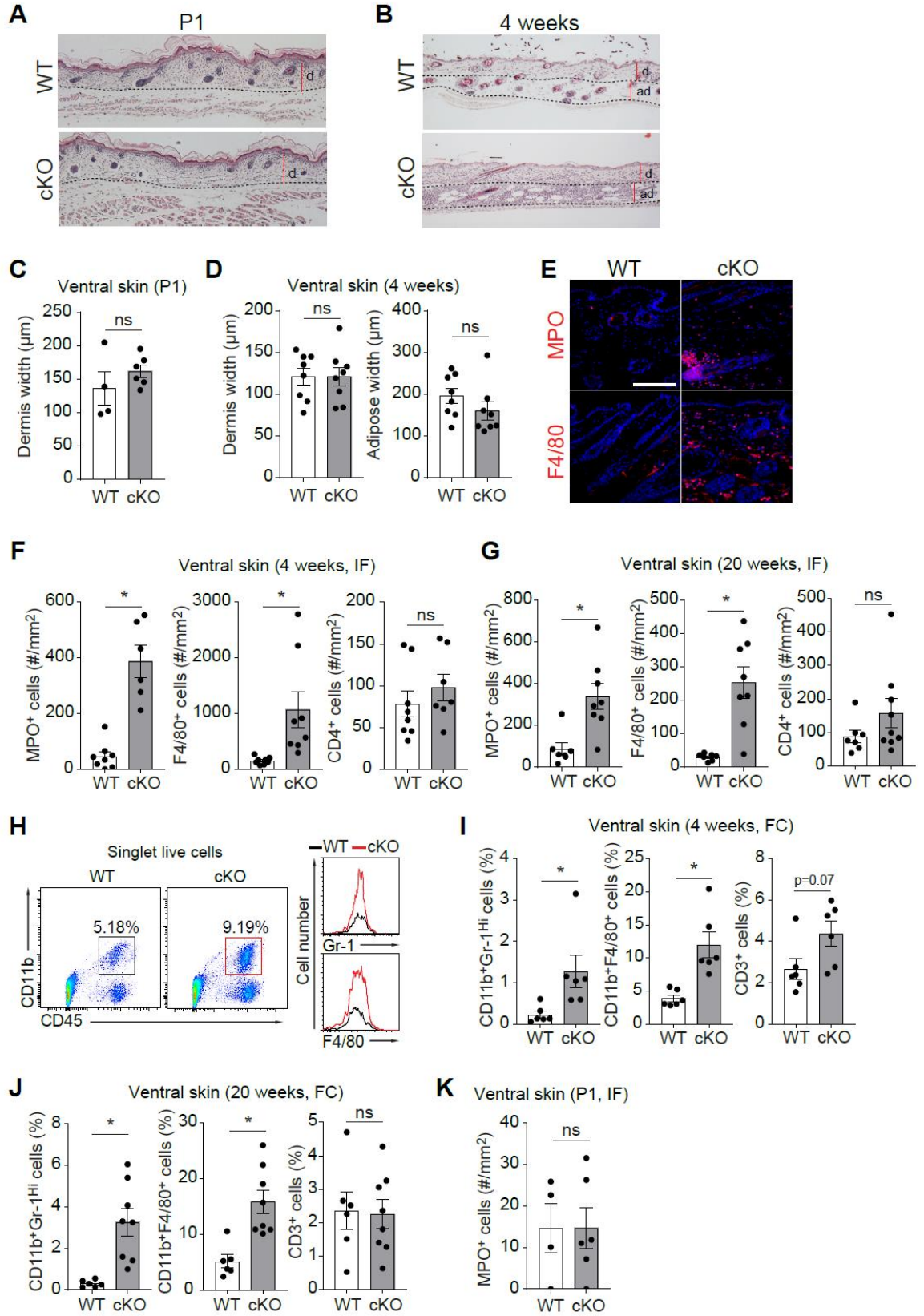




**Figure 3.4. Dermal fibrosis is preceded by myeloid inflammation in young but not neonatal *Ikkβ<sup>ff</sup>* mice.** **A.** H&E images of ventral skin in P1 neonatal wildtype (WT) or *Prx1Cre<sup>+</sup>Ikkβ<sup>ff</sup>* (cKO) mice; d: dermis. **B.** H&E images of ventral skin in 4 weeks old young WT or cKO mice; ad: adipose layer. Note overt inflammatory infiltrate in the skin of cKO mice. **C.** Quantification of dermis thickness between WT versus cKO neonatal mice. **D.** Quantification of dermis and adipose layer thickness between WT versus cKO 4 weeks old mice. **E.** Representative immunofluorescent images with myeloperoxidase antibody (MPO, marker of neutrophils) and F4/80 antibody (marker of macrophages) in 4 weeks old wildtype (WT) or *Prx1Cre<sup>+</sup>Ikkβ<sup>ff</sup>* (cKO) mice, scale bar = 50um. **F-G.** Quantification of immunopositive cells for MPO, F4/80, or CD4 expression in 4 weeks (C) or 16 weeks old (D) WT and cKO mice; IF = immunofluorescence experiment. **H.** Representative flow cytometry plot for myeloid cell gating (Live CD45<sup>+</sup>CD11b<sup>+</sup> cells) and quantification of Gr-1<sup>Hi</sup> cells for neutrophil population and F4/80<sup>+</sup> cells for macrophage population. **I-J.** Quantification of neutrophils, macrophages and CD3 T cells per live cells in 4 weeks (E) or 16 weeks old mice (F) by flow cytometry analysis (FC). **K.** Quantification of MPO immunopositive cells in the skin of P1 neonatal WT or cKO mice. Data are represented as mean ± SEM. \*p<0.05, ns = not significant; students t-test comparing WT to cKO groups. N = 4-6 for P1 groups, N = 6-8 for 4 weeks and 20 weeks old groups.

### **3.5 Dermal inflammation is characterized by excessive myeloid cell infiltration**

To determine the type of inflammation caused by NF- $\kappa$ B inactivation in Prx1<sup>+</sup> skin mesenchymal cells, I broadly examined the number of neutrophils, macrophages and CD3 or CD4 T cells by immunofluorescence and flow cytometry. In the skin of 4 weeks old experimental mice that lacked *Ikkb*, there was a significant increase in the number of MPO<sup>+</sup> neutrophils and F4/80<sup>+</sup> macrophages, whereas the number of CD4<sup>+</sup> T cells did not change when compared to control littermates (Figure 3.4E, F). Similar pattern was observed in the skin of adult (16 weeks old) mice (Figure 3.4G). Flow cytometry analysis revealed a similarly drastic increase in Gr1<sup>Hi</sup> neutrophils and F4/80<sup>+</sup> macrophage numbers, whereas CD3<sup>+</sup> T cell number did not differ compared to control groups, in both 4- and 16-weeks old mice (Figure 3.4H-J). Consistent with our histologic observation, there was no significant difference in the number of neutrophils between control and experimental group at P1 (Figure 3.4K). These results demonstrate that *Ikkb* deletion in Prx1<sup>+</sup> cells cause severe inflammatory reaction that is dominated by myeloid cells and point to a significant contribution of these cells in regulating inflammatory immune cells.

Given that the inflammation is present in relatively young (4 weeks old) but not in neonatal (1 day old) mice, it is possible that the lesion may be influenced by the exposure of extrinsic factors such as micro-irritation by the corn bedding. I tested this by transferring a pregnant female to a soft paper bedding and housing newborn pups in such environment to minimize skin irritation (Figure 3.5A). Flow cytometry analysis of 4 weeks old mice demonstrated that the softer bedding failed to prevent myeloid inflammation as evidenced by the consistent increase in Gr1<sup>Hi</sup> and F4/80<sup>+</sup> myeloid cell numbers and not CD3<sup>+</sup> T cells



(Figure 3.5B). Therefore, dermal inflammation caused by NF- $\kappa$ B inactivation in *Prx1*-lineage cells is likely due to an intrinsic dysregulation of the immune response.

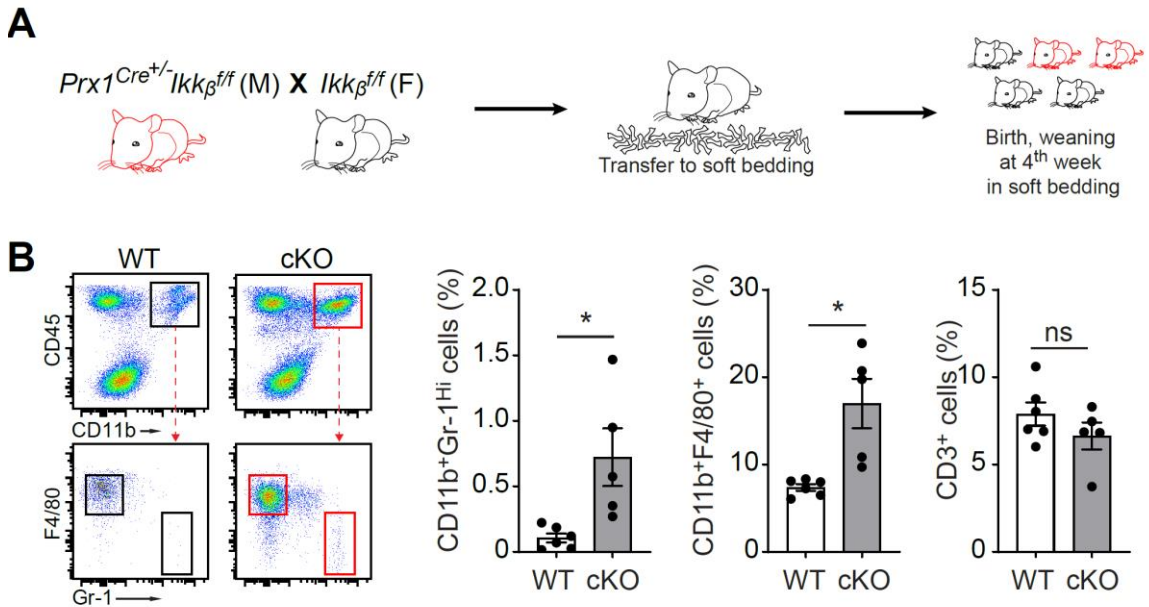


**Figure 3.5. Soft cage bedding does not protect *Prx1Cre<sup>+</sup>Ikkb<sup>f/f</sup>* mice from developing inflammation.**

**A.** Schematic diagram for strategy to wean young 4 weeks old mice in soft paper cage bedding. **B.** Left, flow cytometry gating strategy to quantify neutrophils and macrophages from ventral skin of control (WT) or *Prx1Cre<sup>+</sup>Ikkb<sup>f/f</sup>* mice (cKO); right, quantification of neutrophils (CD45<sup>+</sup>CD11b<sup>+</sup>Gr-1<sup>Hi</sup>), macrophages (CD45<sup>+</sup>CD11b<sup>+</sup>F4/80<sup>+</sup>) and CD3 T cells (CD45<sup>+</sup>SSC<sup>lo</sup>CD3<sup>+</sup>) per live cells. Data are represented as mean ± SEM. \**p*<0.05, ns = not significant; students t-test comparing WT to cKO groups. N = 5-6 each group.

### 3.6 Systemic inflammation in *Prx1Cre<sup>+</sup>IKK $\beta$ <sup>f/f</sup>* mice

*Prx1* gene is active in the stromal cells of spleen and bone marrow, and these cells are important for proper hematopoiesis (Greenbaum et al., 2013). I therefore examined systemic inflammation by quantifying the number of inflammatory cells in peripheral blood, spleen, and bone marrow of the control and experimental animals that lack *Ikkb* gene. Complete blood count with differential analyses of the retinal bleed samples revealed that there was a significant increase in the number of circulating monocytes and eosinophils but not lymphocytes in the experimental *Prx1Cre<sup>+</sup>Ikkb<sup>f/f</sup>* mice compared to control group at 16 weeks old (Figure 3.6A). In addition, I observed splenomegaly in the experimental mice with a concurrent increase in the number of F4/80<sup>+</sup> cells and Gr1<sup>Hi</sup> neutrophils compared to wildtype (Figure 3.6B). There was however no significant difference in the number of neutrophils, monocytes, macrophages or CD3<sup>+</sup> T cells in the bone marrow of control and experimental mice (Figure 3.6C). These results demonstrate that NF- $\kappa$ B inactivation in *Prx1<sup>+</sup>* cells is associated with increased inflammatory cells in the peripheral blood and spleen, but not in the bone marrow, suggesting normal hematopoiesis.

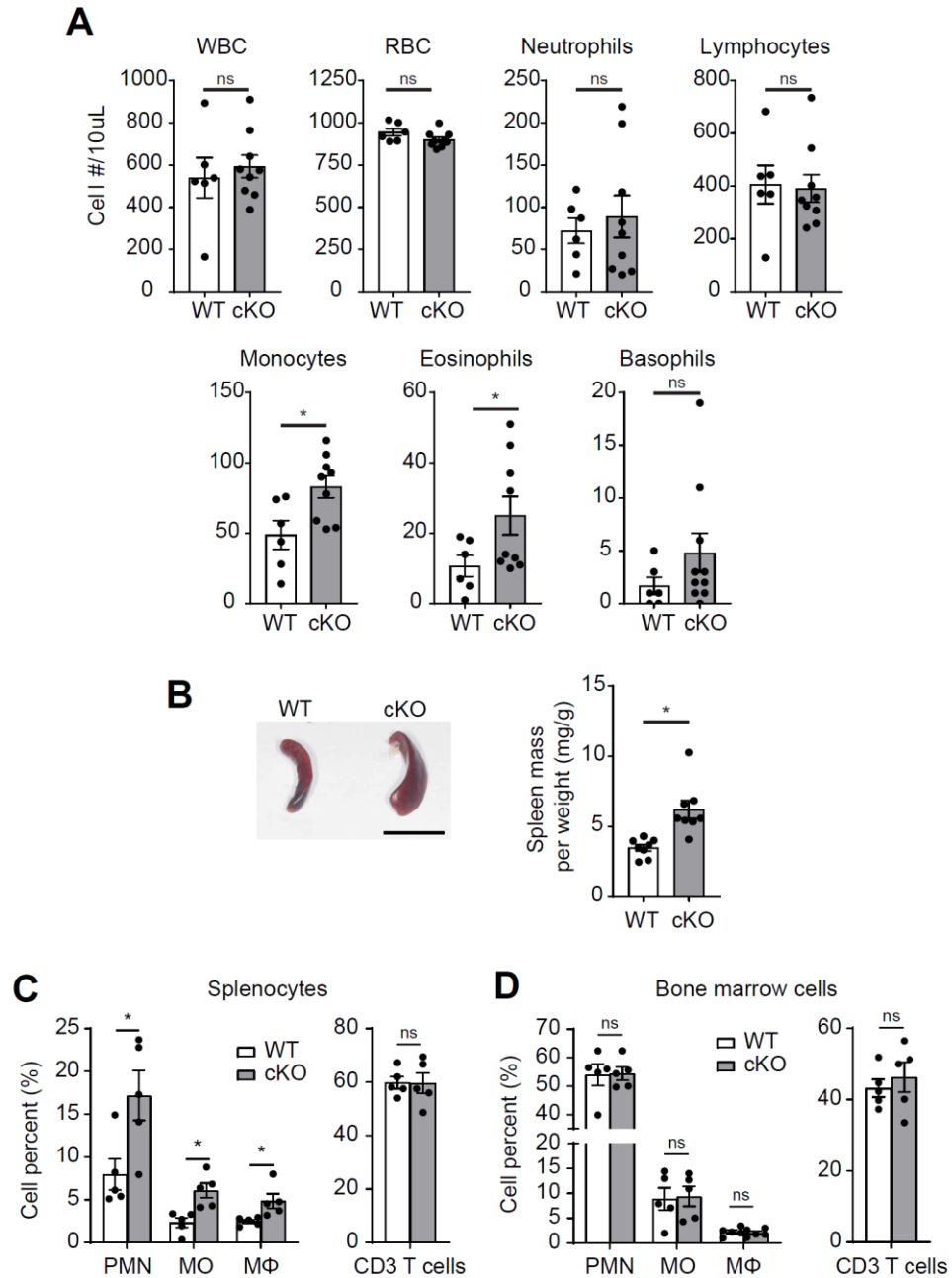


**Figure 3.6. Systemic inflammation in *Prx1Cre<sup>+</sup>Ikkβ<sup>fl/fl</sup>* mice. A.** Quantification of circulating hematopoietic cells from complete blood count and differential analyses of retro-orbital blood samples from the control (WT) or *Prx1Cre<sup>+</sup>Ikkβ<sup>fl/fl</sup>* (cKO) mice at 16 weeks old. WBC: white blood cell, RBC: red blood cell, N = 6-9 each. **B.** Representative micrograph of spleen from WT and cKO mice. Significant splenomegaly is noted in cKO mice. Right, quantification of spleen weight per weight. **C-D.** Quantification of neutrophils (PMN, polymorphonuclear cells, CD45<sup>+</sup>CD11b<sup>+</sup>Gr-1<sup>Hi</sup>), monocytes (MO,

CD45<sup>+</sup>CD11b<sup>+</sup>CD115<sup>+</sup>), macrophages (MΦ, CD45<sup>+</sup>CD11b<sup>+</sup>F4/80<sup>+</sup>) per total live cells; and CD3 T cells (CD45<sup>+</sup>SSC<sup>lo</sup>CD3<sup>+</sup>) per total live SSC<sup>low</sup> cells from splenocyte preparations (C), and from bone marrow preparations (D) of WT and cKO mice; N = 5 each. Data are represented as mean ± SEM. \*p<0.05, ns = not significant; students t-test comparing WT to cKO groups.

### **3.7 NF-κB activity in fibroblasts, not in adipocytes, is critical for immune homeostasis**

What is the mesenchymal cell type responsible for causing dysregulation of immune homeostasis in skin? Because dermal fibroblasts and adipocytes are both derived from Prx1-lineage cell, I generated mice that had *Ikkb* gene deleted specifically in either fibroblasts (*Col1a2CreERT<sup>+</sup>Ikkb<sup>fl/fl</sup>*) or adipocytes (*Adipoq-Cre<sup>+</sup>Ikkb<sup>fl/fl</sup>*). I first performed flow cytometry analysis in 4-weeks old mice that had *Ikkb* gene deleted in adipocytes and found that there was no significant difference in the number of F4/80<sup>+</sup> cells or Gr1<sup>Hi</sup> neutrophils in ventral skin, spleen, and bone marrow samples (Figure 3.7A, B). In contrast, when *Ikkb* was deleted in *Col1a2*-expressing fibroblasts by tamoxifen administration in P1/3 mice, there was a statistically significant increase in F4/80<sup>+</sup> cells in the ventral skin without causing systemic inflammation in the spleen or the bone marrow (Figure 3.7C, D). Consistent with this, activation of Cre-recombinase in postnatal Prx1<sup>+</sup> cells at P1/3 in Prx1CreERT<sup>+</sup>*Ikkb<sup>fl/fl</sup>* mice increased the number of F4/80<sup>+</sup> cells in the skin compared to vehicle control group, as quantified by immunofluorescence (Figure 3.7E), and Gr1<sup>Hi</sup> and F4/80<sup>+</sup> myeloid cells by flow cytometry (Figure 3.7F). These data clearly demonstrate that dermal fibroblasts are the main cell type that is responsible for immune homeostasis in skin and that NF-κB activity is a critical component in the process.

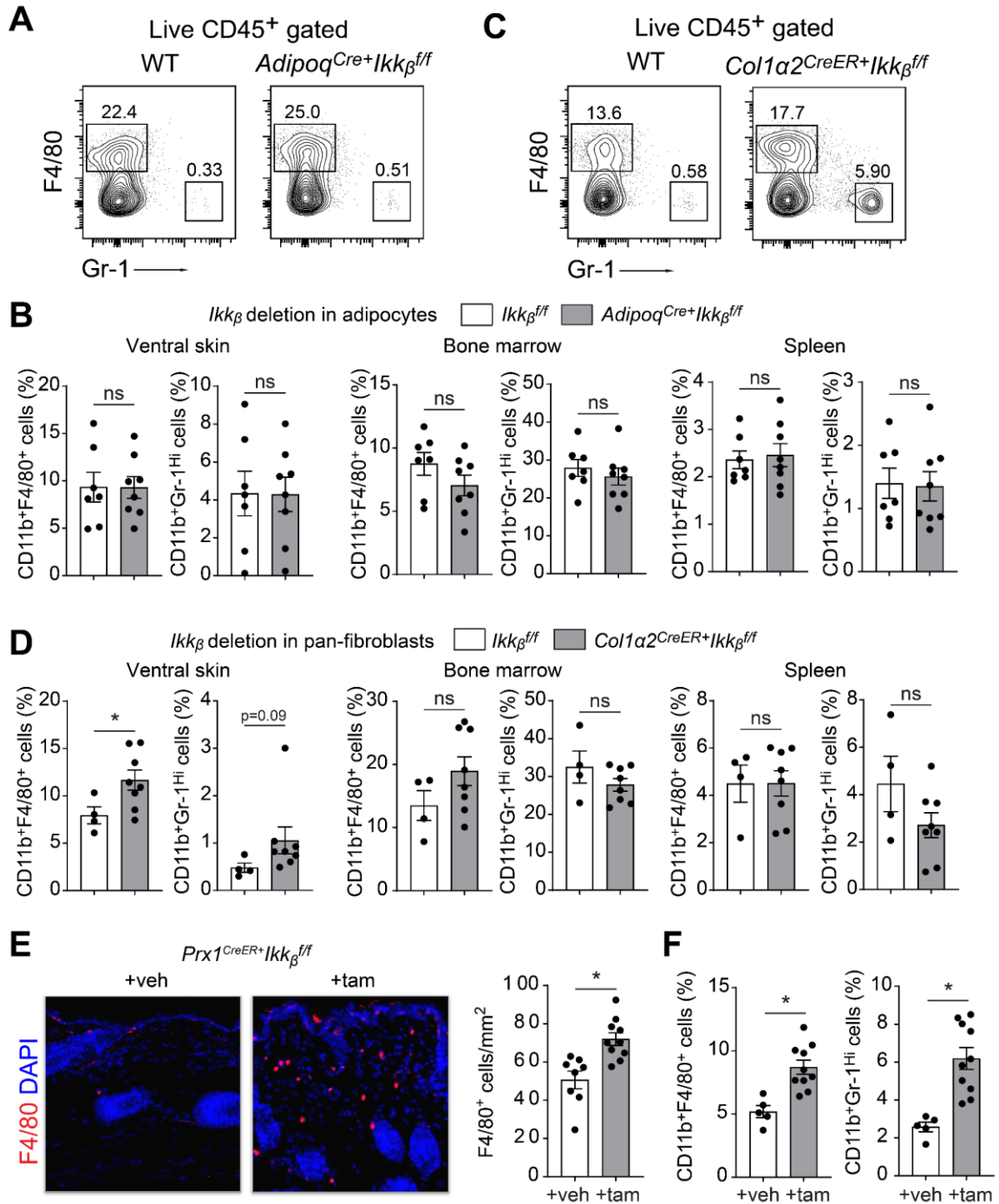


**Figure 3.7. NF-κB activity in fibroblasts, not in adipocytes, is critical for immune homeostasis. A, C.** Flow cytometry analysis of neutrophils and macrophages from ventral skin cell preparations in (A) control (WT) or experimental mice that had *Ikkb* deleted in adipocytes (*Adipoq*-*Cre*<sup>+</sup>*Ikkb*<sup>ff</sup>), and in (C) control or experimental mice that had *Ikkb* deleted in fibroblasts (*Col1a2**CreERT*<sup>+</sup>*Ikkb*<sup>ff</sup>) by tamoxifen injection at P1 and P3 (intragastric, 50ug per dose). Mice were euthanized at 4 week timepoints. **B, D.**

Quantification of macrophages (CD45<sup>+</sup>CD11b<sup>+</sup>F4/80<sup>+</sup>) and neutrophils (CD45<sup>+</sup>CD11b<sup>+</sup>Gr1<sup>Hi</sup>) per live cells from ventral skin (left), bone marrow (middle), and spleen (right). N = 7-8 (B) and 4-8 (D). **E.** Right, representative images of F4/80 immunopositive cells in ventral skin of *Prx1CreERT<sup>+</sup>Ikkb<sup>ff</sup>* mice that received corn oil (+veh) or tamoxifen (+tam, P1/3 injection at 50ug dose) and quantification of F4/80<sup>+</sup> cells per mm<sup>2</sup>. **F.** Quantification of macrophages and neutrophils by flow cytometry analysis in *Prx1CreERT<sup>+</sup>Ikkb<sup>ff</sup>* mice that received corn oil or tamoxifen. Mice were euthanized at 4 week time point. N = 5-10 each. Data are represented as mean ± SEM. \*p<0.05, ns = not significant; students t-test comparing WT to each respective experimental group.

### **3.8 Single cell RNA-sequencing reveals chemokine dysregulation by *Ikkb* deletion in fibroblasts**

To determine the transcriptomic changes caused by *Ikkb* deletion in *Prx1*<sup>+</sup> cells, I performed a droplet-based single cell RNA-sequencing (scRNA-seq) using cells isolated from ventral skin of *Prx1Cre<sup>+</sup>Ikkb<sup>ff</sup>* mice and littermate control groups that lacked Cre recombinase. Of 11084 cells captured, 1014 cells expressing >3-fold absolute median value of mitochondrial genes and number of gene expressed were removed, and 10070 cells were included in the final analysis (Figure 3.8A). Initial dimensionality reduction yielded 15 distinct cell clusters, which were evenly distributed by control and experimental grouping as well as by batch distinction (Figure 3.8B-D). Differentially expressed genes were calculated for each cluster to assign a cell type classification to each cluster, which revealed multiple fibroblast cell identity (cluster 1, 4, 5, 6) and myeloid cell identity (clusters 2, 3, 12, 13) (Figure 3.8E). Other clusters were more distinct in their specific gene expression, such as the exclusive expression of tropomyosin genes by cluster 10 (skeletal myocytes) and *Pecam1*, encoding for protein CD31, by cluster 11 (endothelial cells).

Next, I selected fibroblast population for further downstream analysis to understand the impact of *Ikkb* deletion in *Prx1*<sup>+</sup> cells. Clusters 1, 4, 5 and 6 were chosen by their

expression of putative fibroblast gene expression such as *Dcn*, *Colla2* and *Pdgfra* (Figure 3.9A). Further sub-clustering revealed 6 distinct clusters, in which cluster 3 and 4 belonged mostly to the experimental group whereas clusters 1, 2, 5 and 6 belonged to control groups (Figure 3.9B). Differential gene expression profile revealed that in cluster 3, several ECM-related genes were upregulated such as *Col6a5*, *Col6a6* and *Fn1* genes (Figure 3.9C). A distinct separation of cell clusters between wildtype and the experimental group suggested that *Ikkb* deletion in *Prx1*<sup>+</sup> cells may cause a significant shift in the transcriptome of skin fibroblasts overall. I next carried out a focused analysis by selecting fibroblasts that express *Prx1*<sup>+</sup> genes (Figure 3.10A) and compared that of a control group to the experimental group to explore potential causative mechanism of skin lesion development by *Prx1*<sup>+</sup> cells lacking *Ikkb* gene. I found that *Prx1*<sup>+</sup> fibroblasts in the experimental group had a higher expression of ECM genes such as *Col6a5*, *Fn1*, *Postn*, and importantly, inflammation-related genes such as *Ptx3* and *Ccl11* (Figure 3.10B, C). These data provide crucial evidence in linking *Ikkb* deletion in *Prx1*<sup>+</sup> cells and skin inflammation.

Although our *in vivo* data suggest a higher degree of inflammatory infiltration in the skin of *Prx1Cre*<sup>+</sup>*Ikkb*<sup>ff</sup> animals, the type of inflammation that is predominant is unknown. To address this, I selected immune cells from the scRNA-seq data by the expression of putative leukocyte marker *Ptprc*, encoding for CD45 protein. After selecting for CD45<sup>+</sup> cells and excluding collagen-expressing and clusters with <20 cells, I obtained 11 sub-clusters of immune cells (Figure 3.11A). Interestingly, cluster 1 was almost exclusively derived from control group whereas cluster 4 and 10 were from the experimental group (Figure 3.11B). Differentially expressed genes were examined amongst immune cell clusters to define cell identity, which revealed multiple subgroups of

monocyte/macrophage and T cell types, whereas mast cell (cluster 8) and plasma cell (cluster 11) identification was more distinct (Figure 3.11C). To further understand if the immune cells from the experimental group exhibit distinct inflammatory profile, I selected for monocyte/macrophage cell clusters or T cell clusters and analyzed the expression of known cytokines implicated in pro- and anti-inflammatory process. Of 2448 myeloid cells analyzed, there was a higher expression of *Il1b*, a pro-inflammatory cytokine, in the experimental group, whereas the expression of *Tgfb1*, an anti-inflammatory cytokine, was higher in the control group, and this was consistent throughout the batches (Figure 3.12A, B). These results are consistent with the in vivo data showing elevated dermal inflammation and point to a possible dysregulation in macrophage polarization towards M1 or M2. I next analyzed T cell population (1120 cells) and found a significant upregulation of cytokines implicated in type 2 immunity such as *Il5*, *Il13* and *Areg* (coding for amphiregulin) in the experimental group (Figure 3.12C, D). The results suggest that even though the flow cytometry and immunofluorescence results did not show a change in CD3<sup>+</sup> T cell numbers, their phenotype is biased towards type 2 immunity and thus may have significant impact on pathogenesis of dermal lesion.

The drastic impact on immune cell phenotype by the manipulation of Prx1<sup>+</sup> fibroblasts with *Ikkb* gene deletion suggested an important crosstalk between immune-mesenchymal cell to maintain skin homeostasis. I therefore tested the hypothesis that dermal fibroblasts may be important source of chemokine production. I screened for all known CCL and CXCL chemokines in all cell clusters and found that *Ccl11* was exclusively expressed in fibroblasts (cluster 1, 4, 5, 6) (Figure 3.13A). Although *Ccl2*, *Ccl7*, *Cxcl1* and *Cxcl12* were also expressed in the fibroblasts, their expression was higher



in mast cells, macrophages, smooth muscle cells and endothelial cells, respectively, suggesting that they are less likely to be responsible for the initiation of disease pathogenesis in *Prx1Cre<sup>+</sup>Ikkb<sup>ff</sup>* mice. CCL11, also known as eotaxin-1, is a potent chemoattractant for eosinophils (Ponath et al., 1996). I found that in the myeloid cell cluster, there was a higher average expression of *Ear2*, encoding for eosinophil cationic protein 2 (ECP2), in the experimental group, whereas the expression of other eosinophil granule enzymes such as *Mbp* and *Rnase2a* was less drastic (Figure 3.13B, C). Taken together, these provide evidence that *Prx1<sup>+</sup>* dermal fibroblasts may play an important role in regulating eosinophil recruitment and maintaining immune homeostasis in skin. Furthermore, the data implicate eosinophilic dysregulation by *Ikkb* deletion in *Prx1<sup>+</sup>* fibroblasts as a mechanism for proinflammatory macrophage infiltration and type 2 immune response to cause dermatitis.

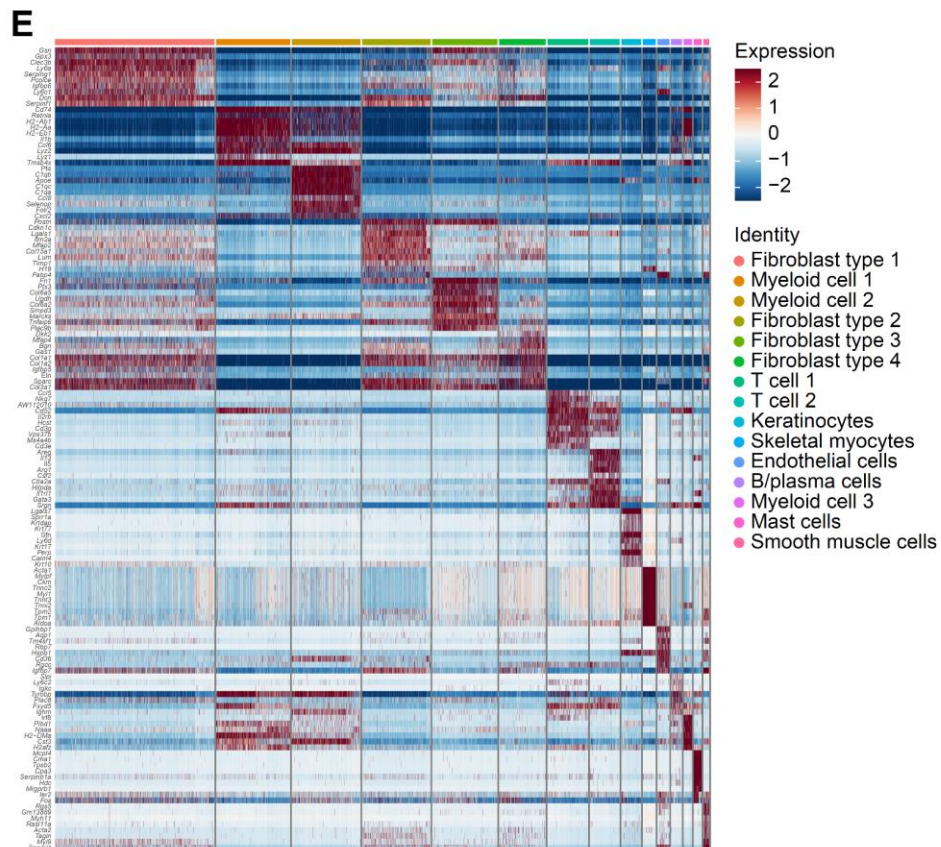
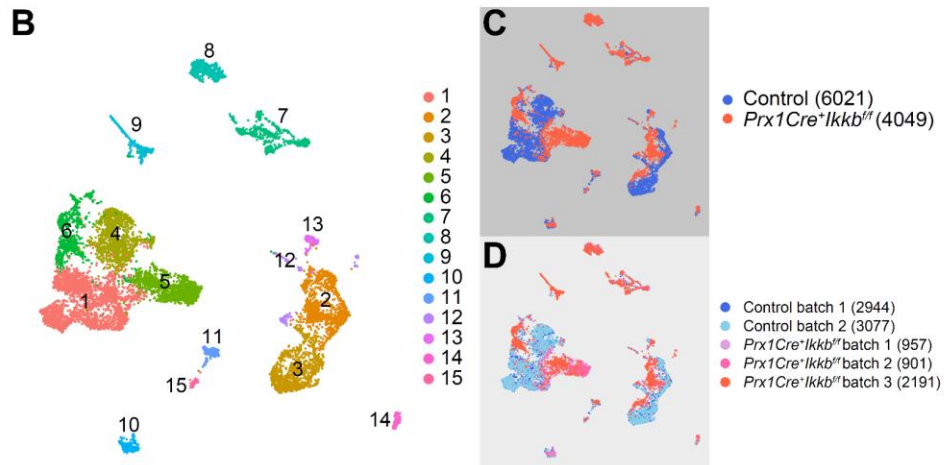
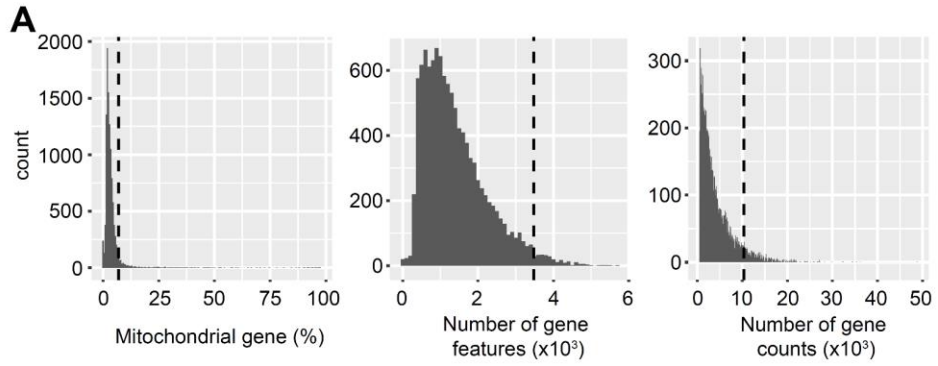


**Figure 3.8. scRNA-seq analysis of skin cells from control vs. *Ikkb* deleted mice.** **A.** Quality control parameters to exclude cells with high mitochondrial gene expression (apoptotic cells) and high mRNA features and counts (cell aggregates). The threshold was determined at 6.93% mitochondrial gene, 3476 features and 10392 gene counts. **B.** UMAP projection of 10070 cells resulting in 15 distinct clusters. **C-D.** UMAP projection by control or experimental (*Prx1Cre<sup>+</sup>Ikkb<sup>fl/fl</sup>*) grouping (C) or by batch numbers (D). Blue hues represent two control batches and red hues three experimental batches, and the number of cells captured is provided. **E.** Differentially expressed genes were calculated, and top 10 most highly expressed genes for each cluster is displayed. Cell identity was assigned based on expression of putative genes for each cell type. Each batch represent cells isolated from the ventral skin pooled from 2 mice that was split into duplicate prior to barcode capture on 10X Genomics machine. Scaled gene expression in z-values.

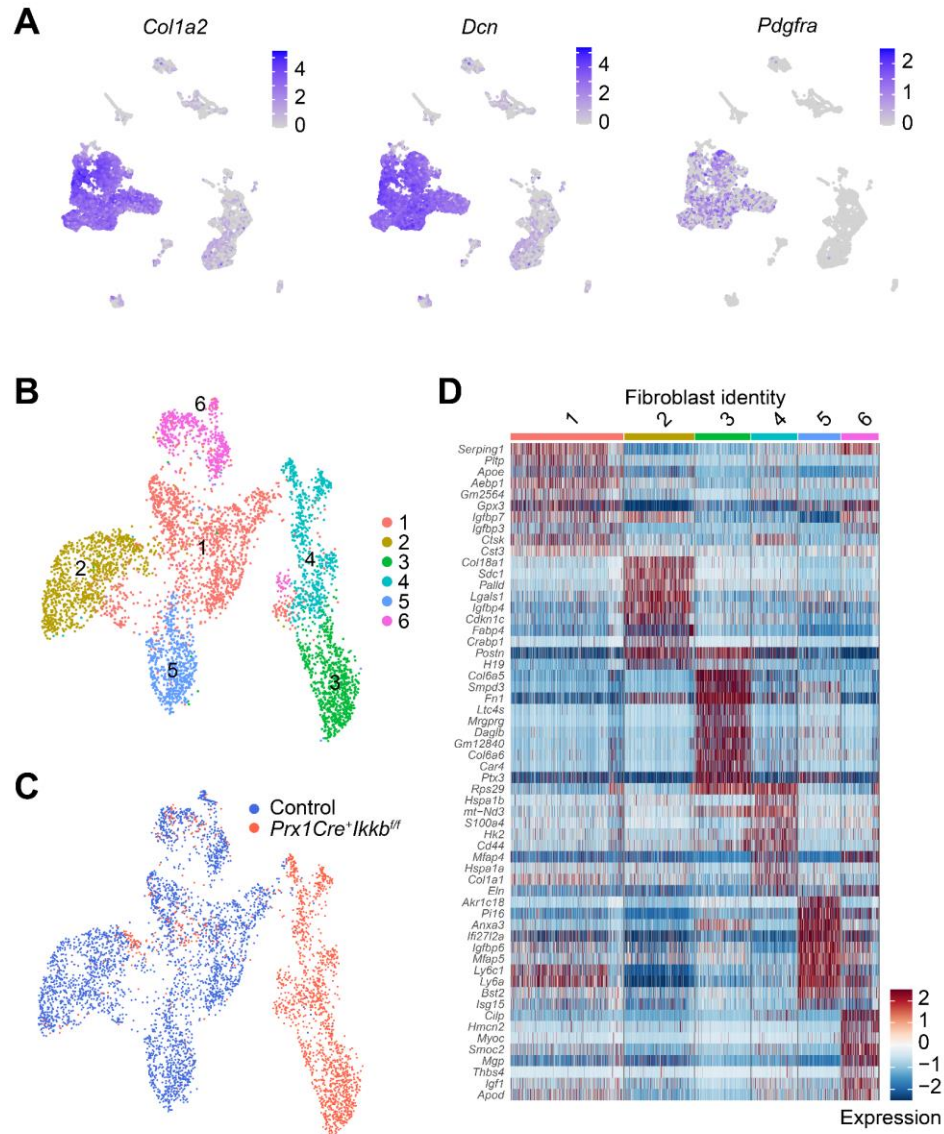


**Figure 3.9. Fibroblast heterogeneity and group-specific populations.** **A.** Feature plot of fibroblast-specific genes, *Col1a2*, *Dcn* (decorin), *Pdgfra* (CD140a). Note highly specific expression in fibroblast clusters originally belonging to cluster 1, 4, 5 and 6 from Figure 3.9.B. **B-C.** Sub-clustering of 5150 fibroblasts generated 6 distinct clusters (B), with clusters 1, 2, 5 and 6 mostly representing cells derived from control group whereas clusters 3 and 4 were exclusively derived from the experimental (*Prx1Cre<sup>+</sup>Ikkb<sup>fl</sup>*). **D.** Heat map of differentially expressed gene among 6 fibroblast clusters. Scaled gene expression is shown in z-values.

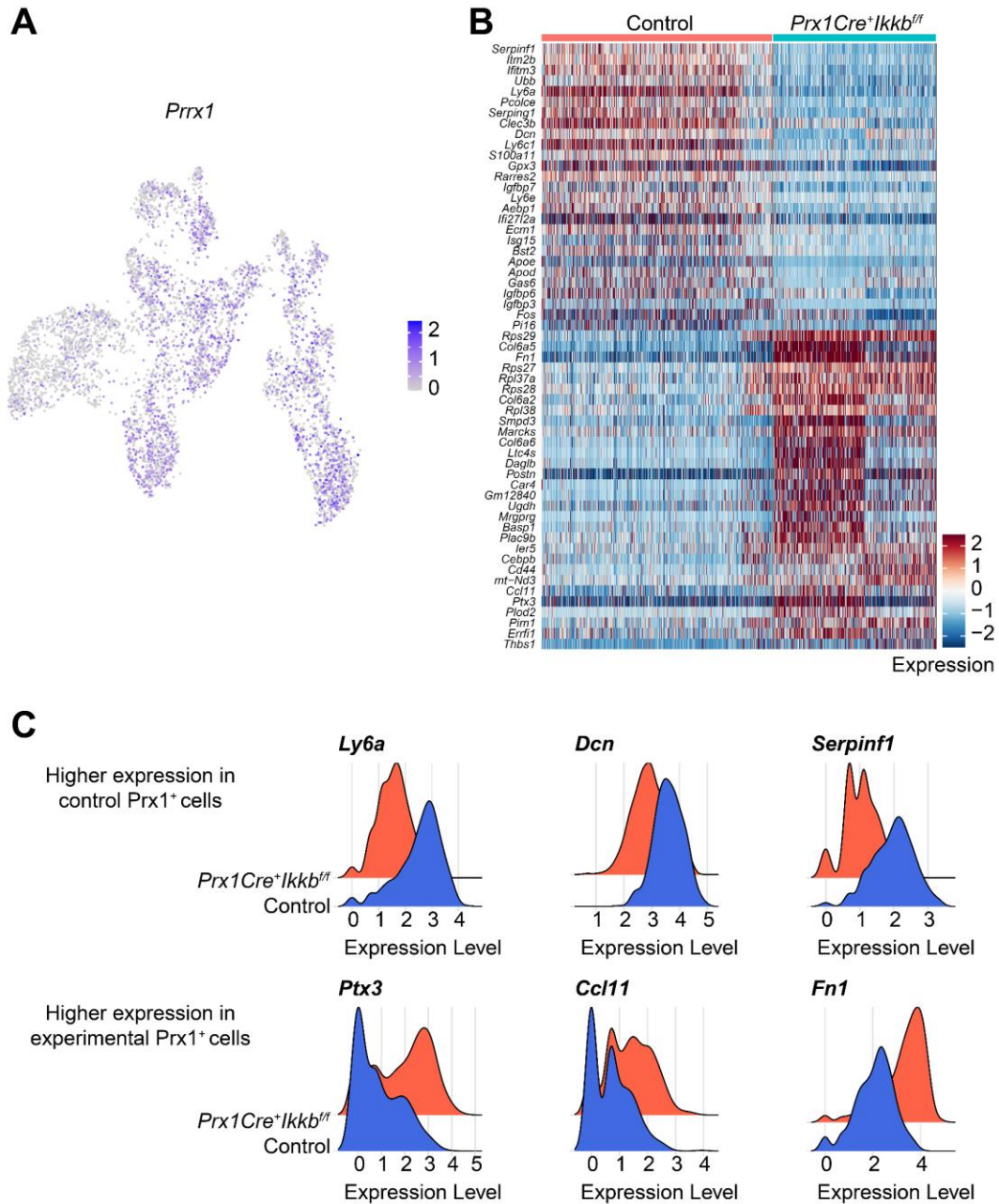


**Figure 3.10. Differentially expressed genes in  $Prx1^+$  fibroblasts between control and  $Ikkb^{fl/fl}$  mice. A.** Feature plot of  $Prx1$ -expressing cells in fibroblast subsets. **B.** Heat map showing differentially expressed genes in  $Prx1^+$  cells ( $Prrx1 > 1$ ) from control and experimental ( $Prx1Cre^+Ikkb^{fl/fl}$ ) mice. **C.** Ridge plot of three representative genes that are highly enriched in control  $Prx1^+$  fibroblasts (top row) and in experimental  $Prx1^+$  fibroblasts (bottom row).



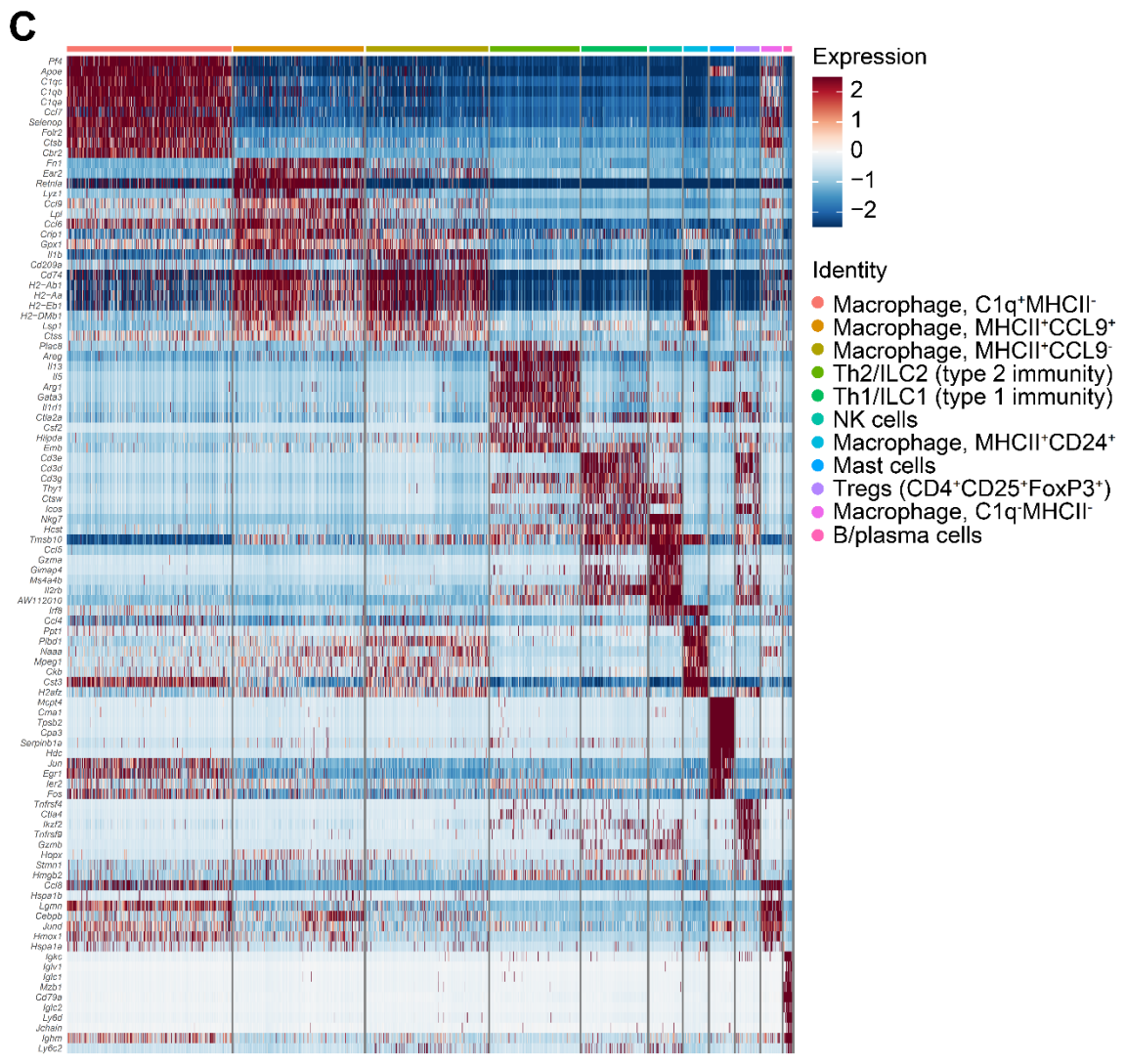
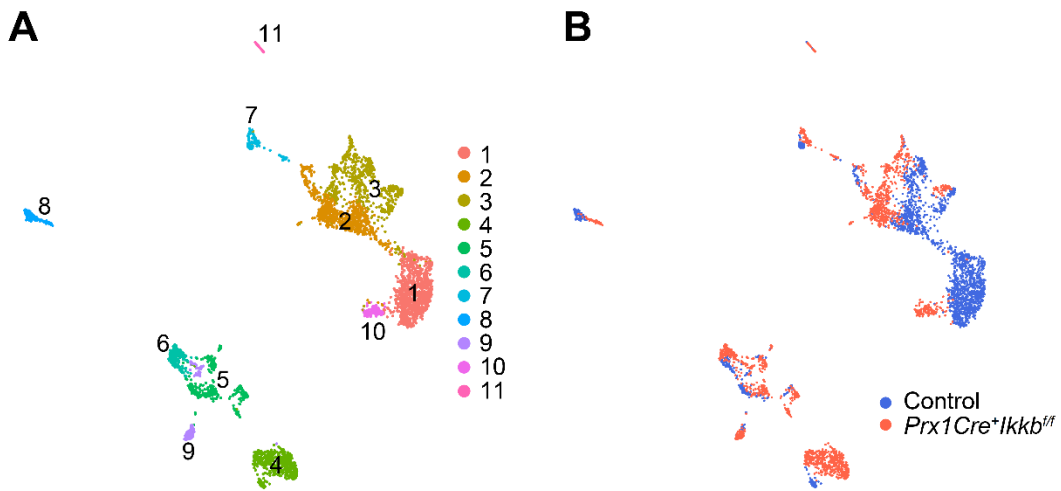


**Figure 3.11. Immune cell subclusters in the skin of control and *Ikkb* deleted mice.** **A.** UMAP projection of immune cells selected based on *Ptprc* (CD45) expression. 11 clusters were identified. **B.** UMAP projection of cells belonging to either control (blue) group or experimental (*Prx1Cre<sup>+</sup>Ikkb<sup>fl/fl</sup>*, red) group. **C.** Heat map of top 10 differentially expressed genes that are enriched for each cluster. Cell identity was assigned based on the expression of canonical markers such as *Tpsb2* (tryptase) for mast cells and immunoglobulin genes for B/plasma cells.

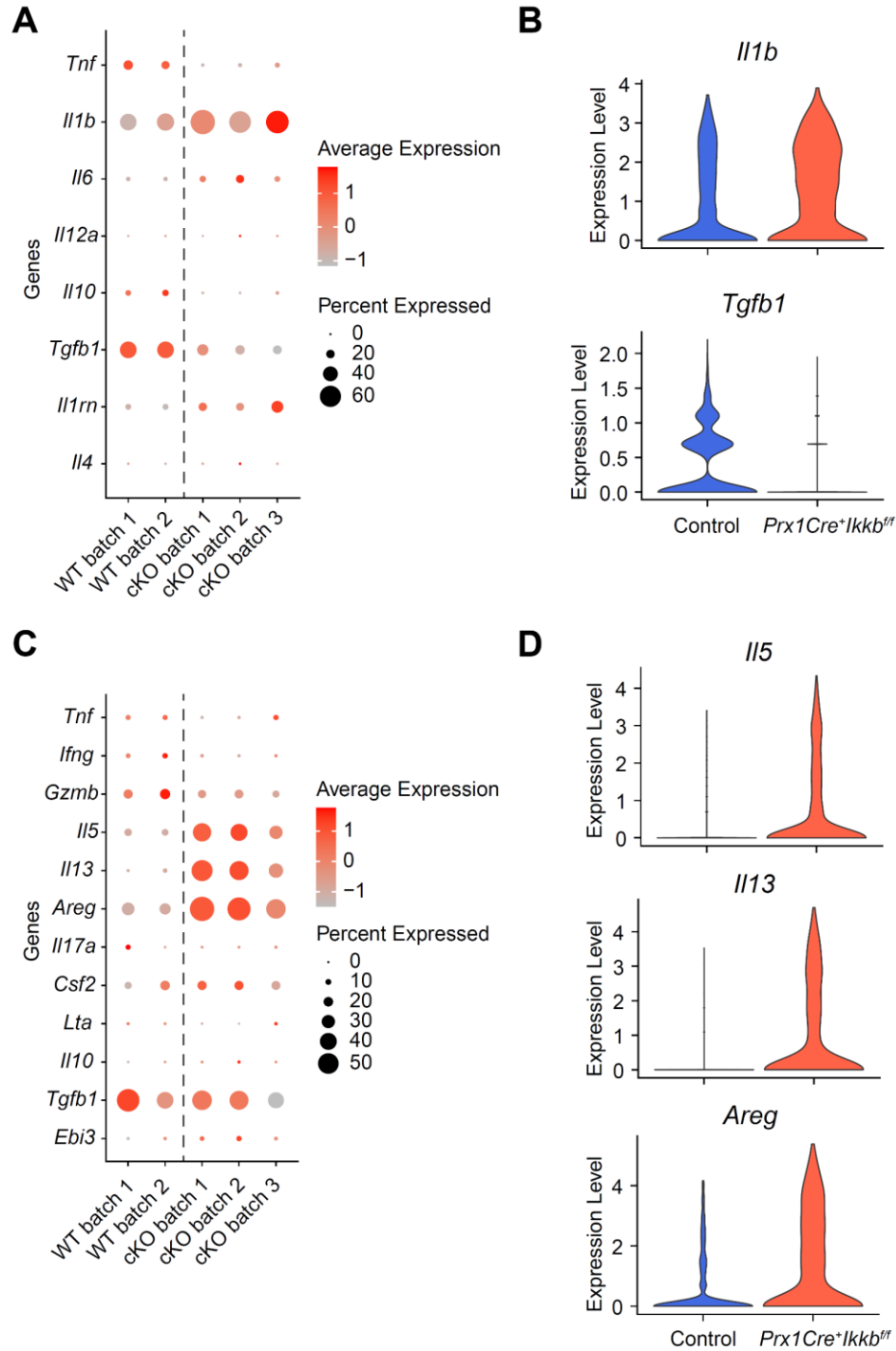


**Figure 3.12. *Ikkb* deletion in *Prx1*<sup>+</sup> cells upregulates pro-inflammatory cytokines in macrophages and causes type 2 immune response from lymphoid cells. **A.** Dot plot of pro- and anti-inflammatory cytokine genes (*Tnf*, *Il1b*, *Il6*, *Il12a* and *Il10*, *Tgfb1*, *Il1rn*, *Il4*, respectively) in myeloid cells, separated by batch groups. Gene expression was scaled. **B.** Violin plot for *Il1b*, showing significant upregulation in**



the myeloid cells of experimental (*Prx1Cre<sup>+</sup>Ikkb<sup>fl/fl</sup>*) group compared to control (top), and for *Tgfb1*, an anti-inflammatory cytokine that was upregulated in control group compared to experimental groups. Gene levels were normalized,  $p < 0.05$ , Wilcoxon rank sum test. **C.** Dot plot of genes implicated in type 1, 2, 3 immunity and anti-inflammatory response (type 1: *Tnf*, *Ifng*, *Gzmb*; type 2: *Il5*, *Il13*, *Areg*; type 3: *Il17a*, *Csf2*, *Lta*; anti-inflammatory: *Il10*, *Tgfb1*, *Ebi3*). Drastic upregulation of type 2 immunity genes are shown. **D.** Violin plot for the type 2 immunity genes (interleukin-5, interleukin-13, and amphiregulin) that were significantly upregulated in the experimental group compared to control.  $P < 0.05$ , Wilcoxon rank sum test.

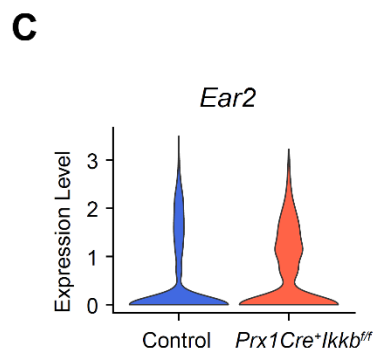
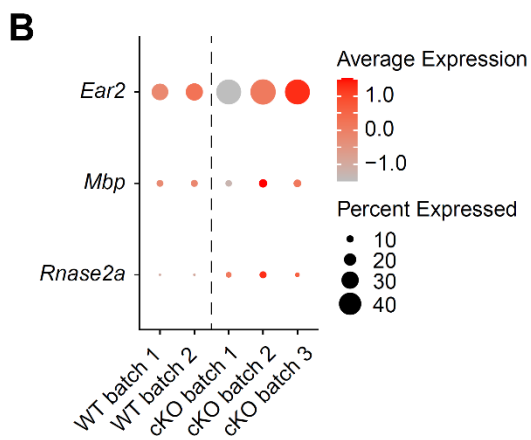
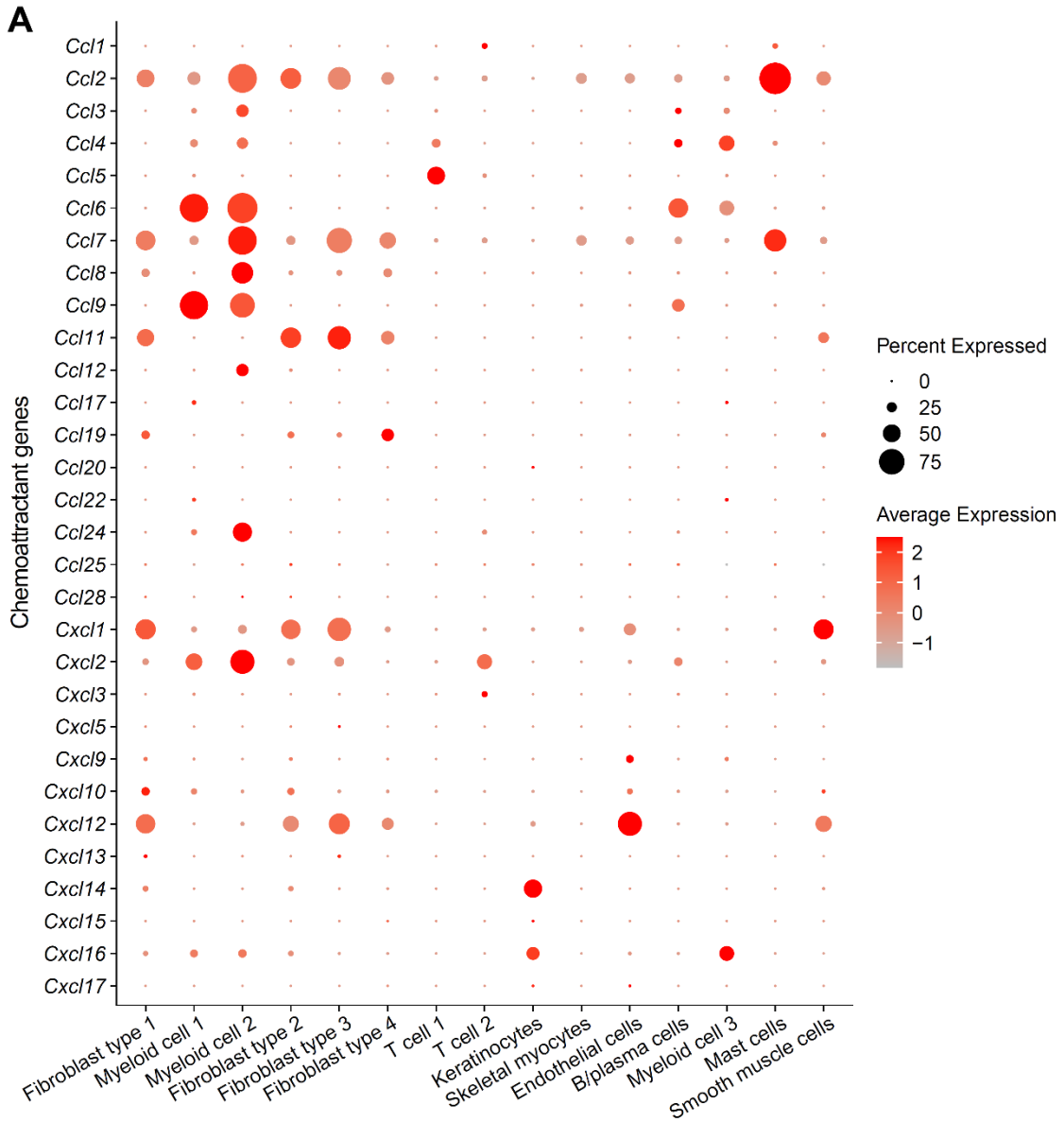


**Figure 3.13. Fibroblast-specific expression of *Ccl11* (eotaxin-1) and increased eosinophil-related genes in *Ikkb* deleted mice.** **A.** Dot plot demonstrating global screening of known CC and CXC chemokines in all cell types. *Ccl11* was the only gene that showed exclusive expression in fibroblast subsets, which are targeted by the Prx1Cre-mediated *Ikkb* deletion. **B.** Dot plot showing scaled expression of *Ear2*, *Mbp*, and *Rnase2a*, which encodes eosinophilic proteins. **C.** Violin plot showing normalized *Ear2* expression from control and experimental group.

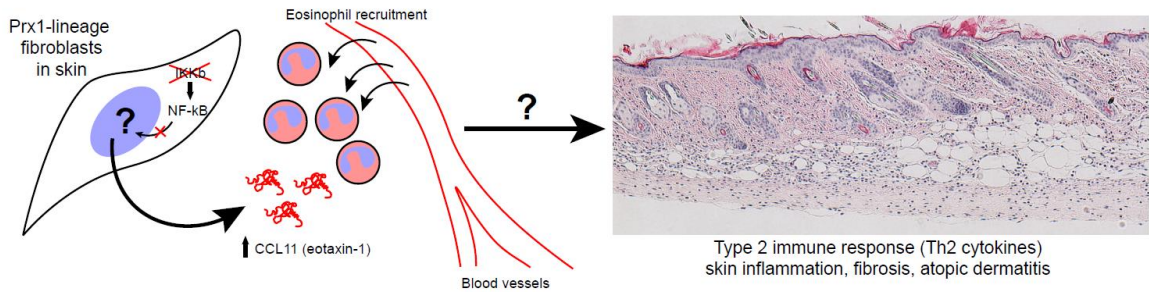


**Figure 3.14. *Ikkb* deletion in fibroblasts and experimental atopic dermatitis.** Cartoon depicting dysregulation of basal NF-kB and its impact on eosinophilia through CCL11. Eosinophilia is closely linked to Th2 immune response, the mechanism of which is yet unclear.

### 3.9 Discussion

Here I report that *Ikkb* deletion and thereby NF- $\kappa$ B (p65) inactivation in Prx1+ mesenchyme leads to an unexpected inflammatory lesion of the skin. As NF- $\kappa$ B is the master inflammatory transcription factor, I initially expected this to result in suppression of overt immune response. Paradoxically, I found that basal level of inflammation by NF- $\kappa$ B activation is necessary in the fibroblasts to maintain immune homeostasis of the skin. I demonstrated that skin fibrosis is the result of the early perinatal inflammation that develops in young (4 weeks old) experimental mice that had *Ikkb* deleted, and that the inflammation is characterized by the increase of myeloid cell populations such as F4/80+ cells and Gr1<sup>Hi</sup> neutrophils. Though there was systemic inflammation in the experimental mice, the effect is likely due to local changes in Prx1+ expressing cells because the lesion development was specific to the venter and not dorsum, consistent with the location-specific expression pattern of the Prx1-lineage cells. This is further supported by the use of inducible Prx1CreERT.*Ikkb* model, in which I observed a lack of systemic inflammation whereas skin inflammation was induced. Moreover, I demonstrated that the *Ikkb* deletion in *Coll1a2*+ fibroblasts, but not mature adipocytes, caused skin inflammation, suggesting that Prx1+ dermal fibroblasts were responsible for the phenotype. Single cell RNA sequencing revealed an emergence of *Col6a5*+, *Fnl1*-high fibroblast population and immune cells that were characterized by *Il1b*-high inflammatory cells and type 2 immunity by the expression of *Areg*, *Il5* and *Il13*. Importantly, I found that the Prx1+ fibroblasts with *Ikkb* deletion had high expression of *Ccl11*, which is an eosinophil attractant, suggesting that the early infiltration of eosinophils by the fibroblast dysregulation may be an important precipitating event prior to skin lesion development. Overall, our findings demonstrate that

the basal NF- $\kappa$ B activity in fibroblasts is critical in maintaining immune homeostasis in skin by preventing an hyperactive Th2 response (Fig 3.14).

The skin lesion observed in the Prx1Cre.Ikbb<sup>f/f</sup> mice resembles clinical atopic dermatitis, which is characterized by type 2 immunity, eosinophilia, and IgE increase (Kim et al., 2019). Although the pathogenesis of AD is incompletely understood, it is well accepted that type 2 immunity plays a critical role and that interfering with it alleviates severe AD symptoms (Gooderham et al., 2018). In addition to type 2 immune cytokines such as IL-4, IL-5 and IL-13, involvement of other cell types such as Th17, Th22 and ILC2 has been demonstrated in AD-like skin lesions (Guttman-Yassky et al., 2018; Koga et al., 2008). Despite the advances made, very little attention has been paid to fibroblast dysfunction as a potential mechanism behind AD. A recent study demonstrated that Ikbb deletion in facial dermal fibroblasts targeted by Nestin-Cre results in skin lesion that mirrors AD-like lesions by the upregulation of type 2 immune cytokines (Nunomura et al., 2019). Though the study reports a similar phenotype observed in our mouse model, the mechanism by which fibroblasts lead to immune dysfunction and hyperinflammation is still unclear.

Our scRNA-seq data demonstrated that Prx1+ cells with Ikbb deleted exhibit a significantly higher expression of *Ccl11* mRNA. Interestingly, fibroblasts were the major source of *Ccl11* in skin. Given that CCL11 is a potent eosinophil attractant, and that eosinophils are known source of IL-4, a type 2 immune cytokine (Goh et al., 2013; Piehler et al., 2011), it is possible that their initial recruitment may be responsible for the AD-like lesion that is characterized by Th2 response. Classical model of murine AD involves cutaneous administration of ovalbumin as allergen (Wang et al., 2007), and mice that lack

CCR3 (receptor for CCL11 for eosinophil recruitment) still develop AD-like skin lesion in absence of eosinophilia (Ma et al., 2002). While this is in contrary to the possible contribution of eosinophils in AD-like lesion from our model, it poses two possibilities: 1) fibroblast-mediated AD-like lesion may involve different mechanisms compared to classical allergen-induced AD models, and 2) our model of skin lesion may represent an eosinophilic disease and that AD-like lesion is a secondary effect. Investigating mesenchymal cells as a vital source of CCL11 is an active area of research, particularly in hepatic fibrosis and thermal adaptation of the white adipose tissue (Gieseck et al., 2016; Huang et al., 2017). Whether they are important in dermatologic diseases in which fibroblast NF- $\kappa$ B activity is dysregulated will require further investigations, possibly by blocking CCL11 with neutralizing antibody and monitoring disease progression.

In summary, I report an unexpected finding where NF- $\kappa$ B inactivation in Prx1+ cells led to hyper-inflammation and fibrosis in the skin characterized by pro-inflammatory macrophages and Th2 responses, similar to AD-like lesions. The skin inflammation was specific to ventral skin, where Prx1+ fibroblasts are found, thus it is unlikely that the lesion development is a result of a systemic inflammation. *Ikkb* deletion in *Coll1a2*-expressing fibroblasts, but not adiponectin-expressing adipocytes, resulted in skin inflammation, ruling out adipocytes as a potential source of immune dysregulation. The results suggest that basal level of inflammation in fibroblasts by *Ikkb*-NF- $\kappa$ B pathway is essential in subduing overt skin inflammation, and that this may involve trafficking eosinophil recruitment by the expression of CCL11. Future investigations could explore possible therapeutic methods to prevent disease progression by blocking fibroblast-specific chemokines, eg. CCL11, to prevent eosinophilia and subsequent Th2 immune response.

### 3.10 Methods

**Animal studies.** All animal experiments were carried out conforming to a protocol approved by the University of Pennsylvania Institutional Animal Care and Use Committee. The following mice were purchased from Jackson Laboratory: *B6.Cg-Tg(Prrx1-cre)1Cjt/J (Prx1Cre)*, *B6.Cg-Tg(Prrx1-cre/ERT2,-EGFP)1Smkm/J (Prx1CreER)*, *B6.Cg-Gt(ROSA)26Sor<sup>tm9(CAG-tdTomato)Hze/J (R26<sup>tdTomato</sup>)</sup>*, *Tg(Adipoq-cre)1Evdr (Adipoq-Cre)*, *Tg(Coll1a2-cre/ERT,-ALPP)7Cpd/J (Coll1a2-CreER)*. Floxed *Ikk $\beta$*  mice (*Ikk $\beta$ <sup>ff</sup>*) were obtained from Dr. Michael Karin (UCSD, La Jolla). Mice were housed in regular corn bedding and were euthanized at 1 day, 4 weeks, and 16-20 weeks old time points. In another set of experiment, animals were housed in Cellu-nest<sup>TM</sup> (Shepherd Specialty Papers) soft bedding from birth to 4<sup>th</sup> week euthanasia time point.

**Mechanics.** Ventral skins of 12-14 weeks old mice (wildtype and *Prx1Cre<sup>+</sup>Ikk $\beta$ <sup>ff</sup>*) were harvested and transported in 60% ethanol solution to Penn Center for Musculoskeletal Disorders Biomechanics Core for mechanical testing. Skin was trimmed to dimensions as shown in Appendix 1. The sample was pre-loaded at 0.1mm/sec to 0.1N, held for 120 seconds, and ramped to fail at 0.24mm/sec, with image captured 4 frames/sec.

**Immunofluorescence.** Full thickness skin samples were harvested and oriented in a sagittal plane. The samples were fixed in 10% formalin at 4°C for 24h, washed and processed in paraffin or frozen blocks. Immunofluorescence was performed using following primary antibodies: anti-RFP (600-901-379, Rockland), anti-NF- $\kappa$ B (ab16502, Abcam), anti-F4/80 (ab6640, Abcam), anti-CD4 (ab183685, Abcam), anti-MPO (ab9535, Abcam), anti-CD34 (ab8158, Abcam), anti-vimentin (ab39376, Abcam), and anti-perilipin (ab61682, Abcam). Species-specific IgG control was used for all experiments with

negative background signal. Percent-positive cells and absolute numbers were quantified using NIS-Element software (Nikon).

**Flow cytometry.** Ventral skin (20x20mm) was isolated and minced to approximately 1x1mm dimension. The tissues were enzymatically digested at 37°C with constant agitation in DMEM media containing collagenase type IV (3.2mg/ml, Gibco) and dispase (2.6mg/ml, Sigma) for 1 hr, with 10 sec of vortex every 15 min. Splenocytes were prepared by homogenizing spleen with slide surface, and bone marrow cells were prepared by flushing femoral marrow space with a syringe. Cells were filtered through 70 um nylon mesh, and red blood cells were lysed in ACK buffer and washed. Prior to staining, Fc receptors were blocked with anti-CD16/32 IgG (clone 93), and dead cells were labeled with Zombie Aqua™ (Biolegend). The cells were stained with the following antibodies purchased from Biolegend unless indicated otherwise: anti-CD3 (clone GK1.5), anti-CD45 (clone 30-F11), anti-CD11b (clone M1/70), anti-Gr-1 (clone RB6-8C5), anti-F4/80 (clone Cl:A3-1, BioRad). Isotype IgG was used as a control.

**Tamoxifen injection.** For perinatal gene deletion, 50ug of tamoxifen was administered (50ul of 1mg/ml) via injecting directly into the stomach of neonatal mice that were 1-day old, and a second dose was given on 3<sup>rd</sup> day.

**Peripheral blood analysis.** Immediately after euthanizing the retro-orbital blood was collected using heparin-coated capillary tubes (Fisher Scientific) into EDTA-covered collection tube (Sarstedt Inc.) to prevent coagulation. Approximately 200ul of blood samples were obtained from each animal. The samples were analyzed the same day on Sysmex XT-2000iV Hematology Analyzer.



**Single cell RNA sequencing.** Cells from ventral skin of B6 mice were isolated by enzymatic digestion as described above and immediately sorted on FACS Aria II SORP instrument to exclude debris, dead cells (DAPI-positive) and aggregates. Single cell barcode capture was performed on a GemCode instrument platform with the 10X single-cell 3' v2 chemistry (10X Genomics). cDNA library was prepared and sequenced on HiSeq 4000 instrument (Illumina). Single cell barcode capture, quality control using BioAnalyzer, cDNA amplification and RNA sequencing were performed at the University of Pennsylvania Next Generation Sequencing Core. The resulting raw reads were aligned and filtered, and unique molecular identifier (UMI) counts were obtained using Cell Ranger software (10X Genomics). Data were analyzed using Seurat package (version 3.0). To remove doublets and broken cells, any cells with insufficient number of genes (<500/cell) and unusually high number of UMI counts or percent of mitochondrial gene expression (above 3 median absolute deviations) were discarded from downstream analyses. Prior to cell clustering, gene expression profile was normalized and transformed followed by principal component analysis (PCA) for dimensionality reduction. A shared nearest neighbor (SNN) modularity optimization based clustering algorithm was used to identify cell clusters (Waltman and van Eck, 2013). Cell clusters were visualized using uniform manifold approximation and projection (UMAP) algorithm (McInnes et al., 2018). Visualization of the data was done using Seurat functions such as Heatmap, Featureplot, Vlnplot, Ridgeplot and Dotplot. Differentially expressed genes were calculated using Findmarker function and Wilcoxon test.

**Statistical analyses.** Statistical analysis was performed using Prism software (GraphPad-ver.7.03). All data are expressed as the mean  $\pm$  SEM. Student's T-test was performed in

comparing two groups (wildtype versus experimental mice).  $P < 0.05$  was considered statistically significant. Individual animal was used as a unit of measurement, and sex was not considered as a factor in the analyses.

## CHAPTER 4: CONCLUSION AND FUTURE DIRECTIONS

### 4.1 Summary

Here I sought to investigate the role of *Ikkb*/NF- $\kappa$ B in Prx1+ mesenchymal cells in bone and skin. The most striking difference between these two models was the finding that *Ikkb* deletion caused a significant skin lesion development under normoglycemic, basal condition whereas it had little to no effect in long bones. The result suggested a protective role of *Ikkb*/NF- $\kappa$ B in Prx1+ cells in skin under homeostatic condition. In sharp contrast, fracture induction in diabetic mice caused hyper-activation of NF- $\kappa$ B in Prx1+ cells, and *Ikkb* deletion prevented this and improved fracture healing. Thus, under pathologic injury perturbation, NF- $\kappa$ B plays a detrimental role in Prx1+ cells of the skeleton. Taken together, these models demonstrate a functional duality of *Ikkb*/NF- $\kappa$ B in Prx1+ mesenchymal cells, in which their protective or negative roles are heavily dependent on biological niche and perturbation status.

I found that in bone, *Ikkb* deletion and thereby NF- $\kappa$ B inactivation in Prx1+ SSCs had little to no effect under basal condition. This was evident by the lack of effect in skeletal development and by the minimal NF- $\kappa$ B activation upon fracture injury in normoglycemic mice. These findings suggest that NF- $\kappa$ B activation may be dispensable in the SSCs in order to maintain skeletal homeostasis. In contrast, diabetes caused a drastic hyper-activation of NF- $\kappa$ B in these SSCs and delayed early fracture healing, which was reversed by *Ikkb* deletion in Prx1+ SSCs. Mechanistically this was due to NF- $\kappa$ B-mediated downregulation of TGF $\beta$ 1 by the SSCs, an important cytokine that is responsible for resolution of inflammation. Further experiments revealed that TGF $\beta$ 1 expression by the SSCs is critical for regulating macrophage polarization towards pro-resolving M2

phenotype, demonstrating an important interplay between mesenchymal and immune cells. Thus, diabetes causes NF- $\kappa$ B over-activation in Prx1+ cells during fracture healing, which plays a negative role in Prx1+ SSCs by interfering with their immune-modulatory function and delaying fracture healing.

In skin, *Ikkb* deletion and NF- $\kappa$ B inactivation in Prx1+ cells caused an unexpected dermal lesion, suggesting a protective role of NF- $\kappa$ B under basal condition. The lesion was characterized by exaggerated myeloid and type 2 immune response, which may be due to a dysregulation of eosinophil chemotaxis by the dermal fibroblasts. The findings were unexpected because *Ikkb*/NF- $\kappa$ B is often implicated in mediating inflammatory reaction and deleting it would presumably suppress, not promote, inflammation. While unexpected, the concept is not foreign – inflammation is an essential component of the immune system that is beneficial when activated transiently, but harmful if persistent. Indeed, hepatocytes require basal inflammatory signaling through IKK-beta for normal glucose homeostasis to occur (Liu et al., 2016). While the results clearly demonstrate an important role of *Ikkb*/NF- $\kappa$ B for normal skin homeostasis, the precise mechanism of inflammation by the *Ikkb* deletion in dermal fibroblasts warrant further investigation.

What is the reason for differential tissue response by the *Ikkb* deletion in Prx1+ cells? A likely explanation is the distinct identity of Prx1+ cells in the bone and skin. Prx1+ cells are fibroblastic cells of dermis and hypodermis (subcutaneous adipose layer), which are scar-forming and possess little regenerative potential. The skin acts as an external barrier to a myriad of microbial insult and/or allergens, thus these dermal Prx1+ cells may be primed to regulate basal level of innate immunity by the activity of *Ikkb*/NF- $\kappa$ B. In the

long bones, Prx1 labels periosteal SSCs, which may be less primed for functions that require Ikkb/NF-kB activity to maintain skeletal homeostasis.

The contrasting roles of NF-kB have significant implications for future therapeutic approaches targeting Ikkb/NF-kB. As diabetes causes aberrant activation of NF-kB, the use of Ikkb inhibitors may be an effective treatment strategy to prevent diabetic complications in healing wounds. However, its inhibition in skin may have an untoward effect because under homeostatic condition, the basal activity of NF-kB is critical in regulating the number of myeloid cell infiltrate. Conversely, although our data suggest that the use of NF-kB pathway agonist may be implicated in treating eosinophilic/dermatologic disorders where Ikkb gene is absent in fibroblasts, extra caution must be applied in patients suffering from other comorbidities such as diabetes. As NF-kB can be both protective and detrimental, future investigations are warranted to identify downstream effector signals as an alternative therapeutic target to Ikkb/NF-kB.

#### **4.2 Future directions on diabetic healing and NF-kB**

Diabetes is a significant risk factor for periodontal disease and negatively affects oral wound healing. While the effect of diabetes on keratinocytes is well studied, the impact of diabetes on oral fibroblasts is not as clear. Given that fibroblasts are the most common cell type in the connective tissue layer of gingiva and that diabetes delays oral wound healing, it is logical to hypothesize that diabetes may negatively affect gingival fibroblasts that participate in oral wound healing. Similar to the hyperactivation of NF-kB in SSCs and the subsequent impact on fracture healing, it is possible that NF-kB may be involved in fibroblasts during diabetic oral wound healing. However, oral wound healing differs from fracture healing in that the oral cavity is rich in microflora that may influence the role

of NF- $\kappa$ B in oral fibroblasts. It is highly likely that the oral fibroblasts require NF- $\kappa$ B activity under physiologic condition to respond accordingly to commensal microbiome during wound healing. Thus, it would be critical to delineate the negative impact of diabetes on NF- $\kappa$ B versus the physiologic role of NF- $\kappa$ B in oral fibroblasts by the use of antibiotic treatment during wound healing. These future investigations may reveal a significant role of oral fibroblasts that are responsible for accelerated wound healing, and the mechanism by which diabetes affects it.

#### **4.3 Future directions on skin lesion by *Ikkb* deletion**

The study presented here provides a clear rationale to investigate fibroblast-eosinophil interaction that may be responsible for the dermatologic phenotype in mice that lack *Ikkb* gene. One advantage of using mouse model in which *Ikkb* is deleted in *Prx1* is that it closely mirrors human dermatitis model. Other murine models investigating the role of NF- $\kappa$ B had focused on keratinocytes, which result in severely widespread skin lesion soon after birth and subsequent impact on postnatal growth and animal survivability. In sharp contrast, atopic dermatitis in humans develops often during adolescence without significant developmental issues. This is similar to our observation in which young mice had inflammation in the skin but not in the neonatal mice. It is possible that the fibroblast dysregulation by the lack of basal NF- $\kappa$ B activity may be the underlying reason for the large proportion of clinical atopic dermatitis cases, which remains to be proven. Our future investigations will focus on the impact of *Ikkb* deletion on eosinophil population. While I report here that the significant myeloid cell infiltration in the experimental mice by the use of F4/80 antibody, a common marker for pan-macrophage, it is known that eosinophils also express F4/80. If I find that high proportion of F4/80+ cells are in fact eosinophils, it would

build a strong case for aberrant upregulation of CCL11 by the fibroblast to be the pathogenic mechanism for the skin inflammation in the experimental mice. Further experiments will investigate if blocking CCL11 with neutralizing antibody reverses the inflammation and clinical lesion development in the experimental mice, the outcome of which may lead to development of monoclonal antibody targeting CCL11 to treat eosinophilic skin diseases.

## REFERENCES

- Alblowi, J., Kayal, R.A., Siqueira, M., McKenzie, E., Krothapalli, N., McLean, J., Conn, J., Nikolajczyk, B., Einhorn, T.A., Gerstenfeld, L., et al. (2009). High levels of tumor necrosis factor-alpha contribute to accelerated loss of cartilage in diabetic fracture healing. *The American journal of pathology* *175*, 1574-1585.
- Alblowi, J., Tian, C., Siqueira, M.F., Kayal, R.A., McKenzie, E., Behl, Y., Gerstenfeld, L., Einhorn, T.A., and Graves, D.T. (2013). Chemokine expression is upregulated in chondrocytes in diabetic fracture healing. *Bone* *53*, 294-300.
- Alvarez, R., Lee, H.L., Hong, C., and Wang, C.Y. (2015). Single CD271 marker isolates mesenchymal stem cells from human dental pulp. *International journal of oral science* *7*, 205-212.
- Arnold, L., Henry, A., Poron, F., Baba-Amer, Y., van Rooijen, N., Plonquet, A., Gherardi, R.K., and Chazaud, B. (2007). Inflammatory monocytes recruited after skeletal muscle injury switch into antiinflammatory macrophages to support myogenesis. *The Journal of experimental medicine* *204*, 1057-1069.
- Baker, R.G., Hayden, M.S., and Ghosh, S. (2011). NF-kappaB, inflammation, and metabolic disease. *Cell metabolism* *13*, 11-22.
- Bannon, P., Wood, S., Restivo, T., Campbell, L., Hardman, M.J., and Mace, K.A. (2013). Diabetes induces stable intrinsic changes to myeloid cells that contribute to chronic inflammation during wound healing in mice. *Disease models & mechanisms* *6*, 1434-1447.
- Beg, A.A., Sha, W.C., Bronson, R.T., Ghosh, S., and Baltimore, D. (1995). Embryonic lethality and liver degeneration in mice lacking the RelA component of NF-kappa B. *Nature* *376*, 167-170.
- Chang, J., Liu, F., Lee, M., Wu, B., Ting, K., Zara, J.N., Soo, C., Al Hezaimi, K., Zou, W., Chen, X., et al. (2013). NF-kappaB inhibits osteogenic differentiation of mesenchymal stem cells by promoting beta-catenin degradation. *Proceedings of the National Academy of Sciences of the United States of America* *110*, 9469-9474.
- Chang, J., Wang, Z., Tang, E., Fan, Z., McCauley, L., Franceschi, R., Guan, K., Krebsbach, P.H., and Wang, C.Y. (2009). Inhibition of osteoblastic bone formation by nuclear factor-kappaB. *Nature medicine* *15*, 682-689.
- Chen, C., Wang, D., Moshaverinia, A., Liu, D., Kou, X., Yu, W., Yang, R., Sun, L., and Shi, S. (2017). Mesenchymal stem cell transplantation in tight-skin mice identifies miR-151-5p as a therapeutic target for systemic sclerosis. *Cell research* *27*, 559-577.
- Chen, F.E., Huang, D.B., Chen, Y.Q., and Ghosh, G. (1998). Crystal structure of p50/p65 heterodimer of transcription factor NF-kappaB bound to DNA. *Nature* *391*, 410-413.



- Chiesa Fuxench, Z.C., Block, J.K., Boguniewicz, M., Boyle, J., Fonacier, L., Gelfand, J.M., Grayson, M.H., Margolis, D.J., Mitchell, L., Silverberg, J.I., et al. (2019). Atopic Dermatitis in America Study: A Cross-Sectional Study Examining the Prevalence and Disease Burden of Atopic Dermatitis in the US Adult Population. *J Invest Dermatol* 139, 583-590.
- Chow, A., Lucas, D., Hidalgo, A., Mendez-Ferrer, S., Hashimoto, D., Scheiermann, C., Battista, M., Leboeuf, M., Prophete, C., van Rooijen, N., et al. (2011). Bone marrow CD169+ macrophages promote the retention of hematopoietic stem and progenitor cells in the mesenchymal stem cell niche. *The Journal of experimental medicine* 208, 261-271.
- Claes, L., Recknagel, S., and Ignatius, A. (2012). Fracture healing under healthy and inflammatory conditions. *Nature reviews. Rheumatology* 8, 133-143.
- Colnot, C. (2009). Skeletal cell fate decisions within periosteum and bone marrow during bone regeneration. *Journal of bone and mineral research : the official journal of the American Society for Bone and Mineral Research* 24, 274-282.
- Cramer, C., Freisinger, E., Jones, R.K., Slakey, D.P., Dupin, C.L., Newsome, E.R., Alt, E.U., and Izadpanah, R. (2010). Persistent high glucose concentrations alter the regenerative potential of mesenchymal stem cells. *Stem cells and development* 19, 1875-1884.
- Currie, J.D., Grosser, L., Murawala, P., Schuez, M., Michel, M., Tanaka, E.M., and Sandoval-Guzman, T. (2019). The Prrx1 limb enhancer marks an adult subpopulation of injury-responsive dermal fibroblasts. *Biol Open* 8.
- Duchamp de Lageneste, O., Julien, A., Abou-Khalil, R., Frangi, G., Carvalho, C., Cagnard, N., Cordier, C., Conway, S.J., and Colnot, C. (2018). Periosteum contains skeletal stem cells with high bone regenerative potential controlled by Periostin. *Nature communications* 9, 773.
- Durland, J.L., Sferlazzo, M., Logan, M., and Burke, A.C. (2008). Visualizing the lateral somitic frontier in the Prx1Cre transgenic mouse. *J Anat* 212, 590-602.
- Edin, S., Wikberg, M.L., Dahlin, A.M., Rutegard, J., Oberg, A., Oldenborg, P.A., and Palmqvist, R. (2012). The distribution of macrophages with a M1 or M2 phenotype in relation to prognosis and the molecular characteristics of colorectal cancer. *PloS one* 7, e47045.
- Einhorn, T.A., and Gerstenfeld, L.C. (2015). Fracture healing: mechanisms and interventions. *Nature reviews. Rheumatology* 11, 45-54.
- El-Osta, A., Brasacchio, D., Yao, D., Poci, A., Jones, P.L., Roeder, R.G., Cooper, M.E., and Brownlee, M. (2008). Transient high glucose causes persistent epigenetic changes and

altered gene expression during subsequent normoglycemia. *The Journal of experimental medicine* *205*, 2409-2417.

Engler, A.J., Sen, S., Sweeney, H.L., and Discher, D.E. (2006). Matrix elasticity directs stem cell lineage specification. *Cell* *126*, 677-689.

English, K., Barry, F.P., Field-Corbett, C.P., and Mahon, B.P. (2007). IFN-gamma and TNF-alpha differentially regulate immunomodulation by murine mesenchymal stem cells. *Immunol Lett* *110*, 91-100.

Eyerich, S., Eyerich, K., Traidl-Hoffmann, C., and Biedermann, T. (2018). Cutaneous Barriers and Skin Immunity: Differentiating A Connected Network. *Trends Immunol* *39*, 315-327.

Finley, P.J., DeClue, C.E., Sell, S.A., DeBartolo, J.M., and Shornick, L.P. (2016). Diabetic Wounds Exhibit Decreased Ym1 and Arginase Expression with Increased Expression of IL-17 and IL-20. *Advances in wound care* *5*, 486-494.

Fiorentino, T.V., Prioleta, A., Zuo, P., and Folli, F. (2013). Hyperglycemia-induced oxidative stress and its role in diabetes mellitus related cardiovascular diseases. *Current pharmaceutical design* *19*, 5695-5703.

Fiorina, P., Jurewicz, M., Augello, A., Vergani, A., Dada, S., La Rosa, S., Selig, M., Godwin, J., Law, K., Placidi, C., et al. (2009). Immunomodulatory function of bone marrow-derived mesenchymal stem cells in experimental autoimmune type 1 diabetes. *Journal of immunology* *183*, 993-1004.

Fullerton, J.N., and Gilroy, D.W. (2016). Resolution of inflammation: a new therapeutic frontier. *Nature reviews. Drug discovery* *15*, 551-567.

Ganesh Yerra, V., Negi, G., Sharma, S.S., and Kumar, A. (2013). Potential therapeutic effects of the simultaneous targeting of the Nrf2 and NF-kappaB pathways in diabetic neuropathy. *Redox biology* *1*, 394-397.

Ghosh, S., May, M.J., and Kopp, E.B. (1998). NF-kappa B and Rel proteins: evolutionarily conserved mediators of immune responses. *Annu Rev Immunol* *16*, 225-260.

Giacco, F., and Brownlee, M. (2010). Oxidative stress and diabetic complications. *Circulation research* *107*, 1058-1070.

Gieseck, R.L., 3rd, Ramalingam, T.R., Hart, K.M., Vannella, K.M., Cantu, D.A., Lu, W.Y., Ferreira-Gonzalez, S., Forbes, S.J., Vallier, L., and Wynn, T.A. (2016). Interleukin-13 Activates Distinct Cellular Pathways Leading to Ductular Reaction, Steatosis, and Fibrosis. *Immunity* *45*, 145-158.

- Goh, Y.P., Henderson, N.C., Heredia, J.E., Red Eagle, A., Odegaard, J.I., Lehwald, N., Nguyen, K.D., Sheppard, D., Mukundan, L., Locksley, R.M., et al. (2013). Eosinophils secrete IL-4 to facilitate liver regeneration. *Proceedings of the National Academy of Sciences of the United States of America* *110*, 9914-9919.
- Gong, D., Shi, W., Yi, S.J., Chen, H., Groffen, J., and Heisterkamp, N. (2012). TGFbeta signaling plays a critical role in promoting alternative macrophage activation. *BMC immunology* *13*, 31.
- Gooderham, M.J., Hong, H.C., Eshtiaghi, P., and Papp, K.A. (2018). Dupilumab: A review of its use in the treatment of atopic dermatitis. *J Am Acad Dermatol* *78*, S28-S36.
- Granero-Molto, F., Weis, J.A., Miga, M.I., Landis, B., Myers, T.J., O'Rear, L., Longobardi, L., Jansen, E.D., Mortlock, D.P., and Spagnoli, A. (2009). Regenerative effects of transplanted mesenchymal stem cells in fracture healing. *Stem Cells* *27*, 1887-1898.
- Greenbaum, A., Hsu, Y.M., Day, R.B., Schuettpelz, L.G., Christopher, M.J., Borgerding, J.N., Nagasawa, T., and Link, D.C. (2013). CXCL12 in early mesenchymal progenitors is required for haematopoietic stem-cell maintenance. *Nature* *495*, 227-230.
- Grinberg-Bleyer, Y., Dainichi, T., Oh, H., Heise, N., Klein, U., Schmid, R.M., Hayden, M.S., and Ghosh, S. (2015). Cutting edge: NF-kappaB p65 and c-Rel control epidermal development and immune homeostasis in the skin. *Journal of immunology* *194*, 2472-2476.
- Guttman-Yassky, E., Krueger, J.G., and Lebwohl, M.G. (2018). Systemic immune mechanisms in atopic dermatitis and psoriasis with implications for treatment. *Exp Dermatol* *27*, 409-417.
- Hayden, M.S., and Ghosh, S. (2011). NF-kappaB in immunobiology. *Cell research* *21*, 223-244.
- Hoesel, B., and Schmid, J.A. (2013). The complexity of NF-kappaB signaling in inflammation and cancer. *Molecular cancer* *12*, 86.
- Huang, Z., Zhong, L., Lee, J.T.H., Zhang, J., Wu, D., Geng, L., Wang, Y., Wong, C.M., and Xu, A. (2017). The FGF21-CCL11 Axis Mediates Beiging of White Adipose Tissues by Coupling Sympathetic Nervous System to Type 2 Immunity. *Cell metabolism* *26*, 493-508 e494.
- Jiao, H., Xiao, E., and Graves, D.T. (2015). Diabetes and Its Effect on Bone and Fracture Healing. *Current osteoporosis reports* *13*, 327-335.
- Jin, P., Zhang, X., Wu, Y., Li, L., Yin, Q., Zheng, L., Zhang, H., and Sun, C. (2010). Streptozotocin-induced diabetic rat-derived bone marrow mesenchymal stem cells have impaired abilities in proliferation, paracrine, antiapoptosis, and myogenic differentiation. *Transplant Proc* *42*, 2745-2752.

- Karimkhani, C., Dellavalle, R.P., Coffeng, L.E., Flohr, C., Hay, R.J., Langan, S.M., Nsoesie, E.O., Ferrari, A.J., Erskine, H.E., Silverberg, J.I., et al. (2017). Global Skin Disease Morbidity and Mortality: An Update From the Global Burden of Disease Study 2013. *JAMA Dermatol* 153, 406-412.
- Kassan, M., Choi, S.K., Galan, M., Bishop, A., Umezawa, K., Trebak, M., Belmadani, S., and Matrougui, K. (2013). Enhanced NF-kappaB activity impairs vascular function through PARP-1-, SP-1-, and COX-2-dependent mechanisms in type 2 diabetes. *Diabetes* 62, 2078-2087.
- Kato, H., Taguchi, Y., Tominaga, K., Kimura, D., Yamawaki, I., Noguchi, M., Yamauchi, N., Tamura, I., Tanaka, A., and Umeda, M. (2016). High Glucose Concentrations Suppress the Proliferation of Human Periodontal Ligament Stem Cells and Their Differentiation Into Osteoblasts. *Journal of periodontology* 87, e44-51.
- Kawanami, A., Matsushita, T., Chan, Y.Y., and Murakami, S. (2009). Mice expressing GFP and CreER in osteochondro progenitor cells in the periosteum. *Biochemical and biophysical research communications* 386, 477-482.
- Kayal, R.A., Siqueira, M., Alblowi, J., McLean, J., Krothapalli, N., Faibish, D., Einhorn, T.A., Gerstenfeld, L.C., and Graves, D.T. (2010). TNF-alpha mediates diabetes-enhanced chondrocyte apoptosis during fracture healing and stimulates chondrocyte apoptosis through FOXO1. *Journal of bone and mineral research : the official journal of the American Society for Bone and Mineral Research* 25, 1604-1615.
- Kim, J., Kim, B.E., and Leung, D.Y.M. (2019). Pathophysiology of atopic dermatitis: Clinical implications. *Allergy Asthma Proc* 40, 84-92.
- Klement, J.F., Rice, N.R., Car, B.D., Abbondanzo, S.J., Powers, G.D., Bhatt, P.H., Chen, C.H., Rosen, C.A., and Stewart, C.L. (1996). IkappaBalpha deficiency results in a sustained NF-kappaB response and severe widespread dermatitis in mice. *Mol Cell Biol* 16, 2341-2349.
- Ko, K.I., Coimbra, L.S., Tian, C., Alblowi, J., Kayal, R.A., Einhorn, T.A., Gerstenfeld, L.C., Pignolo, R.J., and Graves, D.T. (2015). Diabetes reduces mesenchymal stem cells in fracture healing through a TNFalpha-mediated mechanism. *Diabetologia* 58, 633-642.
- Koga, C., Kabashima, K., Shiraishi, N., Kobayashi, M., and Tokura, Y. (2008). Possible pathogenic role of Th17 cells for atopic dermatitis. *J Invest Dermatol* 128, 2625-2630.
- Kuo, Y.R., Wang, C.T., Cheng, J.T., Wang, F.S., Chiang, Y.C., and Wang, C.J. (2011). Bone marrow-derived mesenchymal stem cells enhanced diabetic wound healing through recruitment of tissue regeneration in a rat model of streptozotocin-induced diabetes. *Plast Reconstr Surg* 128, 872-880.

- Li, Q., Van Antwerp, D., Mercurio, F., Lee, K.F., and Verma, I.M. (1999a). Severe liver degeneration in mice lacking the IkappaB kinase 2 gene. *Science* 284, 321-325.
- Li, Z.W., Chu, W., Hu, Y., Delhase, M., Deerinck, T., Ellisman, M., Johnson, R., and Karin, M. (1999b). The IKKbeta subunit of IkappaB kinase (IKK) is essential for nuclear factor kappaB activation and prevention of apoptosis. *The Journal of experimental medicine* 189, 1839-1845.
- Li, Z.W., Omori, S.A., Labuda, T., Karin, M., and Rickert, R.C. (2003). IKK beta is required for peripheral B cell survival and proliferation. *Journal of immunology* 170, 4630-4637.
- Liang, J., Zhang, H., Hua, B., Wang, H., Lu, L., Shi, S., Hou, Y., Zeng, X., Gilkeson, G.S., and Sun, L. (2010). Allogenic mesenchymal stem cells transplantation in refractory systemic lupus erythematosus: a pilot clinical study. *Annals of the rheumatic diseases* 69, 1423-1429.
- Liang, Y., Seymour, R.E., and Sundberg, J.P. (2011). Inhibition of NF-kappaB signaling retards eosinophilic dermatitis in SHARPIN-deficient mice. *J Invest Dermatol* 131, 141-149.
- Lim, H.W., Collins, S.A.B., Resneck, J.S., Jr., Bologna, J.L., Hodge, J.A., Rohrer, T.A., Van Beek, M.J., Margolis, D.J., Sober, A.J., Weinstock, M.A., et al. (2017). The burden of skin disease in the United States. *J Am Acad Dermatol* 76, 958-972 e952.
- Ling, L., Cao, Z., and Goeddel, D.V. (1998). NF-kappaB-inducing kinase activates IKK-alpha by phosphorylation of Ser-176. *Proceedings of the National Academy of Sciences of the United States of America* 95, 3792-3797.
- Liu, J., Ibi, D., Taniguchi, K., Lee, J., Herrema, H., Akosman, B., Mucka, P., Salazar Hernandez, M.A., Uyar, M.F., Park, S.W., et al. (2016). Inflammation Improves Glucose Homeostasis through IKKbeta-XBP1s Interaction. *Cell* 167, 1052-1066 e1018.
- Loder, R.T. (1988). The influence of diabetes mellitus on the healing of closed fractures. *Clin Orthop Relat Res*, 210-216.
- Logan, M., Martin, J.F., Nagy, A., Lobe, C., Olson, E.N., and Tabin, C.J. (2002). Expression of Cre Recombinase in the developing mouse limb bud driven by a Prxl enhancer. *Genesis* 33, 77-80.
- Ma, S., Xie, N., Li, W., Yuan, B., Shi, Y., and Wang, Y. (2014). Immunobiology of mesenchymal stem cells. *Cell Death Differ* 21, 216-225.
- Ma, W., Bryce, P.J., Humbles, A.A., Laouini, D., Yalcindag, A., Alenius, H., Friend, D.S., Oettgen, H.C., Gerard, C., and Geha, R.S. (2002). CCR3 is essential for skin eosinophilia

and airway hyperresponsiveness in a murine model of allergic skin inflammation. *J Clin Invest* 109, 621-628.

Mahmoudi, S., Mancini, E., Xu, L., Moore, A., Jahanbani, F., Hebestreit, K., Srinivasan, R., Li, X., Devarajan, K., PreLOT, L., et al. (2019). Heterogeneity in old fibroblasts is linked to variability in reprogramming and wound healing. *Nature* 574, 553-558.

Marsell, R., and Einhorn, T.A. (2011). The biology of fracture healing. *Injury* 42, 551-555.  
McInnes, L., Healy, J., and Melville, J. (2018). UMAP: Uniform Manifold Approximation and Projection for Dimension Reduction. arXiv:1802.03426 [stat.ML].

Mercurio, F., Zhu, H., Murray, B.W., Shevchenko, A., Bennett, B.L., Li, J., Young, D.B., Barbosa, M., Mann, M., Manning, A., et al. (1997). IKK-1 and IKK-2: cytokine-activated I $\kappa$ B kinases essential for NF- $\kappa$ B activation. *Science* 278, 860-866.

Mirza, R.E., Fang, M.M., Ennis, W.J., and Koh, T.J. (2013). Blocking interleukin-1 $\beta$  induces a healing-associated wound macrophage phenotype and improves healing in type 2 diabetes. *Diabetes* 62, 2579-2587.

Murao, H., Yamamoto, K., Matsuda, S., and Akiyama, H. (2013). Periosteal cells are a major source of soft callus in bone fracture. *Journal of bone and mineral metabolism* 31, 390-398.

Nunomura, S., Ejiri, N., Kitajima, M., Nanri, Y., Arima, K., Mitamura, Y., Yoshihara, T., Fujii, K., Takao, K., Imura, J., et al. (2019). Establishment of a Mouse Model of Atopic Dermatitis by Deleting *Ikk2* in Dermal Fibroblasts. *J Invest Dermatol* 139, 1274-1283.

Oeckinghaus, A., and Ghosh, S. (2009). The NF- $\kappa$ B family of transcription factors and its regulation. *Cold Spring Harb Perspect Biol* 1, a000034.

Oeckinghaus, A., Hayden, M.S., and Ghosh, S. (2011). Crosstalk in NF- $\kappa$ B signaling pathways. *Nature immunology* 12, 695-708.

Ouyang, Z., Chen, Z., Ishikawa, M., Yue, X., Kawanami, A., Leahy, P., Greenfield, E.M., and Murakami, S. (2014). *Prx1* and 3.2kb *Col1a1* promoters target distinct bone cell populations in transgenic mice. *Bone* 58, 136-145.

Ovchinnikov, D.A., Deng, J.M., Ogunrinu, G., and Behringer, R.R. (2000). *Col2a1*-directed expression of Cre recombinase in differentiating chondrocytes in transgenic mice. *Genesis* 26, 145-146.

Pacios, S., Xiao, W., Mattos, M., Lim, J., Tarapore, R.S., Alsadun, S., Yu, B., Wang, C.Y., and Graves, D.T. (2015). Osteoblast Lineage Cells Play an Essential Role in Periodontal Bone Loss Through Activation of Nuclear Factor- $\kappa$ B. *Scientific reports* 5, 16694.

Page, A., Navarro, M., Garin, M., Perez, P., Casanova, M.L., Moreno, R., Jorcano, J.L., Cascallana, J.L., Bravo, A., and Ramirez, A. (2010). IKKbeta leads to an inflammatory skin disease resembling interface dermatitis. *J Invest Dermatol* 130, 1598-1610.

Pahl, H.L. (1999). Activators and target genes of Rel/NF-kappaB transcription factors. *Oncogene* 18, 6853-6866.

Palacios, D., Mozzetta, C., Consalvi, S., Caretti, G., Saccone, V., Proserpio, V., Marquez, V.E., Valente, S., Mai, A., Forcales, S.V., et al. (2010). TNF/p38alpha/polycomb signaling to Pax7 locus in satellite cells links inflammation to the epigenetic control of muscle regeneration. *Cell stem cell* 7, 455-469.

Pannicke, U., Baumann, B., Fuchs, S., Henneke, P., Rensing-Ehl, A., Rizzi, M., Janda, A., Hese, K., Schlesier, M., Holzmann, K., et al. (2013). Deficiency of innate and acquired immunity caused by an IKBKB mutation. *N Engl J Med* 369, 2504-2514.

Pasparakis, M., Courtois, G., Hafner, M., Schmidt-Supprian, M., Nenci, A., Toksoy, A., Krampert, M., Goebeler, M., Gillitzer, R., Israel, A., et al. (2002). TNF-mediated inflammatory skin disease in mice with epidermis-specific deletion of IKK2. *Nature* 417, 861-866.

Patel, S.A., Meyer, J.R., Greco, S.J., Corcoran, K.E., Bryan, M., and Rameshwar, P. (2010). Mesenchymal stem cells protect breast cancer cells through regulatory T cells: role of mesenchymal stem cell-derived TGF-beta. *Journal of immunology* 184, 5885-5894.

Perdiguerro, E., Sousa-Victor, P., Ruiz-Bonilla, V., Jordi, M., Caelles, C., Serrano, A.L., and Munoz-Canoves, P. (2011). p38/MKP-1-regulated AKT coordinates macrophage transitions and resolution of inflammation during tissue repair. *The Journal of cell biology* 195, 307-322.

Philipp, D., Suhr, L., Wahlers, T., Choi, Y.H., and Paunel-Gorgulu, A. (2018). Preconditioning of bone marrow-derived mesenchymal stem cells highly strengthens their potential to promote IL-6-dependent M2b polarization. *Stem Cell Res Ther* 9, 286.

Piehler, D., Stenzel, W., Grahnert, A., Held, J., Richter, L., Kohler, G., Richter, T., Eschke, M., Alber, G., and Muller, U. (2011). Eosinophils contribute to IL-4 production and shape the T-helper cytokine profile and inflammatory response in pulmonary cryptococcosis. *The American journal of pathology* 179, 733-744.

Ponath, P.D., Qin, S., Ringler, D.J., Clark-Lewis, I., Wang, J., Kassam, N., Smith, H., Shi, X., Gonzalo, J.A., Newman, W., et al. (1996). Cloning of the human eosinophil chemoattractant, eotaxin. Expression, receptor binding, and functional properties suggest a mechanism for the selective recruitment of eosinophils. *J Clin Invest* 97, 604-612.

Potter, C.S., Wang, Z., Silva, K.A., Kennedy, V.E., Stearns, T.M., Burzenski, L., Shultz, L.D., Hogenesch, H., and Sundberg, J.P. (2014). Chronic proliferative dermatitis in Sharpin

null mice: development of an autoinflammatory disease in the absence of B and T lymphocytes and IL4/IL13 signaling. *PLoS one* 9, e85666.

Pradhan, L., Cai, X., Wu, S., Andersen, N.D., Martin, M., Malek, J., Guthrie, P., Veves, A., and Logerfo, F.W. (2011). Gene expression of pro-inflammatory cytokines and neuropeptides in diabetic wound healing. *J Surg Res* 167, 336-342.

Sanchez-Gurmaches, J., Hsiao, W.Y., and Guertin, D.A. (2015). Highly selective in vivo labeling of subcutaneous white adipocyte precursors with Prx1-Cre. *Stem Cell Reports* 4, 541-550.

Sato, K., Ozaki, K., Oh, I., Meguro, A., Hatanaka, K., Nagai, T., Muroi, K., and Ozawa, K. (2007). Nitric oxide plays a critical role in suppression of T-cell proliferation by mesenchymal stem cells. *Blood* 109, 228-234.

Schwingen, J., Kaplan, M., and Kurschus, F.C. (2020). Review-Current Concepts in Inflammatory Skin Diseases Evolved by Transcriptome Analysis: In-Depth Analysis of Atopic Dermatitis and Psoriasis. *Int J Mol Sci* 21.

Sehgal, A., Donaldson, D.S., Pridans, C., Sauter, K.A., Hume, D.A., and Mabbott, N.A. (2018). The role of CSF1R-dependent macrophages in control of the intestinal stem-cell niche. *Nature communications* 9, 1272.

Sellmeyer, D.E., Civitelli, R., Hofbauer, L.C., Khosla, S., Lecka-Czernik, B., and Schwartz, A.V. (2016). Skeletal Metabolism, Fracture Risk, and Fracture Outcomes in Type 1 and Type 2 Diabetes. *Diabetes* 65, 1757-1766.

Sen, R., and Baltimore, D. (1986). Multiple nuclear factors interact with the immunoglobulin enhancer sequences. *Cell* 46, 705-716.

Seymour, R.E., Hasham, M.G., Cox, G.A., Shultz, L.D., Hogenesch, H., Roopenian, D.C., and Sundberg, J.P. (2007). Spontaneous mutations in the mouse Sharpin gene result in multiorgan inflammation, immune system dysregulation and dermatitis. *Genes Immun* 8, 416-421.

Shanmugam, N., Reddy, M.A., Guha, M., and Natarajan, R. (2003). High glucose-induced expression of proinflammatory cytokine and chemokine genes in monocytic cells. *Diabetes* 52, 1256-1264.

Shin, L., and Peterson, D.A. (2012). Impaired therapeutic capacity of autologous stem cells in a model of type 2 diabetes. *Stem Cells Transl Med* 1, 125-135.

Silverberg, J.I., Margolis, D.J., Boguniewicz, M., Fonacier, L., Grayson, M.H., Ong, P.Y., Chiesa Fuxench, Z.C., Simpson, E.L., and Gelfand, J.M. (2019). Distribution of atopic dermatitis lesions in United States adults. *J Eur Acad Dermatol Venereol* 33, 1341-1348.



- Simpson, E.L., Bieber, T., Guttman-Yassky, E., Beck, L.A., Blauvelt, A., Cork, M.J., Silverberg, J.I., Deleuran, M., Kataoka, Y., Lacour, J.P., et al. (2016). Two Phase 3 Trials of Dupilumab versus Placebo in Atopic Dermatitis. *N Engl J Med* 375, 2335-2348.
- Siqueira, M.F., Li, J., Chehab, L., Desta, T., Chino, T., Krothpali, N., Behl, Y., Alikhani, M., Yang, J., Braasch, C., et al. (2010). Impaired wound healing in mouse models of diabetes is mediated by TNF-alpha dysregulation and associated with enhanced activation of forkhead box O1 (FOXO1). *Diabetologia* 53, 378-388.
- Stolzing, A., Sellers, D., Llewelyn, O., and Scutt, A. (2010). Diabetes induced changes in rat mesenchymal stem cells. *Cells Tissues Organs* 191, 453-465.
- Sui, B.D., Hu, C.H., Zheng, C.X., Shuai, Y., He, X.N., Gao, P.P., Zhao, P., Li, M., Zhang, X.Y., He, T., et al. (2017). Recipient Glycemic Micro-environments Govern Therapeutic Effects of Mesenchymal Stem Cell Infusion on Osteopenia. *Theranostics* 7, 1225-1244.
- Sun, S.C., Chang, J.H., and Jin, J. (2013). Regulation of nuclear factor-kappaB in autoimmunity. *Trends Immunol* 34, 282-289.
- Suryavanshi, S.V., and Kulkarni, Y.A. (2017). NF-kappabeta: A Potential Target in the Management of Vascular Complications of Diabetes. *Frontiers in pharmacology* 8, 798.
- Taniguchi, K., and Karin, M. (2018). NF-kappaB, inflammation, immunity and cancer: coming of age. *Nat Rev Immunol* 18, 309-324.
- Tevlin, R., Seo, E.Y., Marcic, O., McArdle, A., Tong, X., Zimdahl, B., Malkovskiy, A., Sinha, R., Gulati, G., Li, X., et al. (2017). Pharmacological rescue of diabetic skeletal stem cell niches. *Science translational medicine* 9.
- Tsai, K.H., Wang, W.J., Lin, C.W., Pai, P., Lai, T.Y., Tsai, C.Y., and Kuo, W.W. (2012). NADPH oxidase-derived superoxide anion-induced apoptosis is mediated via the JNK-dependent activation of NF-kappaB in cardiomyocytes exposed to high glucose. *Journal of cellular physiology* 227, 1347-1357.
- van de Vyver, M. (2017). Intrinsic Mesenchymal Stem Cell Dysfunction in Diabetes Mellitus: Implications for Autologous Cell Therapy. *Stem cells and development* 26, 1042-1053.
- Van Linthout, S., Miteva, K., and Tschöpe, C. (2014). Crosstalk between fibroblasts and inflammatory cells. *Cardiovasc Res* 102, 258-269.
- Wada, J., and Makino, H. (2013). Inflammation and the pathogenesis of diabetic nephropathy. *Clinical science* 124, 139-152.
- Waltman, L., and van Eck, N.J. (2013). A smart local moving algorithm for large-scale modularity-based community detection. *Eur. Phys. J. B* 86.

- Wang, G., Savinko, T., Wolff, H., Dieu-Nosjean, M.C., Kemeny, L., Homey, B., Lauerma, A.I., and Alenius, H. (2007). Repeated epicutaneous exposures to ovalbumin progressively induce atopic dermatitis-like skin lesions in mice. *Clin Exp Allergy* 37, 151-161.
- Wang, X., Wang, Y., Gou, W., Lu, Q., Peng, J., and Lu, S. (2013). Role of mesenchymal stem cells in bone regeneration and fracture repair: a review. *Int Orthop* 37, 2491-2498.
- Wang, Y., Chen, X., Cao, W., and Shi, Y. (2014). Plasticity of mesenchymal stem cells in immunomodulation: pathological and therapeutic implications. *Nature immunology* 15, 1009-1016.
- Weber, D.R., and Schwartz, G. (2016). Epidemiology of Skeletal Health in Type 1 Diabetes. *Current osteoporosis reports* 14, 327-336.
- Wilk, K., Yeh, S.A., Mortensen, L.J., Ghaffarigarakani, S., Lombardo, C.M., Bassir, S.H., Aldawood, Z.A., Lin, C.P., and Intini, G. (2017). Postnatal Calvarial Skeletal Stem Cells Expressing PRX1 Reside Exclusively in the Calvarial Sutures and Are Required for Bone Regeneration. *Stem Cell Reports* 8, 933-946.
- Wong, J.W., Gallant-Behm, C., Wiebe, C., Mak, K., Hart, D.A., Larjava, H., and Hakkinen, L. (2009). Wound healing in oral mucosa results in reduced scar formation as compared with skin: evidence from the red Duroc pig model and humans. *Wound Repair Regen* 17, 717-729.
- Xiao, J., Yang, X., Jing, W., Guo, W., Sun, Q., Lin, Y., Liu, L., Meng, W., and Tian, W. (2013). Adipogenic and osteogenic differentiation of Lin(-)CD271(+)Sca-1(+) adipose-derived stem cells. *Molecular and cellular biochemistry* 377, 107-119.
- Xu, F., Zhang, C., and Graves, D.T. (2013). Abnormal cell responses and role of TNF-alpha in impaired diabetic wound healing. *BioMed research international* 2013, 754802.
- Yi, T., and Song, S.U. (2012). Immunomodulatory properties of mesenchymal stem cells and their therapeutic applications. *Arch Pharm Res* 35, 213-221.
- Yoshitomi, H. (2019). Regulation of Immune Responses and Chronic Inflammation by Fibroblast-Like Synoviocytes. *Front Immunol* 10, 1395.
- Zhang, F., Wang, H., Wang, X., Jiang, G., Liu, H., Zhang, G., Wang, H., Fang, R., Bu, X., Cai, S., et al. (2016). TGF-beta induces M2-like macrophage polarization via SNAIL-mediated suppression of a pro-inflammatory phenotype. *Oncotarget* 7, 52294-52306.
- Zhang, G., and Ghosh, S. (2001). Toll-like receptor-mediated NF-kappaB activation: a phylogenetically conserved paradigm in innate immunity. *J Clin Invest* 107, 13-19.

Zhang, Q., Lenardo, M.J., and Baltimore, D. (2017). 30 Years of NF-kappaB: A Blossoming of Relevance to Human Pathobiology. *Cell* 168, 37-57.

Zhou, Y., Jiang, X., Gu, P., Chen, W., Zeng, X., and Gao, X. (2012). Gsdma3 mutation causes bulge stem cell depletion and alopecia mediated by skin inflammation. *The American journal of pathology* 180, 763-774.

Zimmermann, G., Henle, P., Kusswetter, M., Moghaddam, A., Wentzensen, A., Richter, W., and Weiss, S. (2005). TGF-beta1 as a marker of delayed fracture healing. *Bone* 36, 779-785.

Zou, J.P., Huang, S., Peng, Y., Liu, H.W., Cheng, B., Fu, X.B., and Xiang, X.F. (2012). Mesenchymal stem cells/multipotent mesenchymal stromal cells (MSCs): potential role in healing cutaneous chronic wounds. *Int J Low Extrem Wounds* 11, 244-253.